Genetic modules for sensing and detoxification of antimicrobial compounds in *Listeria monocytogenes*

Thesis

for the degree of

doctor rerum naturalium (Dr. rer. nat.)

approved by the Faculty of Natural Sciences of Otto von Guericke University Magdeburg

by M.Sc. Tim Engelgeh

born on the 12th of May 1996 in Kronach

Examiner: Prof. Dr. Sven Halbedel

Prof. Dr. Kürsad Turgay

submitted on: 14.11.2023 defended on: 18.04.2024

Zusammenfassung

ATP-binding cassette (ABC)-Transporter erfüllen eine Vielzahl von Funktionen in allen Bereichen des Lebens. Die wichtigsten Funktionen prokaryotischer ABC-Transporter sind die Aufnahme von Nährstoffen aus der Umwelt, aber auch der Transport von Zuckern und Lipiden über die Zellmembran und die Entgiftung antimikrobieller Substanzen. Ein Transporter, welcher mehrere solcher antimikrobieller Verbindungen exportiert, wird als Multi-Drug-Resistance (MDR)-Transporter bezeichnet, da der Export solcher Verbindungen die Resistenz gegen die jeweiligen antimikrobiellen Substanzen vermittelt.

Listeria monocytogenes ist ein grampositives Bakterium, welches in vielen ökologischen Nischen in der Natur vorkommt, und zeitgleich ein Krankheitserreger des Menschen, der oral aufgenommen wird und schwere Symptome hervorrufen kann. Zwanzig bisher nicht charakterisierte ABC-Typ MDR-Transporter wurden *in silico* im *L. monocytogenes* Genom identifiziert und die Promotoren ihrer Gene mit *lacZ* fusioniert. Stämme, die diese Konstrukte trugen, wurden auf Promotor-Induktion durch sekundäre Metaboliten, die von Kompetitoren von *L. monocytogenes* im Boden ausgeschieden werden getestet. Der Promotor, der die Expression der *lmo1964-lmo1962*-Gene steuert, wurde durch das Makrodiolid Tartrolon B induziert. Die Tartrolon B-Resistenz von *L. monocytogenes* war von den *lmo1964-lmo1963*-Transportergenen abhängig, und das Operon wurde in das *tim*-Operon umbenannt.

Ein Tartrolon-B-Suppressor-Screen führte zur Isolierung von Stämmen mit einem inaktiven *clpP2*-Allel, die hochgradig resistent gegen Tartrolon B waren. Die hohe Resistenz war jedoch vom Vorhandensein der *timAB*-Gene abhängig. Weitere Experimente deuteten darauf hin, dass der Grund für die Tartrolon-B-Resistenz von Stämmen, die ein dysfunktionales ClpXP2- und ClpCP2-Proteasom besitzen, in der Akkumulation von SpxA1, einem Transkriptionsregulator, liegt, welcher vermutlich weitere Gene, die zur Tartrolon B-Resistenz beitragen, aktiviert.

Summary

ATP binding cassette (ABC) transporters fulfill a wide variety of functions in all domains of life. The most important functions of prokaryotic ABC transporters are the uptake of nutrients from the environment, but also the transport of sugars and lipids and the detoxification of antimicrobial compounds. A transporter exporting a variety of such antimicrobial compounds is called an multi drug resistance (MDR) transporter, since its export of such compounds is mediating resistance to the respective molecules.

Listeria monocytogenes is a gram-positive bacterium and a food-borne pathogen, which can cause severe symptoms upon ingestion. Twenty so far uncharacterized ABC-type MDR transporters were identified *in silico* in the *L. monocytogenes* genome, and their respective promoters fused to the *lacZ* reporter gene to monitor their induction by secondary metabolites secreted by natural competitors of *L. monocytogenes* present in the soil. The promoter controlling the expression of the *lmo1964-lmo1962* genes was induced by the macrodiolide tartrolon B, which is toxic to gram-positive bacteria. The tartrolon B resistance of *L. monocytogenes* was dependent on the *lmo1964-lmo1963* transporter genes and the operon renamed to the *tim* operon.

A tartrolon B suppressor screen led to the isolation of strains with an inactive *clpP2* allele, which were highly resistant to the drug. However, the high-level resistance was dependent on the presence of the *timAB* genes. Further experiments demonstrated that the reason for the tartrolon B resistance-gain of strains carrying a dysfunctional ClpXP2 and ClpCP2 proteasome was caused by the accumulation of SpxA1, a transcriptional regulator, which probably activates genes involved in detoxification of tartrolon B.

1 Introduction

1.1 *Listeria monocytogenes*

1.1.1 General characteristics

The microbe *Listeria monocytogenes*, first described as *Bacterium monocytogenes* in 1926 by the group around E.G.D. Murray as they investigated a plague affecting rabbits (Murray *et al.*, 1926) is part of the genus of *Listeria*. This genus consists of 28 recognized species (spp.) (*https://www.bacterio.net/genus/listeria*), which fall into four subgroups, namely the *Listeria sensu stricto* spp., *Paenilisteria*, *Mesolisteria* und *Murraya* (Orsi & Wiedmann, 2016). *Listeria* belong to the class of the *Bacilli* (Sivalingam *et al.*, 1992, Nyarko & Donnelly, 2015) and the phylum of *Bacillota*, formerly known as *Firmicutes* (Gibbons & Murray, 1978, Collins *et al.*, 1991, Oren & Garrity, 2021). This phylum is restricted to gram-positive bacteria with a low G+C content in their DNA (Lightfield *et al.*, 2011) and contains physiologically and morphologically diverse types of bacteria, which mostly vary in their shape and ability to sporulate (Briggs *et al.*, 2012). *L. monocytogenes* is a rod-shaped species, which is motile through its peritrichous flagella between 24°C and 28°C and is unable to form spores (Farber & Peterkin, 1991). The bacterium is about 0.5 µm in width and 1 µm to 1.5 µm in length (Matle *et al.*, 2020). The *Listeria* spp. can grow at temperatures between -0.4 to 45°C, with a growth optimum at 37°C (Matle *et al.*, 2020). Like most other oxygen-exposed species, *Listeria* spp. are catalase-positive, meaning they can protect themselves from oxidative damage by decomposing hydrogen peroxide to water and oxygen. However, catalase negative strains have also been reported (Cepeda *et al.*, 2006). Unlike in the well-studied *B. subtilis* species, the citric acid cycle is incomplete in *Listeria* species, since it is lacking the ketoglutarate dehydrogenase, succinyl-CoA synthetase and succinate dehydrogenase (Kim *et al.*, 2006a).

Out of the 28 *Listeria* species, *L. monocytogenes* is the only species able to frequently infect both animals and humans, while *L. ivanovii* has been shown to be an animal pathogen, infecting mostly ruminants like sheep, although rare cases of human infections with *L. ivanovii* have been reported (Cummins *et al.*, 1994, Guillet *et al.*, 2010). However, containment of the spread of *L. monocytogenes* specifically is crucial for limiting the infection rate of humans with *Listeria* spp.

1.1.2 Occurrence in environmental habitats and on food products

L. monocytogenes can live in the environment and covers its nutritional requirements by uptake of organic material present in the soil or on plants (Freitag *et al.*, 2009). This saprophytic lifestyle enables *L. monocytogenes* to colonize several environmental niches. The bacterium is mostly found in the soil and on plants, but also in saline and non-saline waters (Weis & Seeliger, 1975, Gartley *et al.*, 2022). Although *L. monocytogenes* is unable to form spores, it shows a high tolerance to various stress factors, like its ability to grow at low temperatures or in high sodium chloride conditions of up to 10% and in a broad pH range between 4.4 and 11 (Walker, 1987, Vasseur *et al.*, 1999, Saklani-Jusforgues *et al.*, 2000, Gardan *et al.*, 2003, Begley *et al.*, 2006). The ability of the bacterium to cope with these stress factors is key for its widespread natural occurrence, but also for its survival in various food processing facilities. *L. monocytogenes* can enter these facilities by contaminating unprocessed crops, fruits or vegetables or by infection of farm animals. While farm animals usually get infected by eating contaminated food, wild birds regularly spread *L. monocytogenes* to agricultural land through their feces (Konosonoka *et al.*, 2012). *L. monocytogenes* usually occurs on food, which has not been heated to a point of over 72°C, since this temperature has been shown to effectively kill the bacterium (Mackey & Bratchell, 1989, Selby *et al.*, 2006). It has also been shown, that *L. monocytogenes* can survive the harsh conditions in some food processing applications like the

low pH present in fermentation processes or the high salt present in some meat products (Bucur *et al.*, 2018). Consequently, cases, where *L. monocytogenes* was found on processed fruits and vegetables, in dairy products and on all sorts of processed meat and fish are constantly being reported (Beuchat, 1996, Swaminathan & Gerner-Smidt, 2007, Kuttappan *et al.*, 2021, Simonetti *et al.*, 2021, Halbedel *et al.*, 2023, Madad *et al.*, 2023).

1.1.3 Clinical Aspects

L. monocytogenes is an opportunistic pathogen and the cause of listeriosis, a disease first reported in 1929 that is mainly acquired through consumption of contaminated food (Nyfeldt, 1929, Farber & Peterkin, 1991). Over the years, the disease has become increasingly prevalent all throughout the world and, due to its high fatality rate of up to 30% (Lecuit, 2005), it is a notifiable disease in several countries, including Germany and the United States. However, a high bacterial titer of 10^9 bacteria is required for otherwise healthy individuals to experience symptoms such as a non-invasive gastroenteritis (Schlech III *et al.*, 1983, Radoshevich & Cossart, 2018). The main risk groups for *L. monocytogenes* infections are people with a weakened immune system, such as the elderly or immunosuppressed patients, but also pregnant women and newborns (Gellin & Broome, 1989). In these vulnerable groups, even a low infection dose of 10^2-10^4 ingested bacteria can be sufficient for *L. monocytogenes* to enter the bloodstream, causing an invasive listeriosis (Radoshevich & Cossart, 2018). This invasive listeriosis can lead to severe symptoms such as sepsis or bacterial meningitis, and in patients with a weak immune system, even a low infection dose of 10^2-10^4 ingested bacteria can cause such severe symptoms (Radoshevich & Cossart, 2018). The primary organs being infected by *L. monocytogenes* are the liver and the spleen, however, since *L. monocytogenes* is also able to breach the blood-brain barrier, the brain can also get infected (Ghosh & Higgins, 2018, Chávez-Arroyo & Portnoy, 2020). The placenta is also susceptible for *L. monocytogenes* infection,

leading to premature birth or miscarriage, while newborns can display symptoms of sepsis, asphyxia, pneumonia or meningitis (Smith *et al.*, 2009, Girma *et al.*, 2021, Johnson *et al.*, 2021).

For a patient infected with *L. monocytogenes*, the treatment of choice are antibiotics. The standard therapy for *L. monocytogenes* infections is based on a β-lactam antibiotic, most commonly penicillin and ampicillin, which is often combined with an aminoglycoside like gentamycin (Olaimat *et al.*, 2018). However, alternative antibiotics like cotrimoxazole, several fluoroquinolones, rifampicin, vancomycin or the combination of a sulfonamide like sulfamethoxazole with trimethoprim are also used (Jones & MacGowan, 1995, Charpentier & Courvalin, 1999, Baquero *et al.*, 2020). The antibiotic dosage, in which antibiotics need to be taken is mostly dependent on the severity and the types of symptoms of a patient, where brain abscesses require the highest dosage of antibiotic treatment, and ranges between 3 to 6 weeks (Jones & MacGowan, 1995).

1.1.4 Infection cycle

While *L. monocytogenes* is taken up by macrophages passively through phagocytosis, it needs certain virulence factors to infect other mammalian cell types like the epithelial cells in the intestine (Hamon *et al.*, 2006). The expression of these virulence genes is controlled by the transcriptional activator PrfA. PrfA controls the level of the surface proteins internalin A (InlA) and internalin B (InlB), which are essential for successful invasion of epithelial cells (Dramsi *et al.*, 1995, Gaillard *et al.*, 1996). InlA is anchored to the peptidoglycan on the bacterial cell wall and binds to the epithelial receptor protein E-cadherin on the host cell, mediating invasion. InlB is retained on the cell surface by non-covalent interactions with the bacterial cell wall, from where it interacts with the multifunctional protein gC1q-R, a Met receptor tyrosine kinase as well as glycosaminoglycans (Ghebrehiwet *et al.*, 1994, Braun *et al.*, 2000, Shen *et al.*, 2000, Jonquières *et al.*, 2001, Wampler *et al.*, 2004, Phelps *et al.*, 2018). These two internalin proteins

are necessary and sufficient in promoting *L. monocytogenes* internalization into several cell types (Lecuit *et al.*, 1997).

Once *L. monocytogenes* is inside the host cell, PrfA induces the expression of virulence genes encoded on the *Listeria* Pathogenicity Island 1 (LIPI-1) (Vazquez-Boland *et al.*, 2001, Hadjilouka *et al.*, 2018, Quereda *et al.*, 2018). This LIPI-1 locus is essential for growth within the host cell and only present in the invasive *Listeria* spp. *L. monocytogenes* and *L. ivanovii* and the weakly hemolytic *L. seeligeri*, but not in other non-hemolytic *Listeria* (Gouin *et al.*, 1994). One gene encoded on LIPI-1, that is essential for virulence is the *hly* gene, which encodes for listeriolysin O (LLO). LLO is disrupting the vacuole carrying phagocytosed or internalized *L. monocytogenes* cells, releasing the bacteria into the host cell (Mengaud *et al.*, 1987, Cossart *et al.*, 1989). This step is essential for subsequent replication and cell-to-cell spread of *L. monocytogenes* cells, as disruption of *hly* leads to a substantial decrease in intracellular replication rate (Gaillard *et al.*, 1987, Cossart *et al.*, 1989). Vacuolar escape of *L. monocytogenes* is also accomplished by the two phospholipases PlcA and PlcB. Just like the *hly* gene, their respective genes are located on LIPI-1 and thus controlled by PrfA (Quereda *et al.*, 2018). These phospholipases are responsible for the cleavage of phosphatidylinositol (PlcA) and phosphatidylcholine (PlcB), which are phospholipids present in the vacuolar membrane (Smith *et al.*, 1995). Consequently, a mutant lacking the *plcAB* genes shows a significantly decrease in plaque-size and intracellular growth rate in human cell lines (Smith *et al.*, 1995).

After lysis of the vacuole, *L. monocytogenes* is able to replicate within the host cell. Once inside the cytosol of the host cell, the protein ActA has been shown to be essential for actin-polymerization and hence movement of *L. monocytogenes* within the host cell and cell-to-cell spread, which also enables *L. monocytogenes* to infect different tissues (Pistor *et al.*, 1994). Just like the genes mentioned above, *actA* is also encoded in LIPI-1 (Disson *et al.*, 2021). By

spreading to a different cell, *L. monocytogenes* is enclosed by a secondary vacuole consisting of a lipid bilayer. Here, PlcA and PlcB work together to lyse the inner membrane, while LLO is responsible for the lysis of the other membrane, allowing a new infection cycle to begin (Pizarro-Cerda *et al.*, 2016).

During this infection cycle, *L. monocytogenes* faces several different types of stresses, which are summarized below.

1.2 Stress factors experienced by *L. monocytogenes* in the environment and during infection

1.2.1 Stress factors during infection

1.2.1.1 Acidity

Upon ingestion of contaminated food, *L. monocytogenes* enters the stomach of the host, where it faces a highly acidic pH value of around 1.5 (Beasley *et al.*, 2015). The importance of this barrier in killing *L. monocytogenes* has been shown by the fact, that patients treated with proton pump inhibitors, which raise the pH in the stomach, are more susceptible to *Listeria* infections (Kvistholm Jensen *et al.*, 2017). There are intrinsic mechanisms within the bacteria that contribute to its survival in the stomach, which revolve around increasing the pH within the cell by indirectly exporting protons to the outside of the cell. This is accomplished by two systems that depend on the antiporters GadT1/2 and ArcD, which are only active at pH values below 5.0 (Ryan *et al.*, 2009, Karatzas *et al.*, 2012): The GadT1/2 antiporters import glutamate to the cytoplasm, where it is converted by the GadD1-3 decarboxylases to γ-aminobutyrate. This conversion is done via a decarboxylation reaction, which consumes an intracellular proton and hence raises the pH of the cell. The γ-aminobutyrate is then being exported in exchange for another glutamate (Cotter *et al.*, 2001, Cotter *et al.*, 2005). The ArcD antiporter imports

arginine, which is being converted to an acidic arginine derivate, namely ornithine, in the cytoplasm. Ornithine is then being exported in exchange for another arginine. The basic ammonia, which was cleaved off in this reaction reacts with protons in the cytoplasm and therefore also raises the intracellular pH (Ryan *et al.*, 2009).

L. monocytogenes has another operon designated for dealing with acidic stress, which encodes genes for the F_0F_1 ATPase. This ATPase is capable of synthesizing ATP aerobically using the protons passing into the cell in an acidic environment and use the generated ATP as an energy source to pump out the protons anaerobically (Cotter *et al.*, 2000).

1.2.1.2 Osmolarity

High concentrations of salts are stress factors, which *L. monocytogenes* faces in the intestine of a host (Davis *et al.*, 2019, Quereda *et al.*, 2021). The water loss within the cell, which would be caused by this high osmolarity can be counteracted by importing certain osmolytes, which increase the osmolarity within the cytoplasm and hence stabilize the lowered turgor pressure within the cell upon exposure to high salt concentrations (Csonka, 1989). There are three main osmolytes, which help *L. monocytogenes* survive these conditions, namely glycine betaine, carnitine and proline (Beumer *et al.*, 1994). Import of glycine betain can be accomplished by two specific transporters, namely GbuAB and BetL, both of which have been shown to vastly increase glycine betaine levels in *L. monocytogenes* cells (Sleator *et al.*, 1999, Ko & Smith, 1999). Carnitine can also be imported by GbuAB, but also by another importer named OpuC (Angelidis & Smith, 2003). Consequently, deletion of the mentioned transporters have been shown to negatively affect growth rates of *L. monocytogenes* in high salt concentrations (Wemekamp-Kamphuis *et al.*, 2002).

1.2.1.3 Bile

Bile acids are present in the duodenum, and have been shown to lead to bacterial protein aggregation and cell wall damage (Cremers *et al.*, 2014). In *L. monocytogenes*, resistance to bile salts is mediated by the *bsh* gene, which encodes for a bile salt hydrolase, catalyzing the cleavage of amide bonds present in conjugated bile salts (Begley *et al.*, 2005, Bourgin *et al.*, 2021, Quereda *et al.*, 2021). There are also several other factors, which have been shown to impact bile resistance, like the *pva* and the *btlB* gene, however the precise roles of these genes have been weakly studied (Begley *et al.*, 2005). Additionally, the *bilE*-operon is encoding for a system excluding bile from *L. monocytogenes* cells, as a mutant lacking the *bilE* locus shows a ~30% decreased level of the bile acid chenodeoxycholic acid (Sleator *et al.*, 2005).

1.2.1.4 Host microbiota

In the intestine, *L. monocytogenes* also faces host microbiota, which provide a line of defense against the pathogen. The bacteriocin-producing *Lactobacilli* and several *Clostridiales*, both of which are known gut colonizers, have been shown to be of special importance in inhibiting *L. monocytogenes* growth, mostly by secreting so-called bacteriocins, which are toxins inhibiting growth of different bacterial species (Bien *et al.*, 2013, Becattini *et al.*, 2017). However, *L. monocytogenes* can also secrete bacteriocins itself to battle competitors in the intestine. The most important *L. monocytogenes* bacteriocin is listeriolysin S, which promotes colonization of *L. monocytogenes* through its antimicrobial properties. Listeriolysin S has also been shown to be produced specifically in the intestine of orally infected mice (Quereda *et al.*, 2017, Lee, 2020).

1.2.2 Stress factors in the environment

1.2.2.1 Temperature

Although *L. monocytogenes* does not possess an extremely high tolerance to heat, it could be shown that the bacterium is more resistant to higher temperatures than other non-spore-forming pathogens like *E. coli* or *Salmonella* (Huang, 2004, Sallami *et al.*, 2006). Upon exposure to higher temperatures, *L. monocytogenes* induces the expression of heat-shock genes. There are different classes of heat-shock genes, with class I and class III being the ones most specific to heat (Bucur *et al.*, 2018). Class I heat-shock genes encode for intracellular chaperones, which are needed for the stabilization of proteins and the reassembly of misfolded proteins. Some genes encoding for these class I heat-shock proteins are *grpE*, *dnaK*, *dnaJ*, *groES* and *groEL*, all of which are controlled by the transcriptional repressor HrcA (Grandvalet *et al.*, 1998, Hanawa *et al.*, 2000). Class III heat-shock genes encode for the caseinolytic protease ClpP2 and their adaptor proteins ClpC and ClpE and are also induced at elevated temperatures to deal with the increased rate of misfolded proteins by proteolytic degradation (Nair *et al.*, 2000).

L. monocytogenes also possesses a system of cold shock proteins (Csps), which is induced at low temperature. Csps are nucleotide-binding proteins, which may act as RNA chaperones that melt secondary structures of mRNAs to enable an efficient protein translation rate under cold conditions (Muchaamba *et al.*, 2021). There are three Csps encoded within the *L. monocytogenes* genome, namely *cspA*, *cspB* and *cspD*. Among these, *cspA* appears to be the most critical one, as its expression is elevated at the highest rate at 4°C (Schmid *et al.*, 2009).

1.2.2.2 UV light

UV light is used in various food processing methods to kill off pathogens by causing damage to their DNA. As a consequence, DNA repair pathways like the nucleotide excision repair (NER) pathway increase in importance upon exposure of *L. monocytogenes* to UV light. In this

pathway, the UvrA protein is of great importance and cells lacking *uvrA* become more susceptible to UV light (Kim *et al.*, 2006b). It has been hypothesized, that a plasmid encoded gene named *uvrX* is also involved in mediating resistance to UV light (Anast & Schmitz-Esser, 2021). While *L. monocytogenes* is more resistant to UV light than *E. coli*, no precise mechanisms regarding resistance to UV light has been revealed (Beauchamp & Lacroix, 2012). However, UV induced stress is not being regulated by the σ^B-dependent stress response, which is involved in coping with other stress factors like temperature, acidic pH or high osmolarity (Gayan *et al.*, 2015, Quereda *et al.*, 2021).

1.2.2.3 Antibiotics

As mentioned previously in chapter 1.1.3, antibiotics are used in the clinical context to deal with *L. monocytogenes* infections. However, *L. monocytogenes* also faces antibiotic exposure in its natural habitats, where other bacterial species secrete antimicrobial compounds to battle competitors (Cornforth & Foster, 2013). Both of these factors lead to a constant selection pressure of *L. monocytogenes* to develop resistance against these antibiotics and strains carrying antibiotic resistances are frequently isolated from food products as well as in clinical settings (Charpentier & Courvalin, 1999, Walsh *et al.*, 2001, Yücel *et al.*, 2005, Arslan & Özdemir, 2008, Baquero *et al.*, 2020). In principle, *L. monocytogenes* can be intrinsically resistant to certain types of antibiotics, which lack affinity to the target structure in *L. monocytogenes* cells (Luque-Sastre *et al.*, 2018). However, most resistance mechanisms are acquired by mutations of chromosomal genes, which weakens the affinity of the antimicrobial agent to its target structure, or by acquisition of resistance genes from plasmids or conjugative transposons (Charpentier *et al.*, 1999) originating from other bacterial species. Genes encoding for multi drug resistance (MDR) transporters constitute an important class of antibiotic resistance genes and can either be intrinsically encoded in the *L. monocytogenes* genome or acquired through

the acquisition of mobile genetic elements (Collins *et al.*, 2010, Müller *et al.*, 2014, Hauf *et al.*, 2019). MDR transporters pump the antibiotic to the outside of the cell, hence mediating resistance (Godreuil *et al.*, 2003). In gram-positive bacteria, MDR transporters belong to four different classes: (1) the major facilitator superfamily (MFS), (2) the small MDR (SMR) transporters, (3) the multidrug and toxic extrusion (MATE) transporters and (4) the ATP binding cassette (ABC)-type MDR transporters. While the three first mentioned types of MDR transporters all use transmembrane cation gradients as energy source for compound extrusion, the ABC-type MDR transporters energize compound export by ATP hydrolysis (Lubelski *et al.*, 2007).

1.3 ABC-type MDR transporters

1.3.1 Domain organisation

Although there are several subclasses of ABC transporters, their main constitution is very similar. An ABC transporter consists of four membrane-associated domains, two of which are highly hydrophobic and consist of six to twelve transmembrane helices (forming a permease unit), and two domains located at the cytoplasmic side of the membrane, which form the ABCs (Higgins, 1992). ATP transporters can be assembled in various ways. If the ATPase and permease are encoded on the same gene, a simple dimerization of these two polypeptides is sufficient to form the transporter. However, more complex ways, like heterodimerization of different ATPase or transmembrane domains, are also possible when the ATPase and permease subunits are encoded as separate polypeptides (Holland & Blight, 1999). ABC transporters can transport a wide range of substrates such as lipids, sugars or nutrients (Ekiert *et al.*, 2022, Webb *et al.*, 2008, Lewis *et al.*, 2012). The main difference between ABC importers and exporters is that the importers use a soluble substrate binding protein to capture the ligand. This protein is either soluble in the periplasm, bound to the membrane via a protein anchor or directly fused to

the transporter (Swier *et al.*, 2016). After binding of this protein to its substrate, this complex binds to the importer and the substance is being imported (Locher, 2004). The topology of ABC transporters is summarized in Fig. 1-1A.

1.3.2 Structural motifs

The ABC domains are well conserved in the ABC transporter family, with sequence identities between 30% and 50%, even when comparing bacterial to eukaryotic ABCs. This conservation is linked to several common motifs required for the conserved tertiary structure and the mechanism of ATP hydrolysis (Wilkens, 2015).

In general, ABC domains can be divided into two conserved subdomains: The catalytic core domain consists of two β-sheets and seven α-helices, which fold into a characteristic tertiary structure. The second subdomain, the signaling domain consists of five α-helices (Schmitt *et al.*, 2003). The catalytic core contains most of the conserved motifs of ABC domains: The phosphate binding loop (P-loop), also known as the Walker A motif, is a glycine-rich sequence followed by a lysine and either a serine or threonine is required for nucleotide binding (Saraste *et al.*, 1990). This binding only occurs in conjunction with the Walker B motif, which consists of four hydrophobic amino acids, followed by an aspartic acid residue (Walker *et al.*, 1982). The Q-loop contains a highly conserved glutamine (Q) and is required for coupling of substrate binding to the catalytic cycle, as a transporter carrying dysfunctional Q-loops has been shown to retain affinity for its substrate, but is unable to trigger export mechanisms (Jones & George, 2002, Zolnerciks *et al.*, 2014). Finally, a H- and a D-loop, consisting of a conserved histidine (H) and an aspartic acid (D) residue, respectively, are also required for ATP binding and hydrolysis, since they make direct contacts with the nucleotide (Buchaklian & Klug, 2006, Westfahl *et al.*, 2008, Aittoniemi *et al.*, 2010). The function of the signaling domain is defined by the coupling of the catalytic core domain to the transmembrane domain (Holland & Blight,

1999). However, it also contains a highly conserved LSGGQ sequence, which, when mutated negatively affects ATP binding and hydrolysis (Schmees *et al.*, 1999). Fig. 1-1B shows a schematic representation of the mentioned key structural motifs in an ABC domain needed for nucleotide binding and hydrolysis.

The transmembrane domain is the domain determining the substrates for an ABC transporter (Wilkens, 2015). In order to transport a wide variety of substrates, the transmembrane domains display poor homologies even within related organisms. The membrane spanning domains consist of multiple hydrophobic α-helices and can vary in their conformation, number of transmembrane α-helices and size, which classifies them as Type I ABC importers, Type II ABC importers or ABC exporters (Locher, 2009). However, all α-helices are oriented in a

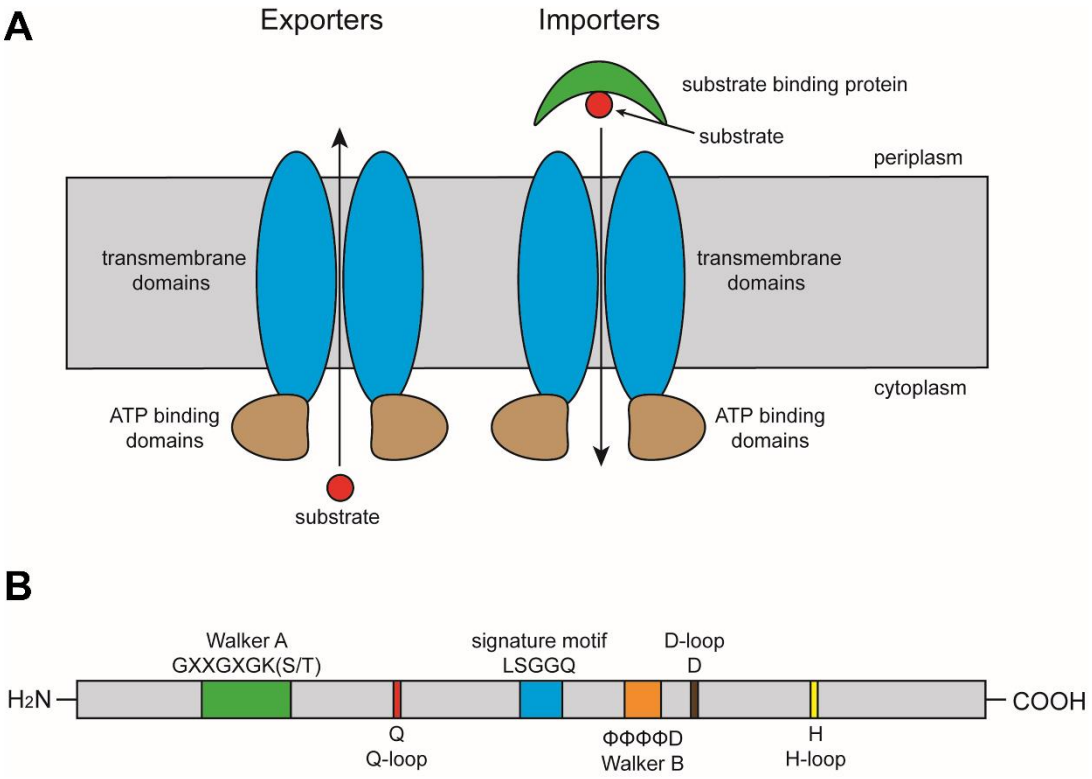

Figure 1-1: Schematic structure and motifs of ABC transporters. (A) Illustration of the structure of an ABC exporter (left side) and an importer (right side)**.** An ABC transporter consists of two ATP binding domains located in the cytoplasm (brown) and two transmembrane domains (blue). Importers need an additional substrate binding protein (green), which binds to the substrate of the importer to function. **(B)** Schematic representation of an ATP binding domain. Key structural motifs for nucleotide binding and the catalytic mechanism are marked in various colors and the name and protein sequence of each motif is indicated.

specific way, so they form a pore, that is open to the outside of the cell in the case of an ABC importer or to the cytoplasm when the transporter functions as an exporter (Wilkens, 2015).

1.3.3 Transport mechanism

The diverse topology of different types of transmembrane domains, as well as the varying size of substrates and their different chemical properties are the main reasons as to why detailed transport mechanisms vary strongly between ABC transporters. Thus, in the following only the basic, conserved steps of substrate transport are being discussed.

The catalytic cycle of an ABC transporter starts with the binding of the substrate, or the substrate binding proteins (in the case of importers), to the transmembrane domain. Afterwards, two molecules of ATP bind to their binding sites on the ABC domains, inducing a conformational change within these domains, which leads to their dimerization (Hellmich *et al.*, 2015). This conformational change in the ABC domain is transmitted to the transmembrane domain through interactions at their shared interface (Dawson & Locher, 2006). For this, the coupling helices of the transmembrane domains are of special importance, as they contact key nucleotide-binding domains on the ABC domain (Dawson & Locher, 2006). These conformational changes lead to opening of the ABC transporter on its trans-site and substrate transport. After ATP hydrolysis, the ABC domains lose their affinity to each other, which leads to the release of ADP, phosphate and the substrate on the other side of the membrane, and the transporter resets to its apo state (Wilkens, 2015).

1.3.4 Substrate binding site of ABC-type MDR transporters

An antibiotic is being exported by an ABC-type MDR transporter by binding to the binding site on the transporter, followed by conformational changes in the ABC and transmembrane domains. However, the exact mechanisms of antibiotic binding are still unclear and may also

vary between different MDR transporters. In principle, antibiotic binding could occur by capturing the antibiotic when it is already present in the cell, or the drug could be extruded directly upon diffusion of the molecule into the membrane (Bolhuis *et al.*, 1997). While a general detoxification mechanism, where the antibiotic is being exported from the cytoplasm has been proposed (Altenberg *et al.*, 1994), there is increasing evidence, that an MDR transporter can bind its substrate when it is still present within the cell membrane, where most antibiotics don't have the opportunity to implement their toxic activities (Bolhuis *et al.*, 1996b, Nishino *et al.*, 2021, Dickey *et al.*, 2023). The detoxification of antibiotics directly from the membrane has been studied in detail for the *L. lactis* MDR transporters LmrA and LmrP using the hydrophobic fluorescent membrane substrate diphenylhexatriene, which can be directly exported by both transporters from the inner leaflet of the lipid bilayer to the outside of the cell (Bolhuis *et al.*, 1996a, Bolhuis *et al.*, 1996b). Therefore, these types of MDR transporters are often referred to as "hydrophobic vacuum cleaners" that detect and expel drugs as they enter the plasma membrane (Gottesman & Pastan, 1993, Bolhuis *et al.*, 1996a, Poelarends *et al.*, 2002). These data are consistent with the fact, that the substrate binding cavity in the well-studied *S. aureus* MDR transporter SAV1866 (PDB: 2HYD) is not exposed to the cytoplasm (Dawson & Locher, 2006).

1.3.5 Transcriptional regulation of expression of MDR transporter genes

In general, gene expression must be fine-tuned in order to save energy and other resources and to prevent accumulation of unneeded substances in the cell (Bervoets & Charlier, 2019). Exposure of a bacterium to antimicrobials is usually transient, making MDR transporters only necessary when the drug that the transporter can export is present. Thus, prokaryotes have evolved regulatory mechanisms for expression of their MDR transporter genes.

While a system in *B. subtilis* has been reported, in which the expression of the *blt* and *bmr* MDR transporter genes is activated by a transcriptional activators called BltR and BmrR respectively (Ahmed *et al.*, 1995), expression of most MDR transporter genes are regulated by repressor proteins, which bind to the operator region of the transporter genes. An antibiotic can act as a ligand for this repressor, preventing the repressor from binding to the operator, which controls expression of the transporter genes (Wex *et al.*, 2021). Often times, this repressor protein is encoded in the same operon as the transporter. Several systems have been described following this principle, out of which two are exemplarily mentioned here:

The LmrCD transporter was initially identified as an exporter of daunomycin (Lubelski *et al.*, 2004, Lubelski *et al.*, 2006). The *lmrCD* genes were found to be regulated by LmrR, a repressor protein encoded in the same operon as LmrCD. Structural biology experiments showed an interaction of daunomycin with LmrR, which prevents LmrR from binding to its operator site, inducing the expression of the *lmrCD* genes in the presence of daunomycin (Madoori *et al.*, 2009).

A similar system has been reported for the *lmrAB* operon in *B. subtilis*. In this system, *lmrB* encodes the MDR transporter and *lmrA* a transcriptional repressor. The binding of the repressor protein LmrA to the *lmrAB* promoter was shown *in vitro* (Murata *et al.*, 2003, Yoshida *et al.*, 2004). However, while LmrB is mediating resistance against lincomycin and puromycin, neither antibiotic is able to induce the operon (Murata *et al.*, 2003). Instead, repression of the *lmrAB* genes is relieved in presence of flavonoids like quercetin, fisetin and catechin (Hirooka *et al.*, 2007).

1.3.6 ABC-type MDR transporters in *L. monocytogenes*

There are several MDR transporters in *L. monocytogenes*, which share this type of regulatory mechanism. Using the TransportDB 2.0 database (Elbourne *et al.*, 2017), 22 putative ABC-type

MDR transporters can be identified in the *L. monocytogenes* EGD-e genome. Substrate identification has only been accomplished for two out of these 22 ABC-type MDR transporters. One of these transporters is encoded by the *anrAB* genes. The AnrAB transporter has been identified via a transposon mutagenesis and subsequent identification of mutants which were sensitive to nisin. Nisin is an antimicrobial peptide produced by *Lactococcus lactis* using the *nisABTCIPR* gene cluster (Kuipers *et al.*, 1993, Collins *et al.*, 2010). As an multi drug transporter, AnrAB also mediates resistance to bacitracin, a non-ribosomally synthesized dodecyl peptide antibiotic synthesized by various *Bacillus* strains and gallidermin, an antimicrobial peptide produced by *Staphylococcus gallinarum* (Kellner *et al.*, 1988, Konz *et al.*, 1997). The *anrAB* genes are being controlled by the VirR regulator and are induced upon exposure of *L. monocytogenes* to bacitracin or nisin, enabling an efficient detoxification of all antibiotics (Mandin *et al.*, 2005, Jiang *et al.*, 2019).

The second MDR transporter which could be assigned with a substrate is the LieAB transporter. LieAB is an exporter of aurantimycin A, a depsipeptide secreted by *Streptomyces aurantiacus* (Gräfe *et al.*, 1995). Aurantimycin A was identified as a LieAB substrate by screening of a natural compound collection containing ~700 naturally occurring substances induction of the *lieAB* genes. For this screen, the *lieAB* promoter was fused to the *lacZ* reporter gene, which enabled monitoring of promoter induction when exposing this strain to various substances (Hauf *et al.*, 2019). The transcriptional regulator of the *lieAB* genes is the LftR repressor. LftR binds to the *lieAB* promoter via an imperfect palindromic sequence to repress *lieAB* transcription (Hauf *et al.*, 2021). The *lftR* gene is encoded together with *lftS* in the *lftRS* operon (Hauf *et al.*, 2019). While the function of LftS is unknown (Kaval *et al.*, 2015, Hauf *et al.*, 2019), *lftS* is required for aurantimycin-dependent induction of the *lieAB* promoter (Hauf *et al.*, 2019).

All of the species secreting the antibiotics which are detoxified by AnrAB or LieAB co-occur with *L. monocytogenes* in the soil (Rey *et al.*, 2004, Cavanagh *et al.*, 2015, Komaki, 2023). This suggests, that over time *L. monocytogenes* has evolved more, as of yet uncharacterized MDR transporters, which export antimicrobials secreted by competitors in the soil, in marine habitats or on plant surfaces.

1.4 Regulation of protein stability by controlled degradation

1.4.1 Proteases

While the tight transcriptional regulation of genes encoding MDR transporters has been well-studied, the level of an MDR transporter within the cell can also be regulated by proteolytic degradation. This was also observed in *L. monocytogenes* for the AnrAB transporter, which is being degraded by the protease ClpP2 (Balogh *et al.*, 2022).

Proteases are enzymes, which break down or hydrolyze peptides or proteins into smaller fragments or individual amino acids (Razzaq *et al.*, 2019). Proteases are essential enzymes in all three domains of life responsible for the degradation of misfolded proteins and maintaining protein homeostasis (Solanki *et al.*, 2021).

The majority of bacterial proteases require energy to unfold proteins. This energy is often generated by ATP-hydrolyzing enzymes, which attach to the protease and open its degradation channel. Hence, these types of proteases are called "ATPase associated which cellular activities" (AAA+) proteases (Sauer & Baker, 2011). All AAA+ proteases share some conserved structural motifs. Cleavage of a peptide is performed in an active center on the inside of the proteolytic complex, which is usually established by an assembly of protease monomers into heptameric rings (Kim *et al.*, 2022). The resulting topology allows the protease to form a narrow substrate channel that is too small for properly folded proteins to enter, thus preventing

the uncontrolled degradation of cellular proteins (Olivares *et al.*, 2016). In order for a protein to be degraded by such proteases, it needs to be recognized by an AAA+ ATPase, which then unfolds and translocates the protein into the opened substrate channel of the protease (Kim *et al.*, 2022). These types of ATPases can recognize a substrate directly by N-terminally encoded degradation tags or, or indirectly, where certain substrates first need to bind to an adapter protein (Sauer & Baker, 2011, Kim *et al.*, 2022).

There are multiple types of proteases, which are classified based on their catalytic mechanism. Each protease functions in a similar manner, which is the cleavage of a peptide at its peptide bond (Farady & Craik, 2010). For the commonly found serine and cysteine proteases, this is accomplished by transfer of a proton from the hydroxy- or thiol- side chains of the respective residue to a basic residue, which is usually a histidine. This reaction follows a nucleophilic attack of the deprotonated serine or cysteine to the carbonyl carbon of the peptide bond, which in the end leads to its hydrolysis (Radisky *et al.*, 2006). One of the most crucial bacterial serine proteases is the protease ClpP. ClpP proteases are a central determinants of proteolytic protein turnover and are conserved in most bacteria and eukaryotes (Maupin-Furlow, 2011).

1.4.2 *L. monocytogenes* ClpP2

L. monocytogenes posesses two ClpP isoforms, namely ClpP1 and ClpP2. However, these ClpP isoforms are only distantly related, since they only share a sequence identity of 42%. ClpP1 assembles into an inactive heptamer and only shows low sequence homology to ClpP proteins from other organisms (Balogh *et al.*, 2022). ClpP2 is biologically active and its special importance for proteolysis, growth in high salt concentrations or at elevated temperatures and for survival of *L. monocytogenes* inside macrophages and mice has been demonstrated (Gaillot *et al.*, 2000). While the reduced tolerance of a Δ*clpP2* mutant to heat is mainly caused by the increased importance of ClpP2 at higher temperatures, the impaired pathogenesis is caused by

a lower level of listeriolysin O, which is essential for phagosomal escape (Gaillot *et al.*, 2000, Phelps *et al.*, 2018). In other organisms, ClpP could be assigned with several other functions, such as the acquisition of nutrients, biofilm formation, cell motility and antibiotic resistance (Frees *et al.*, 2014, Bhandari *et al.*, 2018, Moreno-Cinos *et al.*, 2019).

L. monocytogenes ClpP2 oligomerizes into a heptameric ring and can assembly with another heptamer of either ClpP1 or ClpP2 to form a biologically active protease with 14 active sites (Wang *et al.*, 1997, Dahmen *et al.*, 2015, Balogh *et al.*, 2022). The catalytic center of ClpP2 consists of the three residues S98, H123 and D172, which mediate cleavage of the substrates (Dahmen *et al.*, 2015). For proteolytic cleavage, an ATPase bound to ClpP2 unfolds the target protein under hydrolysis of ATP, and enters the unfolded protein into the opened degradation channel, leading to protein degradation (Olivares *et al.*, 2016, Moreno-Cinos *et al.*, 2019). In *L. monocytogenes*, three AAA+ ATPases are known to mediate ClpP2-dependent proteolysis, namely ClpC, ClpE and ClpX (Rouquette *et al.*, 1996, Nair *et al.*, 1999, Gatsogiannis *et al.*, 2019, Aljghami *et al.*, 2022). These ATPases can be specific for certain substrates but can also act synergistically, allowing a fine-tuned control of protein homeostasis. While ClpX is constitutively expressed and has been postulated to be the main ATPase for protein quality control, ClpC and ClpE are under control of CtsR, a repressor protein which negatively regulates the expression of several genes under non-stress conditions (Derré *et al.*, 1999, Flynn *et al.*, 2001, Karatzas *et al.*, 2003, Aljghami *et al.*, 2022). A synergistic relationship between ClpC and ClpE in cell division mechanisms has also been demonstrated (Nair *et al.*, 1999).

The tight regulation of ClpP and its vital role in several cellular processes make the protease an interesting target for antibiotics. A group of acyldepsipeptides (ADEPs) was isolated from *Streptomyces hawaiiensis* and showed antimicrobial properties against *Staphylococcus aureus* and *Enterococcus faecalis* (Brötz-Oesterhelt *et al.*, 2005). ADEPs interact with ClpP directly

and compete with the AAA+ ATPases for their binding site at the hydrophobic groove (Li *et al.*, 2010). Hence, the toxicity of ADEP is caused by mimicking the binding of an ATPase to ClpP, constantly opening the degradation channel of the protease, leading to uncontrolled proteolysis and bacterial cell death (Brötz-Oesterhelt *et al.*, 2005, Kirstein *et al.*, 2009). However, ADEP resistant suppressors carrying inactivating mutations in *clpP* can frequently be isolated in *Bacillota* (Malik *et al.*, 2020).

1.5 Aim of this study

Twenty so far uncharacterized ABC-type MDR transporters could be identified *in silico* in the *L. monocytogenes* genome. The promoters controlling expression of their genes should be fused to the *lacZ* reporter gene, with the intention to identify their respective substrates by screening of natural compound libraries. Upon induction of a promoter by a specific compound, the genes encoded in this operon should then be tested regarding their role in the secretion and in the resistance against the compounds.

2 Materials and Methods

2.1 Primers

Table 2-1 lists all primers used in this work. A total amount of 25 nmol of each primer was ordered from Integrated DNA Technologies and resuspended in ddH_2O to a final concentration of 100 µM. Primers were stored at -20°C.

Table 2-1: List of primers used in this study.

name	sequence	purpose
SaH90	CGGGAAGCCCTGGGACG	control of promoter insertion in pBP117
SaH91	TGGCCTTCCTGTAGCCAGC	control of promoter insertion in pBP117
TE20	GATCTATCGATGCATGCCATGGTACCCGGGCGCGAGGAAACAGGCAACGC	*lmo0744* deletion US FW
TE21	GGCGATATCGGATCCATATGACGTCGACGCCACTGCCTAAGGATGGG	*lmo0744* deletion DS RV
TE22	GGAGAATAAATGCTGCAGTGACCCAACTAACAGAAAAGAGG	*lmo0744* deletion DS FW
TE23	GTTGGGTCACTGCAGCATTTATTCTCCTACTTTCAAATAGTATC	*lmo0744* deletion US RV
TE45	CCGCTCTAGAACTAGTGGATCCCCCGGGGCTACCGCGTCATCTGAATAATGCC	$P_{lmo0606}$ in pBP117 FW
TE46	CGTTGTAAAACGACGGGGAATTCCATTTCTCCACTTCTTTCTATCATTTG	$P_{lmo0606}$ in pBP117 RV
TE47	CCGCTCTAGAACTAGTGGATCCCCCGGGAATTAAAAAAATTTTTTAAAAGCAATAAAAAAACC	$P_{lmo0741}$ in pBP117 FW
TE48	CGTTGTAAAACGACGGGGAATTCCATAATTTCCTCCTTTCGCC	$P_{lmo0741}$ in pBP117 RV
TE49	CCGCTCTAGAACTAGTGGATCCCCCGGGCGAGCCGACTTAGTTCTTC	$P_{lmo0923}$ in pBP117 FW
TE50	CGTTGTAAAACGACGGGGAATTCCATTGCTTTCCCTCCCTTTCTC	$P_{lmo0923}$ in pBP117 RV
TE51	CCGCTCTAGAACTAGTGGATCCCCCGGGGGATGCTGTTGTAGATACTCTTGC	$P_{lmo1635}$ in pBP117 FW
TE52	CGTTGTAAAACGACGGGGAATTCCATTGAATCAACTCCATTCTTGTTCC	$P_{lmo1635}$ in pBP117 RV
TE53	CGTTGTAAAACGACGGGGAATTCCATTTCCATACCTCCTTACGTAATC	$P_{lmo2215}$ in pBP117 RV
TE54	CCGCTCTAGAACTAGTGGATCCCCCGGGCGGTAAAGCTTCTTTTAATGCCCGCGC	$P_{lmo2215}$ in pBP117 FW
TE66	CCGCTCTAGAACTAGTGGATCCCCCGGGCCGAACAAACTGGTGGTAAAAAAG	$P_{lmo0984}$ in pBP117 FW
TE67	CGTTGTAAAACGACGGGGAATTCCATCTGGTTGCCTCCCTTTTTC	$P_{lmo0984}$ in pBP117 RV
TE68	CCGCTCTAGAACTAGTGGATCCCCCGGGCCGAAAACCAATATGGAGTTGCG	$P_{lmo0108}$ in pBP117 FW
TE69	CGTTGTAAAACGACGGGGAATTCCATTTTTTCACATCCTTTAATATTC	$P_{lmo0108}$ in pBP117 RV

TE70	CTCTAGAACTAGTGGATCCCCCGGGGCTAGTCATTAAGCATAACG	$P_{lmo1652}$ in pBP117 FW
TE71	CGTTGTAAAACGACGGGGAATTCCAAACAACAATCCCTCCCTTTTC	$P_{lmo1652}$ in pBP117 RV
TE72	CTCTAGAACTAGTGGATCCCCCGGGGGAATTGAAAAAATTACTTTTTACG	$P_{lmo1725}$ with *lmo1725* in pBP117 FW
TE74	CTCTAGAACTAGTGGATCCCCCGGGCTAAACCGTCCAAAGTTTATG	$P_{lmo1964}$ in pBP117 FW
TE75	CGTTGTAAAACGACGGGGAATTCCATGTTCTCTCCTCCACACTC	$P_{lmo1964}$ in pBP117 RV
TE76	CTCTAGAACTAGTGGATCCCCCGGGGCGGTACAAAAGATCAATGG	$P_{lmo2228}$ in pBP117 FW
TE77	CGTTGTAAAACGACGGGGAATTCCAATTTACTCACCTCATCCTTTTG	$P_{lmo2228}$ in pBP117 RV
TE78	CTCTAGAACTAGTGGATCCCCCGGGGGGGAACTTACGAATTTTAC	$P_{lmo2241}$ in pBP117 FW
TE79	CGTTGTAAAACGACGGGGAATTCCATCTCTCCCCCCGCTTTCATG	$P_{lmo2241}$ in pBP117 RV
TE80	CTCTAGAACTAGTGGATCCCCCGGGCGGTGCGCCTTGGTTAAAAG	$P_{lmo2371}$ in pBP117 FW
TE81	GTAAAACGACGGGGAATTCCATCGGTTATACCAACTCC	$P_{lmo2371}$ in pBP117 RV
TE82	CTCTAGAACTAGTGGATCCCCCGGGCCGTTAGATTGGATTCAAGC	$P_{lmo2745}$ in pBP117 FW
TE83	CGTTGTAAAACGACGGGGAATTCCATTCATTTCACCCTTCCTG	$P_{lmo2745}$ in pBP117 RV
TE86	CTCTAGAACTAGTGGATCCCCCGGGGGATTTGTAGAAGTAGAAATTAAAC	$P_{lmo2751}$ in pBP117 FW
TE87	CGTTGTAAAACGACGGGGAATTCCATGATTTTCCTCCCTTGG	$P_{lmo2751}$ in pBP117 RV
TE88	CTCTAGAACTAGTGGATCCCCCGGGGGGTTATCCTCTTTTGGACC	$P_{lmo2768}$ in pBP117 FW
TE89	CGTTGTAAAACGACGGGGAATTCCATTATTCCACCTCTTTCAC	$P_{lmo2768}$ in pBP117 RV
TE104	GATCTATCGATGCATGCCATGGTACCCGGGGAAATCGCAGAACAAGGTCAAGTCC	*lmo0194/lmo0195* deletion US FW
TE105	GATCTATCGATGCATGCCATGGTACCCGGGGAAATCGCAGAACAAGGTCAAGTCC	*lmo0194/lmo0195* deletion DS RV
TE106	GATCTATCGATGCATGCCATGGTACCCGGGGAAATCGCAGAACAAGGTCAAGTCC	*lmo0194/lmo0195* deletion DS FW
TE107	GATCTATCGATGCATGCCATGGTACCCGGGGAAATCGCAGAACAAGGTCAAGTCC	*lmo0194/lmo0195* deletion US RV
TE124	CCGCTCTAGAACTAGTGGATCCCCCGGGGTCTTTTTCTCGGGTAGTTTGTATG	$P_{lmo0667}$ in pBP117 FW
TE125	CGTTGTAAAACGACGGGGAATTCCATGTAATTGCTGTCTCCTTATAA	$P_{lmo0667}$ in pBP117 RV
TE128	CAAATCCAGATGCTATCACG	control PCR for *lmo0744* deletion
TE129	CAAATCCAGATGCTATCACG	control PCR for *lmo0744* deletion
TE134	GGCGATATCGGATCCATATGACGTCGACCTTGATTCATTTGCGCCTCTGACC	*lmo1963/lmo1964* deletion DS RV
TE135	GATCTATCGATGCATGCCATGGTACCCGGGGTGTTATTTTGACTGTTTAGTAAC	*lmo1963/lmo1964* deletion US FW
TE136	TTTTCATCCATTACTGCAGCATGTTCTCTCCTCCACACTC	*lmo1963/lmo1964* deletion US RV
TE137	GAGAGAACATGCTGCAGTAATGGATGAAAAACGATTAAAAAT	*lmo1963/lmo1964* deletion DS FW

TE146	GGCGATATCGGATCCATATGACGTCGACGCAGAACTCGAAAAAGAAGTAC	*lmo2371/lmo2372* deletion US FW
TE147	GATCTATCGATGCATGCCATGGTACCCGGGGCTAAAGGTAGTTATAATAAGAGTG	*lmo2371/lmo2372* deletion DS RV
TE148	GGTATAACCGATGCTGCAGTAAAAAACCTGCGTGGCTTAAG	*lmo2371/lmo2372* deletion DS FW
TE149	GGTATAACCGATGCTGCAGTAAAAAACCTGCGTGGCTTAAG	*lmo2371/lmo2372* deletion US RV
TE162	AGAAGTAAAAGTCACAGTAACAGC	control PCR for *lmo0193/lmo0194* deletion
TE163	GACAACTTTGTGAATTGTAATC	control PCR for *lmo0193/lmo0194* deletion
TE181	CGTTGTAAAACGACGGGGAATTCTCATTCATGGTTGCGGCTCCT	$P_{lmo1725}$ with *lmo1725* in pBP117 RV
TE188	GATGGCAGCTAGTTTAATATG	control PCR for *lmo1963/lmo1964* deletion
TE189	CGGATGGATCTGCAAATAAAC	control PCR for *lmo1963/lmo1964* deletion
TE208	CCACGACTAACGGTCTTAATG	control PCR for *lmo2371/lmo2372* deletion
TE209	CTATTATCGCTCTTTTTCCG	control PCR for *lmo2371/lmo2372* deletion
TE212	GGCGATATCGGATCCATATGACGTCGACCGAAATCCATATCCATCATGAAATC	*lmo1962* deletion DS RV
TE213	GATCTATCGATGCATGCCATGGTACCCGGGGTTTTTTGGAAAATGATTGGG	*lmo1962* deletion US FW
TE214	GGATTTGGGCTCACTGCAGCATTATACTTTCAAATCCTTTTTCTTA	*lmo1962* deletion US RV
TE215	GAAAGTATAATGCTGCAGTGAGCCCAAATCCTTTTTTTAAC	*lmo1962* deletion DS FW
TE216	CACCTTATTTATCGCGGCG	control PCR for *lmo1962* deletion
TE217	GCAGCACTAATTGGTGCGC	control PCR for *lmo1962* deletion
TE218	GATTCCTAGGATGGGTACCATGGAAGCAATTAAAGTGGAG	*lmo1963/lmo1964* in pSG1154
TE219	GCTTGATAATTCGCGGCCGCTTATACTTTCAAATCCTTTTTCTTATAAAG	*lmo1963/lmo1964* in pSG1154
TE220	GGGCAACAAACTAATGTGCAAC	control of pSG1154 insertions
TE227	GTAGAAGGAGAGTGAAACCCATGGAAGCAATTAAAGTGGAGTCGC	*lmo1963/lmo1964* in pIMK3 FW
TE228	CAAAGCATAATGGGATCGTCGACTTATACTTTCAAATCCTTTTTC	*lmo1963/lmo1964* in pIMK3 RV
TE229	GTAGAAGGAGAGTGAAACCCATGGATGAAAAACGATTAAAAATTTTAG	*lmo1962* in pIMK3 RV
TE230	CAAAGCATAATGGGATCGTCGACTCACTCGCCCAAATCCTTTTTTTC	*lmo1962* in pIMK3 RV
TE237	CTTAATTCCAACAGTAATTAAACAAACTAGCCGCGGTG	*clpP2* E9K mutation in pSW54 FW
TE238	CACCGCGGCTAGTTTGTTTAATTACTGTTGGAATTAAG	*clpP2* E9K mutation in pSW54 RV
TE239	GGAGATATACATATGACTAGTATGGATGAAAAACGATTAAAAATTTT	*lmo1962* in pET11a
TE240	TTTCGAACTGCGGGTGGCTCCACTCGCCCAAATCCTTTTTTTC	*lmo1962* in pET11a
TE241	GATCGAGATCTCGATCCCGCG	control of pET11a insertions
TE257	GTTGGTGCGATTGTTGGGATG	control PCR for *lmo2468* (*clpP2*) deletion

TE271	GCATCAATAACTTGATAGAACGCATTAC	control PCR for *lmo2468* (*clpP2*) deletion
TE277	CTCTAGAACTAGTGGATCCCCCGGGGCTGAAGGCTCTAACGTAGTAATCG	$P_{lmo0193}$ in pBP117 FW
TE278	CGTTGTAAAACGACGGGGAATTCCATGAATGTTCTCCTTCTGCTCC	$P_{lmo0193}$ in pBP117 RV
TE366	GGCGATATCGGATCCATATGACGTCGACCCGTGAAAATATTATCCTTCCTC	*lmo2115* (*anrB*) deletion US FW
TE367	GATCTATCGATGCATGCCATGGTACCCGGGGCAGGTGTTTTCTCGCTTCTTGG	*lmo2115* (*anrB*) deletion DS RV
TE368	ATGACGTTATTTGACCTGCAGTAATAAAAAGAAGCCCTCTAACC	*lmo2115* (*anrB*) deletion DS FW
TE369	GCTTCTTTTTATTACTGCAGGTCAAATAACGTCATCTGAGTCGCCC	*lmo2115* (*anrB*) deletion US RV
TE370	GTCCACTTTCCGACGTGAC	control PCR for *lmo2115* deletion
TE371	CAAGCAAAAGAAATACAAGC	control PCR for *lmo2115* deletion
TE375	GATCTATCGATGCATGCCATGGTACCCGGGCCGACGAATGGCCTTGATCCG	strep-tagging of Ct of Lmo1964 (TimA) US FW
TE376	GGCGATATCGGATCCATATGACGTCGACCGATGCTAAAAAAGTAATCACC	strep-tagging of Ct of Lmo1964 (TimA) DS RV
TE379	TGGAGCCACCCGCAGTTCGAAAAATACGAAGGGGGAGAAATCAAG	strep-tagging of Ct of Lmo1964 (TimA) DS FW
TE380	TTTTTCGAACTGCGGGTGGCTCCATAATGTCATAAATTTATCTTCCAGCTC	strep-tagging of Ct of Lmo1964 (TimA) US RV
TE383	TGGAGCCACCCGCAGTTCGAAAAATATAAGAAAAAGGATTTGAAAGTATAATGG	strep-tagging of Ct of Lmo1963 (TimB) US FW
TE384	TTTTTCGAACTGCGGGTGGCTCCAAAGAACAAATGTCATAGCAAC	strep-tagging of Ct of Lmo1963 (TimB) DS RV
TE387	GGCGATATCGGATCCATATGACGTCGACTGCACGCACAAATGGAAAAAG	*lmo1268* (*clpX*) deletion US FW
TE388	GATCTATCGATGCATGCCATGGTACCCGGGGGATCGCCTTCTGCATCAGTGG	*lmo1268* (*clpX*) deletion DS RV
TE389	GAAATATTTTGCTGCAGTGATTAGAATGCGCGTCGTAATTG	*lmo1268* (*clpX*) deletion DS FW
TE390	CATTCTAATCACTGCAGCAAAATATTTCACCCCTTCGC	*lmo1268* (*clpX*) deletion US RV
TE391	GGCGATATCGGATCCATATGACGTCGACCCAAGAAATTGGGAGCTTCTGG	*lmo0997* (*clpE*) deletion DS RV
TE392	GATCTATCGATGCATGCCATGGTACCCGGGCTACTTATCGTTGCCATCATC	*lmo0997* (*clpE*) deletion US FW
TE393	CCTTTTTATTACTGCAGCATATATAATTTCCTCCTTTTAAAAATGAG	*lmo0997* (*clpE*) deletion US RV
TE394	AATTATATATGCTGCAGTAATAAAAAGGGCTTGAGTTAAC	*lmo0997* (*clpE*) deletion DS FW
TE397	GTTATTTGACCTGCAGTAATAAAAAGAAGCCCTCTAACC	*lmo2115* (*anrB*) deletion DS FW
TE398	TATTACTGCAGGTCAAATAACGTCATCTGAGTCGCCC	*lmo2115* (*anrB*) deletion US RV
TE400	CTAGAACATTCTGTAGAAGCTG	control of *lmo0997* (*clpE*) deletion
TE401	GATATGCTAAAACGTCAGAAAGC	control of *lmo0997* (*clpE*) deletion
TE402	CAAGCACAAGGTCTAACTCCTG	control of *lmo1268* (*clpX*) deletion
TE403	CTCCTAAAACAAAAAGTTCTCC	control of *lmo1268* (*clpX*) deletion

TE410	CAAGCTTGCATGCCTGCAGGTCGACCTGGGGAAGC CTAACTGGTGGC	*lmo0964* (*yjbH*) deletion DS RV
TE411	GCCAGTGAATTCGAGCTCGGTACCGAATCAATCAT GAAGACTTACAAG	*lmo0964* (*yjbH*) deletion US FW
TE412	GTGCTTCTTTTTTACTGCAGCATTTGCTATCACCTG ATTTTC	*lmo0964* (*yjbH*) deletion US RV
TE413	GCAAATGCTGCAGTAAAAAAGAAGCACCCATTCCT GG	*lmo0964* (*yjbH*) deletion DS FW
TE414	GTGATATAGCAATGCGAATG	control of *lmo0964* (*yjbH*) deletion
TE415	CGGTTGGACCTGTTCGTGAC	control of *lmo0964* (*yjbH*) deletion
TE416	CAAGCTTGCATGCCTGCAGGTCGACGACTTGTATCC AGAGCGGACCTTC	*lmo2191* (*spxA1*) deletion DS RV
TE417	GCCAGTGAATTCGAGCTCGGTACCGTAAAACATAT GATCCGACGTCTC	*lmo2191* (*spxA1*) deletion US FW
TE418	CAATCTTACTGCAGCATTAGACATTCACACTCCTTA TC	*lmo2191* (*spxA1*) deletion US RV
TE419	GTGTGAATGTCTAATGCTGCAGTAAGATTGATAAA AGTGGTTGCC	*lmo2191* (*spxA1*) deletion DS FW
TE420	CTTTGCCAGATCCAAATTATG	control of *lmo2191* (*spxA1*) deletion
TE421	CCAATTGTAGCTTTTGTTACG	control of *lmo2191* (*spxA1*) deletion
TE438	GTAGAAGGAGAGTGAAACCCATGGTATTTAAATTT AACGACGAAAAAGGCC	*lmo1268* (*clpX*) into pIMK3
TE439	CAAAGCATAATGGGATCGTCGACTCATGCAGATGT TTTAATTGGAAT	*lmo1268* (*clpX*) into pIMK3
TE452	GGAGAGTGAAACCCATGGTAACGTTATACACTTCA CC	*lmo2191* (*spxA1*) into pIMK3
TE453	GCTTTGGTCGACTTAGTTAACCATTTTTTGCGCTTC	*lmo1268* (*spxA1*) into pIMK3

2.2 Plasmids

In Table 2-2, the plasmids used in this work are listed. All plasmids were isolated from *E. coli* TOP10, and an aliquot of the *E. coli* strain was stored in 25% (v/v) glycerol at -70°C to -80°C.

Table 2-2: List of plasmids used in this study.

name	genotype	construction
pBP117	*lacZ neo*	(Hauf *et al.*, 2019)
pET11a	*bla* P_{T7} *lacI*	Novagen
pIMK3	P_{help}-*lacO lacI neo*	(Monk *et al.*, 2008)
pMAD	*bla erm bgaB*	(Arnaud *et al.*, 2004)
pMinimad	ori^{BsTs} *amp mls*	(Patrick & Kearns, 2008)
pJR127	*bla erm bgaB* Δ*clpC*	Dr. Jeanine Rismondo
pSaH14	$P_{lmo1409}$-*lacZ neo*	Dr. Samuel Hauf
pSaH91	*bla amyE* 3' *spc* P_{xyl}-*lieAB amyE* 5'	Dr. Samuel Hauf
pSH535	*bla* P*T7 lacI lftR-strep* G27S	PD Dr. Sven Halbedel
pSH536	*bla* P*T7 lacI lftR-strep* T46M	PD Dr. Sven Halbedel

pSW54	*bla PT7 lacI clpP2*	Dr. Sabrina Wamp
pPR5	P_{help}-*lacO lacI neo clpP2*	Patricia Rothe
pPR8	*bla erm bgaB* Δ*clpP2*	Patricia Rothe
pTE6	$P_{lmo0925}$-*lacZ neo*	RF cloning of *lmo0925* promoter (TE49, TE50) into pSaH14 linearized with EcoRI
pTE7	$P_{lmo1635}$-*lacZ neo*	RF cloning of *lmo1635* upstream (TE51, TE52) into pSaH14 cut EcoRI
pTE8	$P_{lmo2214}$-*lacZ neo*	RF cloning of *lmo2214* upstream (TE53, TE54) into pSaH14 cut EcoRI
pTE9	*bla erm bgaB* Δ*lmo0744*	*lmo0744* upstream (TE20, TE23) and downstream (TE21, TE22) into pMAD cut EcoRI by RF cloning
pTE10	$P_{lmo0744}$-*lacZ neo*	RF cloning of *lmo0741* upstream (TE47, TE48) into pSaH14 cut EcoRI
pTE12	$P_{lmo0107}$-*lacZ neo*	RF cloning of *lmo0107* upstream (TE68, TE69) into pPB117 cut EcoRI
pTE14	$P_{lmo0984}$-*lacZ neo*	RF cloning of *lmo0984* upstream (TE66, TE67) into pPB117 cut EcoRI
pTE15	$P_{lmo1652}$-*lacZ neo*	RF cloning of *lmo1652* upstream (TE70, TE71) into pPB117 cut EcoRI
pTE16	$P_{lmo1962}$-*lacZ neo*	RF cloning of *lmo1962* upstream (TE74, TE75) into pPB117 cut EcoRI
pTE17	$P_{lmo2226}$-*lacZ neo*	RF cloning of *lmo2228* upstream (TE76, TE77) into pPB117 cut EcoRI
pTE19	$P_{lmo2241}$-*lacZ neo*	RF cloning of *lmo2241* upstream (TE78, TE79) into pPB117 cut EcoRI
pTE23	$P_{lmo0606}$-*lacZ neo*	RF cloning of *lmo0606* upstream (TE45, TE46) into pPB117 cut EcoRI
pTE24	$P_{lmo2751}$-*lacZ neo*	RF cloning of *lmo2751* upstream (TE86, TE87) into pPB117 cut EcoRI
pTE26	$P_{lmo2371}$-*lacZ neo*	RF cloning of *lmo2371* upstream (TE80, TE81) into pPB117 cut EcoRI
pTE30	*bla erm bgaB* Δ*lmo0194/lmo0195*	*lmo0194-lmo0195* upstream (TE104, TE107) and downstream (TE105, TE106) into pMAD cut EcoRI by RF cloning
pTE32	$P_{lmo2745}$-*lacZ neo*	RF cloning of *lmo2745* upstream (TE82, TE83) into pPB117 cut EcoRI
pTE36	$P_{lmo2768}$-*lacZ neo*	RF cloning of *lmo2768* upstream (TE88, TE89) into pPB117 cut EcoRI
pTE39	$P_{lmo0667}$-*lacZ neo*	RF cloning of *lmo2768* upstream (TE124, TE125) into pPB117 cut EcoRI
pTE42	*bla erm bgaB* Δ*lmo1963/lmo1964*	*lmo1963-lmo1964* upstream (TE135, TE136) and downstream (TE134, TE137) into pMAD cut EcoRI by RF cloning
pTE50	*bla erm bgaB* Δ*lmo2371/lmo2372*	*lmo2371-lmo2372* upstream (TE146, TE149) and downstream (TE147, TE148) into pMAD cut EcoRI by RF cloning
pTE52	*bla erm bgaB* Δ*lmo1962*	*lmo1962* upstream (TE213, TE214) and downstream (TE212, TE215) into pMAD cut EcoRI by RF cloning
pTE58	*bla amyE* 3' *spc* P_{xyl}-*timAB amyE* 5'	*lmo1963/lmo1964* (TE218/TE219) into pSaH91 by RF cloning
pTE61	P_{help}-*lacO lacI neo lmo1962*	product of TE229/TE230 cut NcoI, SalI ligated into pIMK3 cut NcoI, SalI
pTE62	P_{help}-*lacO lacI neo lmo1963/lmo1964*	product of TE227/TE228 cut NcoI, SalI ligated into pIMK3 cut NcoI, SalI
pTE64	*bla* P_{T7} *lacI clpP2-strep* E9K	inverse PCR with TE237/TE238 on pSW54
pTE71	*bla* P_{T7} *lacI timR*-strep	product of TE239/TE240 into pTE64 by RF cloning

pTE75	$P_{lmo0193}$-*lacZ neo*	RF cloning of *lmo0193* upstream (TE277/TE278) into pPB117 cut EcoRI
pTE87	ori^{BsTs} *amp mls* Δ*clpP2*	ligation of pPR8 insert cut KpnI, BamHI into pMinimad cut KpnI, BamHI
pTE91	*bla erm bgaB lmo2115*	*lmo2215* +450 bp up- and downstream (TE366-TE367) into pMAD by RF cloning
pTE98	*bla erm bgaB lmo1963-strep*	450 bp upstream (TE213/TE384) and downstream (TE383/TE134) of *lmo1963*-C-terminus into pMAD by RF cloning
pTE99	*bla erm bgaB* Δ*clpE*	*lmo0997* upstream (TE392/TE393) and downstream (TE391/TE394) into pMAD cut EcoRI by RF cloning
pTE100	*bla erm bgaB* Δ*anrB*	inverse PCR with TE397/TE398 on pTE91
pTE101	ori^{BsTs} *amp mls* Δ*clpX*	ligation of pTE97 insert cut KpnI, SalI into pMinimad cut KpnI, SalI
pTE102	ori^{BsTs} *amp mls lmo1964-lmo1963-strep*	ligation of insert in pTE98 cut KpnI, SalI into pMinimad cut KpnI, SalI
pTE103	ori^{BsTs} *amp mls* Δ*clpE*	ligation of pTE99 insert cut KpnI, SalI into pMinimad cut KpnI, SalI
pTE104	ori^{BsTs} *amp mls* Δ*anrB*	ligation of pTE100 insert cut KpnI, SalI into pMinimad cut KpnI, SalI
pTE105	ori^{BsTs} *amp mls lmo1964-strep-lmo1963*	ligation of 450 bp upstream (TE375/TE380) and downstream (TE376/TE379) into pMinimad
pTE107	P_{help}-*lacO lacI neo lmo1964-strep-lmo1963*	ligation of PCR product of TE227/TE228 on LMTE98 cut NcoI, SalI into pTE61 backbone cut NcoI, SalI
pTE108	P_{help}-*lacO lacI neo clpX*	ligation of PCR product of TE438/TE439 cut NcoI, SalI into pTE61 backbone cut NcoI, SalI
pTE111	*bla erm::secY* antisense Δ*clpX*	ligation of pTE97 insert cut KpnI, SalI into pHoss1 cut KpnI, SalI
pTE112	P_{help}-*lacO lacI neo lmo1964-lmo1963-strep*	ligation of PCR product of TE227/TE228 on LMTE99 cut NcoI, SalI into pTE61 cut NcoI, SalI
pTE115	P_{help}-*lacO lacI neo spxA1*	ligation of PCR product of TE452/TE453 cut NcoI, SalI into pTE61 cut NcoI, SalI
pTE116	*bla erm bgaB* Δ*yjbH*	*lmo0964* upstream (TE411/TE412) and downstream (TE410/TE413) cut EcoRI, SalI ligated into pMAD cut EcoRI, SalI
pTE117	*bla erm bgaB* Δ*spxA1*	*lmo2191* upstream (TE417/TE418) and downstream (TE416/TE419) cut EcoRI SalI into pMAD cut EcoRI, SalI
pTE118	ori^{BsTs} *amp mls* Δ*spxA1*	ligation of pTE117 insert cut NcoI, SalI into pTE87 backbone cut NcoI, SalI

2.3 Bacterial strains

All bacterial strains used in this study are summarized in Table 2-3. Strains were stored in 25% (v/v) glycerol at -70°C to -80°C.

Table 2-3: Table of bacterial strains used in this work.

name	genotype	construction
***Bacillus subtilis* strains**		
168	wild type	
BSTE1	*amyE* 3' *spc* P_{xyl}-*timAB amyE* 5'	pTE58 → *B. subtilis* 168
***Listeria monocytogenes* strains**		
EGD-e	wild type, serovar 1/2a	
BPL18	Δ*ktrD*	Dr. Johannes Gibhardt
BPL87	Δ*kdpABCDE*	Mengyi Wang
BPL88	Δ*kimA*	Mengyi Wang
BPL89	Δ*pgpH* Δ*pdeA*	(Wang *et al.*, 2022)
LMJR45	Δ*cdaR*	(Rismondo *et al.*, 2016)
LMJR46	Δ*cdaA attB*::P_{help}-*lacO-cdaA lacI neo*	(Rismondo *et al.*, 2016)
LMJR138	Δ*clpC*	(Rismondo *et al.*, 2017)
LMSH5	*attB*::P_{lieAB}-*lacZ neo*	(Hauf *et al.*, 2019)
LMSH16	*attB*::*lacZ neo*	(Hauf *et al.*, 2019)
LMSH30	*attB*::$P_{lieAB(1-193)}$-*lacZ neo*	(Hauf *et al.*, 2021)
LMSH31	*attB*::$P_{lieAB(1-152)}$-*lacZ neo*	(Hauf *et al.*, 2021)
LMSH32	*attB*::$P_{lieAB(1-122)}$-*lacZ neo*	(Hauf *et al.*, 2021)
LMSH33	*attB*::$P_{lieAB(1-97)}$-*lacZ neo*	(Hauf *et al.*, 2021)
LMSH44	*attB*::$P_{lieAB(1-122)\ transversion\ 69-61}$-*lacZ neo*	(Hauf *et al.*, 2021)
LMSH45	*attB*::$P_{lieAB(1-122)\ transversion\ 60-51}$-*lacZ neo*	(Hauf *et al.*, 2021)
LMSH46	*attB*::$P_{lieAB(1-122)\ transversion\ 50-41}$-*lacZ neo*	(Hauf *et al.*, 2021)
LMSH47	*attB*::$P_{lieAB(1-122)\ transversion\ 40-31}$-*lacZ neo*	(Hauf *et al.*, 2021)
LMSH48	*attB*::$P_{lieAB(1-122)\ transversion\ 30-21}$-*lacZ neo*	(Hauf *et al.*, 2021)
LMSH98	Δ*lftR attB*::$P_{lieAB(1-122)}$-*lacZ neo*	(Hauf *et al.*, 2021)
LMS250	Δ*hly*	(Fischer *et al.*, 2022)
LMTE3	*attB*::$P_{lmo0741}$-*lacZ neo*	pTE10 → EGD-e
LMTE4	*attB*::$P_{lmo0923}$-*lacZ neo*	pTE6 → EGD-e
LMTE5	*attB*::$P_{lmo1635}$-*lacZ neo*	pTE7 → EGD-e
LMTE6	*attB*::$P_{lmo2215}$-*lacZ neo*	pTE8 → EGD-e
LMTE8	Δ*lmo0744*	pTE9 ↔ EGD-e
LMTE10	*attB*::$P_{lmo2241}$-*lacZ neo*	pTE19 → EGD-e
LMTE11	*attB*::$P_{lmo0984}$-*lacZ neo*	pTE14 → EGD-e
LMTE12	*attB*::$P_{lmo2228}$-*lacZ neo*	pTE17 → EGD-e
LMTE13	*attB*::$P_{lmo0194}$-*lacZ neo*	pTE13 → EGD-e
LMTE14	*attB*::$P_{lmo1652}$-*lacZ neo*	pTE15 → EGD-e
LMTE15	*attB*::$P_{lmo0108}$-*lacZ neo*	pTE12 → EGD-e
LMTE16	*attB*::$P_{lmo2751}$-*lacZ neo*	pTE24 → EGD-e
LMTE18	*attB*::$P_{lmo2371}$-*lacZ neo*	pTE26 → EGD-e
LMTE19	*attB*::P_{timA}-*lacZ neo*	pTE16 → EGD-e
LMTE24	*attB*::$P_{lmo2768}$-*lacZ neo*	pTE36 → EGD-e
LMTE26	*attB*::$P_{lmo2745}$-*lacZ neo*	pTE32 → EGD-e
LMTE27	*attB*::$P_{lmo0606}$-*lacZ neo*	pTE23 → EGD-e
LMTE28	*attB*::$P_{lmo0667}$-*lacZ neo*	pTE39 → EGD-e
LMTE30	Δ*lmo0194/lmo0195*	pTE30 ↔ EGD-e
LMTE33	*attB*::$P_{lmo1723}$ *lmo1725-lacZ neo*	pTE37 → EGD-e
LMTE34	Δ*timAB*	pTE42 ↔ EGD-e
LMTE37	Δ*timR*	pTE52 ↔ EGD-e

LMTE38	*attB*::P_{timA}-*lacZ neo clpP2* E9K	tartrolon resistant suppressor
LMTE39	*attB*::P_{timA}-*lacZ neo clpP2* E9K	tartrolon resistant suppressor
LMTE40	*attB*::P_{timA}-*lacZ neo clpP2* E9K	tartrolon resistant suppressor
LMTE42	*attB*::P_{timA}-*lacZ neo clpP2* E9K	tartrolon resistant suppressor
LMTE43	*attB*::P_{timA}-*lacZ neo clpP2* E9K	tartrolon resistant suppressor
LMTE44	*attB*::P_{timA}-*lacZ neo clpP2* E9K	tartrolon resistant suppressor
LMTE45	*attB*::P_{timA}-*lacZ neo clpP2* E9K	tartrolon resistant suppressor
LMTE46	*attB*::P_{timA}-*lacZ neo clpP2* E9K	tartrolon resistant suppressor
LMTE47	*attB*::P_{timA}-*lacZ neo clpP2* E9K	tartrolon resistant suppressor
LMTE48	*attB*::P_{timA}-*lacZ neo clpP2* E9K	tartrolon resistant suppressor
LMTE49	*attB*::P_{timA}-*lacZ neo clpP2* E9K	tartrolon resistant suppressor
LMTE50	Δ*timR attB*::P_{timA}-*lacZ neo*	pTE16 → LMTE37
LMTE51	Δ*timAB attB::*P_{help}-*lacO-timAB lacI neo*	pTE62 → LMTE34
LMTE52	Δ*timR attB::*P_{help}-*lacO-timR lacI neo*	pTE61 → LMTE37
LMTE65	*timR* K202fs	tartrolon resistant suppressor
LMTE66	*yjbH* D143fs	tartrolon resistant suppressor
LMTE69	Δ*lmo2371/lmo2372*	pTE50 ↔ EGD-e
LMTE71	*attB*::$P_{lmo0193}$-*lacZ neo*	pTE75 → EGD-e
LMTE72	*attB*::P_{clpP2}-*lacZ neo*	pTE80 → EGD-e
LMTE74	*clpP2* T90I	tartrolon resistant suppressor
LMTE75	*clpP2* T90I	tartrolon resistant suppressor
LMTE76	*clpP2* T90I	tartrolon resistant suppressor
LMTE77	*clpP2* T90I	tartrolon resistant suppressor
LMTE78	*clpP2* T90I	tartrolon resistant suppressor
LMTE80	Δ*clpP2*	pTE87 ↔ EGD-e
LMTE89	*attB::*P_{help}-*lacO-timAB lacI neo*	pTE61 → EGD-e
LMTE90	Δ*clpP2 attB::*P_{help}-*lacO-clpP2 lacI neo*	pTE87 ↔ LMPR7
LMTE91	P_{timA}G14→T	tartrolon resistant suppressor
LMTE94	Δ*timR attB::*P_{help}-*lacO-timAB lacI neo*	pTE61 ↔ LMTE37
LMTE95	Δ*timAB*Δ*clpP2*	pTE87 ↔ LMTE34
LMTE100	Δ*clpE*	pTE103 ↔ EGD-e
LMTE101	Δ*lmo0744* Δ*lmo0194/0195*	pTE9 ↔ LMTE30
LMTE102	Δ*clpE* Δ*clpC*	pJR127 ↔ LMTE100
LMTE103	Δ*lmo0744* Δ*lmo2371/lmo2372*	pTE50 ↔ LMTE8
LMTE104	Δ*lmo0744* Δ*lmo0194/lmo0195* Δ*lmo2371/lmo2372*	pTE50 ↔ LMTE101
LMTE106	Δ*timAB attB*::P_{help}-*lacO-timA-strep-timB*	pTE107 → LMTE34
LMTE110	Δ*clpP2* Δ*timAB attB*::P_{help}-*lacO-timA-strep-timB*	pTE87 ↔ LMTE106
LMTE112	Δ*clpE* Δ*clpX*	pTE111 ↔ LMTE100
LMTE113	Δ*clpX*	pTE111 ↔ EGD-e
LMTE114	Δ*clpC* Δ*clpX*	pJR127 ↔ LMTE113
LMTE115	Δ*clpC* Δ*clpE* Δ*clpX*	pTE111 ↔ LMTE102
LMTE116	Δ*timAB attB*::P_{help}-*lacO-spxA1 lacI neo*	pTE115 → LMTE34
LMTE117	*attB*::P_{help}-*lacO-spxA1 lacI neo*	pTE115 ↔ EGD-e
LMTE118	Δ*timR attB*::P_{help}-*lacO-spxA1 lacI neo*	pTE115 → LMTE37
LMTE119	Δ*clpP2 attB*::P_{timA}-*lacZ neo*	pTE87 ↔ LMTE19
LMTE120	Δ*yjbH*	pTE116 ↔ EGD-e
LMTE121	Δ*clpC attB*::P_{help}-*lacO-spxA1 lacI neo*	pTE115 → LMJR138
LMTE122	Δ*clpX attB*::P_{help}-*lacO-spxA1 lacI neo*	pTE115 → LMTE113
LMTE139	Δ*spxA1 attB::*P_{help}-*lacO-spxA1 lacI neo*	pTE118 ↔ LMTE117
LMTE140	Δ*clpC* Δ*yjbH*	pJR127 ↔ LMTE120

Arrows (→) indicate the integration of the respective plasmid into the $tRNA^{Arg}$ locus of *L. monocytogenes*, or the *amyE* locus of *B. subtilis*, whereas double arrows (↔) indicate gene deletions obtained by chromosomal insertion and subsequent excision of plasmid derivatives.

2.4 Cultivation conditions

2.4.1 Cultivation media

Cultivation of bacterial strains was done in Luria Bertani (LB) or brain heart infusion (BHI) broth. Each medium was autoclaved prior to usage (121°C, 2 bar, 20 min). Additional components were added immediately before usage. Components, that were solved in ddH_2O were additionally sterilized by filtering the suspension through an MiniSart® syringe filter (Sartorius, pore size 0.2-0.45 µm). Final concentrations of these components are summarized in Table 2-4. Tartrolon A and tartrolon B were obtained from the German Centre of Infection Research (DZIF) and dissolved in DMSO to a 25 mg/ml stock solution. Boromycin was purchased from Hello Bio Ltd. (Ireland) and dissolved to 10 mg/ml in DMSO.

LB broth	10 g tryptone
	5 g yeast extract
	10 g NaCl
	ad. 1 l ddH_2O
LB agar	10 g agar
	ad. 1 l LB broth
BHI broth	37 g brain heart infusion broth
	ad. 1 l ddH_2O
BHI agar	10 g agar
	ad. 1 l ddH_2O

2.4.2 Cultivation of *E. coli*, *B. subtilis* and *L. monocytogenes*

E. coli and *B. subtilis* strains were grown in LB broth, while for growth of *L. monocytogenes* strains BHI medium was used. Additional components were added according to Table 2-4 where necessary. All strains were incubated over night at 37°C, 250 rpm, before being tested

in the respective experimental conditions. Strains were stored in 25% (v/v) glycerol at -70°C to -80°C.

Table 2-4: Concentrations of additional compounds used in different organisms.

compound	stock solution	final concentration		
		E. coli	***L. monocytogenes***	***B. subtilis***
Ampicillin	100 mg/ml in ddH_2O	100 µg/ml	-	-
Kanamycin	50 mg/ml in ddH_2O	50 µg/ml	50 µg/ml	-
Erythromycin	5 mg/ml in EtOH	-	5 µg/ml	-
Spectinomycin	100 mg/ml in ddH_2O	-	-	100 µg/ml
X-Gal	50 mg/ml in DMSO	50 µg/ml	50 µg/ml	-
IPTG	1 M in ddH_2O	1 mM	1 mM	-
Xylose	25% in ddH_2O	-	-	5%

2.5 DNA based work

2.5.1 Preparation of plasmid DNA

Plasmid DNA was isolated from a 5 ml *E. coli* TOP10 culture that was grown in selective medium. 4 ml of this culture was centrifuged (11000 x g, 1 min) and the plasmids purified using the QIAprep Spin Miniprep Kit (QIAGEN) according to the manufacturer´s guidelines. For the final elution step, 50-100 µl ddH_2O were used. Plasmid DNA was stored at -20°C. When applicable, 500 µl of the remaining overnight culture was used to create a glycerol culture (final glycerol concentration: 25% (v/v) and stored at -70°C to -80°C.

2.5.2 Isolation of genomic DNA

For isolation of genomic DNA as a PCR template, 2 ml of an overnight culture was centrifuged and the pellet resuspended in 500 µl ddH_2O. Around 200 mg glass beads (1 mm diameter) were added and the cells lysed using the TissueLyser II (QIAGEN) (30 Hz, 5 min). After lysis, the suspension was centrifuged (11000 x g, 1 min). 100 µl of the supernatant was taken into a new tube and immediately used as a PCR template. The isolated DNA was stored at -20°C until further usage.

2.5.3 Polymerase chain reaction (PCR)

2.5.3.1 PCR for molecular cloning

Amplification of DNA fragments needed for molecular cloning was done using the Phusion®-High Fidelity DNA Polymerase (New England Biolabs (NEB) GmbH) in 1x HF buffer (NEB). The reaction volume varied between 20 µl and 100 µl. Each PCR contained a set concentration of a premade deoxynucleotide triphosphate mix (10 mM each; Thermo Fisher Scientific) and respective primer pairs ordered from Integrated DNA Technologies (IDT). Primers were solved in ddH_2O to a concentration of 100 µM. The reaction mixture for a 100 µl PCR as well as typical PCR conditions used are summarized in Table 2-5. Annealing temperatures were estimated using the online tool OligoCalc (Kibbe, 2007).

Table 2-5: Composition and conditions of PCR reactions.

compound	volume (100 µl)	step	temperature	duration
ddH_2O	77 µl	denaturation	95°C	5 min
5x HF buffer	20 µl			
dNTPs (40 mM)	1 µl	30 cycles of:		
template DNA	1 µl	denaturation	95°C	30 s
primer (100 mM)	0.5 µl	annealing	45-60°C	30 s
Phusion® HF polymerase	0.5 µl	elongation	60-72°C	1 min / kb
		elongation	60-72°C	5 min
		storage	8-16°C	∞

2.5.3.2 Restriction free (RF) cloning

RF cloning was used as an alternative to classical cloning methods. For this, overlaps of 20-30 nucleotides (nt) that are complementary to the insertion site on the plasmid were added to the primers at its 5´-ends. The amplified fragment containing these complementary overlaps was used together with the plasmid in a PCR without primers to obtain the desired construct. For this PCR, the Phusion High-Fidelity PCR Master Mix (2x concentration) (NEB) was used. If possible, the plasmid was linearized prior to RF cloning by digestion with a single-cutting enzyme cutting between the two complementary regions. Composition of the reaction and PCR

conditions are listed in Table 2-6. If uncut plasmid was used, the reaction was incubated with 1 µl DpnI (NEB) afterwards (37°C, 2 h). Afterwards, chemical competent *E. coli* TOP10 cells were transformed with the reaction mix.

Table 2-6: Composition and reaction conditions of PCRs for restriction free cloning and quikchange PCRs.

compound	RF cloning	quikchange PCR	step	temper-ature	duration
ddH_2O	-	7 µl	denaturation	95°C	15 min
plasmid	2 µl	2 µl			
insert	8 µl	-	30 cycles of:		
primer (100 µM)	-	0.5 µl each	denaturation	95°C	5 min
Phusion® HF PCR Master Mix (2x conc.)	10 µl	10 µl	annealing	45-60°C	30 s
			elongation	72°C	14-17 min
			elongation	60-72°C	15 min
			storage	8-16°C	∞

2.5.3.3 Colony PCR

The presence of a specific plasmid or genomic modification was checked in *E. coli* or *L. monocytogenes* cells using colony PCR. A small amount of a single colony was picked into a PCR tube. While *E. coli* cells were untreated, *L. monocytogenes* cells were lysed by heat in a microwave for 2 min. Afterwards, a master mix was prepared depending on the number of clones to be analyzed. The reaction volume for each PCR was 20 µl. Each reaction consisted of the concentrations described for standard PCRs in Table 2-5.

2.5.4 Agarose gel electrophoresis

For agarose gel electrophoresis, agarose was solved in 1x TAE buffer to obtain 1% (w/v) agarose gels. As loading buffers, Purple Loading Dye (6x, NEB) or TriTrack (6x, Thermo Fisher Scientific) were used. Gels were run in 1x TAE buffer at 120-150 V for 20-60 min in a PowerPac™ Basic (BioRad) or a PerfectBlue® (VWR) gel chamber. The agarose gel was stained for >10 min in an ethidium bromide solution and visualized on a Molecular Imager® Gel Doc™ XR+ (BioRad) using the Image Lab 6.0 software (BioRad).

TAE buffer (50x)	0.5 M EDTA, pH 8.0 57.1 ml acetic acid 242 g Tris ad. 1 l ddH_2O
Ethidium bromide solution	3 drops 1% ethidium bromide ad. 300 ml 1x TAE

2.5.5 Extraction of DNA fragments from agarose gels

After preparative DNA digestions or fusion of DNA fragments by PCR, fragments were separated on an agarose gel, stained with ethidium bromide and fragments of interest were cut out. Fragment purification was done using the Macherey-Nagel™ NucleoSpin™ Gel and PCR Clean-up Kit according to manufacturer´s instructions. Elution was done in 25 µl ddH_2O. DNA was stored at -20°C until further usage

2.5.6 Restriction digest

Digestion of plasmids was done analytically to confirm the correct integration of fragments into plasmids (10 µl reaction volume) and on a preparative scale for cloning of new constructs (50 µl reaction volume). The enzymes and buffer (10x CutSmart) used were all ordered from New England Biolabs. The reaction was incubated stationary at the enzyme specific temperature for 2-5 h and then analyzed by agarose gel electrophoresis. The composition of each reaction is summarized in Table 2-7.

Table 2-7: Compositions of restriction digests.

	analytical digestion (10 µl)	**preparative digestion (50 µl)**
plasmid	8 µl	43 µl
enzyme 1	0.5 µl	1 µl
enzyme 2	0.5 µl	1 µl
10x CutSmart buffer	1 µl	5 µl

2.5.7 Ligation

Ligation reactions were performed by creating sticky ends at both sides of an insert and a plasmid. After digestion, DNA fragments were purified using the Macherey-Nagel™ NucleoSpin™ Gel and PCR Clean-up Kit according to manufacturer's instructions. Ligation of DNA fragments was done using 2 µl plasmid DNA and 8 µl of the insert independently of DNA yields. 1.2 µl 10x T4 DNA Ligase Reaction buffer and 0.8 µl T4 DNA Ligase (NEB) were added. The reaction was put to room temperature for 1-2 h and afterwards overnight to 6°C. After 1-3 h at room temperature on the next day, *E. coli* TOP10 cells were transformed with the entire ligation mix.

2.5.8 Determination of DNA concentration

DNA concentrations were determined on a NanoPhotometer® (IMPLEN), where an absorption spectrum from λ=200 nm to λ=400 nm was measured using ddH_2O as reference and the value of the DNA concentration was taken directly from the photometer. The spectrum was also used to check for possible protein or salt impurities by calculating the A_{260}/A_{230} and A_{260}/A_{280} values of the DNA solution. The DNA solution was considered free of any contaminants, if the A_{260}/A_{230} value was above 2.0 and the A_{260}/A_{280} value was above 1.8.

2.5.9 DNA precipitation

40 µl of a plasmid, which needed to be transformed into *L. monocytogenes* was mixed with 4 µl 3 M sodium acetate, pH 7.0 and 100 µl 100% ethanol. The mixture was put to -20°C for at least 2 h, before being centrifuged at 6°C and 15000 x g for 10 min. The supernatant was discarded, 700 µl 70% Ethanol added and the tube centrifuged again (6°C, 15000 x g, 10 min). After discarding the supernatant, the pellet was air-dried at room temperature.

2.5.10 DNA sequencing

For DNA sequencing, the chain termination method established by Sanger (Sanger *et al.*, 1977) was used. The reaction was performed using the ABI BigDye Terminator 3.1 Premix (Thermo Scientific). The composition for each reaction and the PCR program is summarized in Table 2-8. Results of the sequencing reaction were processed in-house by the department MF1. The final evaluation was done using Clone Manager Professional 9 (Sci-Ed-Software).

Table 2-8: Composition and conditions of Sanger sequencing reactions.

compound	volume	step	temperature	duration
ddH_2O	4 µl	denaturation	96°C	2 min
template (plasmid or PCR product)	3 µl (concentration >50 ng/µl)			
ABI buffer (5x)	2 µl	25 cycles of:		
primer (100 mM)	0.5 µl	denaturation	96°C	10 s
BigDye 3.1	0.5 µl	annealing	52°C	5 s
		extension	60°C	4 min
		storage	4°C	∞

2.5.11 Genome sequencing

Three single colonies of strains, whose genome needed to be sequenced were picked and dissolved in 120 µl buffer EB (QIAGEN). Around 40 mg of glass beads (0.1 mm diameter, Roth) were added and the suspension incubated at 95°C for 5 min. Cells were lysed using the TissueLyser II (QIAGEN) at 30 Hz for 5 min. After centrifugation (11000 x g, 5 min), 70 µl of the supernatant was transferred to a new tube, its DNA concentration measured according to chapter 2.5.8 and diluted to a final DNA concentration between 30 and 50 ng/µl. In-house sequencing reactions were performed by the MF1/MF2 department using the Illumina sequencing method. Data was evaluated using Geneious Prime, where *L. monocytogenes* EGD-e (NC_003210) was used as reference where applicable. The genome sequences of published strains were stored on the European nucleotide archive (ENA). The accession number of each strain will be published upon publication.

2.5.12 Transformation of competent cells

2.5.12.1 Transformation of *E. coli*

For cloning purposes, *E. coli* TOP10 cells were transformed with PCR products or ligation reactions. *E. coli* BL21 cells were transformed for gene-overexpression followed by protein purification steps. For these transformations, an overnight culture of the respective *E. coli* strain was diluted 1:100 in 25-50 ml LB broth and shaken at 37°C and 250 rpm for 2-3 h until an OD_{600} of 0.3-0.4. Cells were centrifuged at 11000 x g, the pellet resuspended in 10-20 ml ice cold 0.1 M $CaCl_2$ and the cells incubated on ice for at least 30 min. After centrifugation (5 min, 5000 x g) in a Biofuge 28 RS (Heraeus Sepatech) or a 5810R centrifuge (Eppendorf), cells were resuspended in 1 ml 0.1 M $CaCl_2$ and 100 µl of the suspension was added to the DNA (1 µl for purified plasmids, 12-20 µl for ligation or PCR reactions). Cells were put on ice for at least another 30 min and heat shocked at 42°C for 1 min using a water bath. After 3 more min on ice, 200 µl LB medium was added and the cells incubated at 37°C for 1 h whilst shaking. The entire volume was plated onto selective LB agar plates and incubated over night at 37°C.

2.5.12.2 Transformation of *L. monocytogenes*

For transformation of *L. monocytogenes*, electrocompetent cells were generated (Monk *et al.*, 2008). For this, an overnight culture of the strain to be transformed was diluted 1:50 in 30 ml BHI broth and incubated at 37°C, 250 rpm for 3-4 h. Ampicillin was added at a final concentration of 10 µg/ml and the cells shaken for another 2 h. Cells were harvested by centrifugation (11000 x g, 5 min) and washed in 15 ml ice cold sucrose glycerol wash buffer (SGWB). This washing step was done three times in total, and the cells resuspended in 15 ml (second wash) and 5 ml (third wash) SGWB. 10 µg/ml lysozyme was added and the cells were incubated at 37°C at 250 rpm for 20 min. After centrifugation (11000 x g, 5 min), the cells were washed with 5 ml SGWB, centrifuged again and finally resuspended in 1 ml SGWB. 100 µl of

this cell suspension was used to resuspend the precipitated DNA. Afterwards, the mixture was put on ice for 5 min. The mixture was transferred to an electroporation cuvette (VWR, 2 mm). Electroporation was done using the Gene Pulser Xcell™ Elektroporator (Bio Rad) and the pre-set *A. tumefaciens* protocol (25 µF, 200 Ω and 2400 V). 1 ml BHI broth was added to the cells, followed by an incubation at 37°C for 1 h, if temperature insensitive plasmids were used or 30°C for 1.5 h for temperature sensitive constructs. Cells were centrifuged and resuspended in 200 µl BHI broth, plated on selective BHI agar plates and incubated at 37°C for 1-2 d or 30°C for 2-4 d.

SGWB buffer	10% (v/v) glycerin 500 mM sucrose pH 7.0

2.5.12.3 Transformation of *B. subtilis* 168

For heterologous expression of *timAB* in *Bacillus subtilis* 168, the *timAB* genes were brought under control of a xylose inducible promoter present in plasmid pSG1154. 600 µl of an overnight culture of *Bacillus subtilis* 168 was added to 10 ml MM competence medium and incubated with 250 rpm at 37°C for 3 h. 10 ml starvation medium, which was preheated to 37°C, was added and the culture shaken with 250 rpm for another 2 h at 37°C. 10 µl of purified plasmid DNA was mixed with 400 µl of the culture and shaken with 250 rpm for 45 min at 37°C. 200 µl of the mix was plated onto an LB plate containing 100 µg/ml spectinomycin. The plates were incubated for 1 d at 37°C. To confirm the integration of the plasmid into the *amyE* locus, clones were streaked out onto a new LB-spec plate containing 1% (w/v) starch, iodine crystals were added and clones, which had no halo - indicating loss of amylase activity - were picked for further analysis.

SMM (Spizizen minimal medium)	0.2% ammonium sulphate 1.4% di-potassium phosphate 0.6% potassium dihydrogen phosphate 0.1% sodium citrate dehydrate 0.02% magnesium sulphate
MM competence medium	0.5% (w/v) glucose 0.2 mg tryptophane 6.25 mM $MgSO_4$ 0.2% casamino acids 0.001% Fe-NH_4-citrate ad. 10 ml SMM medium
starvation medium	0.5 (w/v) glucose 6.25 mM $MgSO_4$ ad. 10 ml SMM medium

2.5.13 Genome modifications in *L. monocytogenes*

2.5.13.1 Modifications using pMAD

L. monocytogenes cells were transformed with the respective pMAD construct, which carried a fragment with fused genomic regions roughly 400 bp up- and downstream of the gene to be deleted. Clones were selected on BHI plates with X-Gal and erythromycin at 30°C for 3 d. Two blue-colored clones were streaked out onto a new BHI plate containing X-Gal and erythromycin and incubated at 42°C for 2 d to force the chromosomal integration of the plasmid. Two single, blue colonies were then used to inoculate 5 ml BHI broth and the culture was grown at 30°C and 250 rpm for 2 h and afterwards at 37°C or 42°C and 250 rpm for 4 h. The culture was diluted to 10^{-4} in a total volume of 1 ml BHI broth and 200 µl were plated on 5 BHI plates containing X-Gal. After incubation at 37°C for 1-2 d, white colonies were streaked out on two

separate BHI plates containing X-Gal, where one plate additionally contained erythromycin. White, erythromycin sensitive clones indicated the loss of pMAD. These clones were analyzed for double cross-over events, where the plasmid was lost together with the gene to be deleted by colony PCR. Colonies carrying the desired deletion were streaked out to single colonies on BHI agar plates containing X-Gal. Single colonies were used to inoculate an overnight culture, grown overnight at 37°C and then stored in a glycerol stock culture at -70°C to -80°C.

2.5.13.2 Modifications using pMinimad II

Whenever gene deletions with pMAD were not possible, pMinimad II was used. Here the protocol established by Patrick and Kearns (Patrick & Kearns, 2008) was followed. For obtaining pMinimad II with the fused up- and downstream regions of the gene to be deleted, the fragment was cut out of the respective pMAD construct and subcloned into pMinimad II using the restriction enzymes XmaI and SalI, where possible. Transformation of *L. monocytogenes* was identical to the procedure followed for pMAD plasmids. After streaking out of two single colonies on BHI plates containing erythromycin and incubation at 42°C for 1-2 d, three single colonies were picked and 5 ml BHI broth inoculated. The culture was grown stationary for 20-24 h at room temperature, before it was diluted 1:1000 into fresh 5 ml BHI broth. This dilution step was performed three times, before the culture was grown for 20-24 h at room temperature, diluted 10^{-4} in 1 ml BHI broth and 200 µl plated on 4 BHI plates and 1 BHI plate containing erythromycin plate to estimate the ratio of sensitive clones. Plates were incubated at room temperature for 2-3 d. Single clones were then streaked out on BHI plates with and without erythromycin and erythromycin sensitive clones analyzed for gene deletion and absence of the plasmid by PCR. Positive clones were once again streaked out on BHI plates, a single colony used to inoculate an over-night culture, which was stored as a glycerol stock culture as described above.

2.5.13.3 Modifications using pHoss1

Creation of *clpX* deletion mutants was done with the pMAD-derivate pHoss1 (Abdelhamed *et al.*, 2015) following the authors instructions. After transformation of *L. monocytogenes* cells with the pHoss1 derivate and incubation at 30°C for 3 d on BHI plates containing erythromycin, two single colonies were picked and streaked out for 1 d at 42°C on BHI agar plates containing erythromycin. Two single colonies were then picked and streaked out on a fresh BHI agar plate containing erythromycin. This procedure was performed three times in total. A single colony was then picked and 5 ml BHI broth inoculated and shaken with 250 rpm at 30°C for 20-24 h, before the culture was diluted 1:1000 in fresh 5 ml BHI broth and the culture shaken again (30°C, 250 rpm, 20-24 h). This step was performed twice, before the culture was diluted 1:1000 once more and shaken at 42°C, 250 rpm for 8 h. This culture was plated on BHI agar plates and single colonies streaked out on BHI plates with and without erythromycin. Erythromycin sensitive clones were analyzed for the presence or absence of *clpX* and the parental plasmid, and colonies lacking both were stored as a glycerol stock culture as described above.

2.5.13.4 Modifications using pIMK derivates

pIMK derivates were used for gene overexpression or complementation purposes. In *L. monocytogenes*, pIMK plasmids lack an origin of replication and are forced to integrate into the *L. monocytogenes attB* site at the $tRNA^{Arg}$ locus site (Monk *et al.*, 2008). After transformation of the respective strain, cells were grown on BHI agar plates containing kanamycin at 37°C for 1 d. After streaking out of 2-3 clones, a single colony was picked from each clone to inoculate an overnight culture and the plasmid integration was checked by PCR. Strains carrying the desired construct were stored as a glycerol culture.

2.6 Protein based work

2.6.1 Isolation of heterologous proteins from *E. coli*

2.6.1.1 Protein overproduction

E. coli BL21 cells were transformed with 1 µl of the purified pET11a construct containing the gene to be overexpressed fused to a Strep-tag at its C-terminus and plated on an LB plate containing ampicillin. A single colony was inoculated in 25 ml LB broth containing ampicillin and shaken overnight with 250 rpm at 37°C. Cells were diluted in 500 ml selective LB broth to an OD_{600} of 0.1 and incubated at 37°C and 250 rpm until an OD_{600} of 0.5-0.7 was reached. IPTG was added to a final concentration of 1 mM. After 3 h at 37°C and 250 rpm, cells were harvested at 8000 x g for 5 min in a Beckman Avanti™ J-25 centrifuge. Cells were washed once in buffer W and the pellet was stored at -20°C overnight.

2.6.1.2 Protein purification

Cells were resuspended in 20-40 ml buffer W + 1 mM PMSF and lysed for 3 min using the EmulsiFlex C3 homogenizer (Avestin Europe GmbH). The lysate was separated from insoluble cell material by centrifugation (8000 x g, 20 min) and filtration through MiniSart syringes (0.2 µm, Sartorius) and stored on ice. Purification of Strep-tagged proteins was done using the StrepTactin® superflow system (IBA GmbH). 4 ml StrepTactin suspension was put onto a plastic column. The column material was equilibrated by washing 3 times with 5 ml buffer W. The cell lysate was added to the column and the flow-through collected in a separate tube. Afterwards, the column was washed three times with 5 ml buffer W. Afterwards, protein elution was performed by addition of 5 x 500 µl buffer W + 2.5 mM desthiobiotin (IBA GmbH). Each elution step was collected in a separate tube. Protein concentration was determined by a Bradford assay and possible contaminations with nucleic acids were analyzed with the

NanoPhotometer® (IMPLEN). Purity of the isolated protein was confirmed by SDS-PAGE (chapter 2.6.3). The purified protein was stored at -20°C. The column was regenerated by washing three times with 5 ml buffer R and then stored at 6°C.

buffer W	100 mM Tris-HCl, pH 8.0 150 mM NaCl
buffer E	Buffer W + 2.5 mM desthiobiotin
buffer R	1 mM 2-[4'-hydroxy-benzeneazo]benzoic acid (HABA)

2.6.2 Determination of protein concentration

A 5x Roti®-Nanoquant solution (Roth) was diluted to 1x in ddH_2O and immediately mixed with 2-50 µl cell lysate or 5-10 µl purified protein in a total volume of 1 ml. The suspension was incubated for at least 5 min at room temperature and the absorption at λ=595 nm was measured in a 1 ml plastic cuvette. Measurement was done using the BioSpectrometer® basic photometer (Eppendorf) with the same amount of buffer W in 1x Bradford reagent used for the probes as blank. Protein concentration was determined using the following formula, which was calculated via a bovine serum albumin (BSA) calibration line.

$$c[\mu g/\mu l] = \frac{A595}{(0{,}0536 * x\ \mu l)}$$

2.6.3 Linear SDS-PAGE

For SDS polyacrylamide gel electrophoresis, 6-10 µl of each sample was mixed with 2-4 µl 4x ROTI®Load 1 loading buffer (Roth) and incubated at 95°C for 5 min. The PageRuler™ Prestained Protein Ladder (Thermo Scientific) was used as molecular weight marker. For analysis of protein purity and western blotting purposes, 12.5% (w/v) acrylamide gels were prepared using the ROTIPHORESE® Gel 30 (37.5:1 acrylamide:bisacrylamide) premix (Roth) and run in a Mini-PROTEAN® Tetra Cell gel chamber (BioRad) in 1x ROTIPHORESE® SDS-PAGE buffer (Roth) at 140 V for 90 min. Composition of stacking and resolving gels are summarized in Table 2-9.

Gels that had to be visualized by protein staining after the run were stained in 1x Roti®Blue (Roth) at room temperature and constant shaking overnight. The next day, gels were destained by washing twice with water. For gels used for western blotting this step was omitted.

Table 2-9: Composition of acrylamide gels.

4% (w/v) acrylamide stacking gel:	
component	**volume**
acrylamide/bisacrylamide (30% (w/v))	530 µl
0.5 M Tris-HCl, pH 6.8	1 ml
ddH_2O	2.4 ml
10% SDS	40 µl
10% APS	50 µl
TEMED	4 µl

12.5% (w/v) acrylamide resolving gel:	
component	**volume**
acrylamide/bisacrylamide (30% (w/v))	4.2 ml
1.5 M Tris-HCl, pH 8.8	2.5 ml
ddH_2O	3.1 ml
10% SDS	100 µl
10% APS	100 µl
TEMED	10 µl

2.6.4 Western blotting

For Western blotting a Semi-Dry-Blot chamber was used. Three Whatman paper sheets (Whatman™ Grade GB003; GE Healthcare) were equilibrated in 1x Western blot buffer and put on the bottom of the chamber. An Immobilon®-P^{SQ} polyvinylidendifluorid membrane (PVDF, Merck Millipore GmbH) was activated in methanol, equilibrated in 1x Western blot buffer and added on top of the Whatman papers. After SDS-PAGE, the upper stacking gel was removed and the resolving gel was laid onto the membrane. Three additional Whatman paper sheets were equilibrated in 1x Western blot buffer and put on top of the gel. Protein transfer was performed at 100 mA per gel for 75 min.

1x Western blot buffer	25 mM Tris-HCl 192 mM glycine 10% (v/v) methanol ad. 1 l ddH_2O

2.6.5 Protein detection

After Western blotting, the membrane was shaken in blocking solution for at least 3 h at room temperature or overnight at 4°C. The primary antibody was diluted in blocking solution according to Table 2-10 and added to the membrane. The membrane was shaken for 1-4 h at room temperature or overnight at 4°C. The membrane was washed three times with 1x TBST buffer and the second antibody (diluted in blocking solution according to Table 2-10) was added. After shaking for at least 2 h at room temperature, the membrane was washed three times with 1x TBST buffer. Protein detection was done with the Enhanced Chemiluminescence Substrate (Thermo Scientific) according to manufacturer's instructions. The blot was visualized with a ChemiDoc® MP Imaging System (BioRad). For detection, exposure times between 30 s and 15 min were used. Band intensities were quantified using the ImageJ 1.52a software.

1x TBST	10 mM Tris-HCl; pH 8.0
	137 mM NaCl
	0.1% (v/v) Tween 20
	ad. 1 l ddH_2O
blocking solution	2.5% (w/v) skim milk powder
	ad. 1 l x TBST

Table 2-10: Antibodies used in this work.

name	antibody type	antigen	dilution	reference/source
primary antibodies:				
α MurAA	rabbit IgG	MurA	1:5000	(Kock *et al.*, 2004)
α DivIVA	rabbit IgG	DivIVA	1:5000	(Marston *et al.*, 1998)
secondary antibodies:				
α rabbit IgG-HRP	goat IgG	rabbit IgG	1:10000	Sigma Aldrich
α Strep-HRP		Strep	1:10000	IBA life sciences

2.6.6 Analysis of *in vivo* protein degradation

To analyze proteolytic degradation of a potential ClpP2 substrate *in vivo*, *L. monocytogenes* strains were inoculated to an OD_{600} of 0.1 and grown in presence of the respective agents at 37°C whilst shaking until an OD_{600} of 0.8-1.2. Afterwards, half of the culture was pelleted by centrifugation (5000 x g, 5 min), washed once in buffer W and stored at -20°C. The other half of the culture was treated with 200 µg/ml chloramphenicol to stop protein translation and shaken for another 90 min at 37°C. Afterwards, the culture was pelleted and washed in buffer W. Both samples were resuspended in 1.5 ml buffer W and lysed by sonification using the SONOPULS HD 2070 sonifier (Bandelin) for 10 min at a power output of 40%. The cell debris was removed by centrifugation and the protein concentration of the supernatant was determined according to chapter 2.6.2. A total amount of 6-10 µg protein solution was mixed with 4x ROTI®Load 1, incubated at 95°C for 5 min and loaded onto a 12.5% (w/v) polyacrylamide (PA)-gel. PA gel electrophoresis, followed by Western blotting was performed according to chapters 2.6.3 and 2.6.4, respectively. For detection of TimA-Strep, the α Strep-HRP antibody

was used, and for detection of MurA, the α MurAA and α rabbit IgG-HRP antibodies were used according to Table 2-10. Protein detection was done according to chapter 0.

Buffer W	100 mM Tris-HCl, pH 8.0 150 mM NaCl

2.6.7 Electrophoretic mobility shift assay (EMSA)

To show the interaction of TimR with the P_{timA} promoter, the promotor fragment was amplified using primers TE74-TE75 and purified using the QIAprep Spin Miniprep Kit (QIAGEN GmbH) according to the manufacturer´s guidelines. DNA concentration was measured using the NanoPhotometer® (IMPLEN) and the fragment was added to the reaction mix in a final concentration of 32 nM. After addition of various amounts of purified TimR-Strep (and additional supplements where necessary), EMSA buffer was added to a final volume of 10 µl and the reaction was left at room temperature for 5 min before being loaded onto a 10% (w/v) acrylamide/bisacrylamide gel in 0.6x TBE buffer. The gel was run in 0.6x TBE buffer for 120 min at 120 V and visualized by ethidium bromide staining.

EMSA buffer	120 mM HEPES, pH 8.0 300 mM KCl 30 mM $MgCl_2$ 0.3 mg/ml bovine serum albumin (BSA) 30% glycerol 0.3 mM EDTA
1x TBE buffer	89 mM Tris-HCl, pH 8.3 89 mM borate 2 mM EDTA

2.6.8 ClpP2 activity assay

For analysis of a direct ClpP2 interaction with tartrolon B, an *in vitro* activity assay was performed. 20 µM of purified ClpP2-Strep and ClpP2 E9K-Strep proteins were added to various concentrations of ADEP and tartrolon B (0 µM, 1 µM, 2 µM, 4 µM in DMSO). Buffer W was added to a final volume of 90 µl. The reaction was started by addition of 10 µl 2 mM Suc-Leu-Tyr-7-amido-4-methylcoumarin (Merck) as the substrate in a final concentration of 200 µM, and ClpP2 mediated cleavage of this substrate monitored by measuring in black, flat bottom 96 well plates (Thermo Scientific™ Nunc™ MicroWell) at 32°C in a Tecan infinite M1000 reader with excitation at 380 nm and emission at 440 nm. Assays were conducted for 3 h with 5 min between each measurement step.

Buffer W	100 mM Tris-HCl, pH 8.0
	150 mM NaCl

2.6.9 β-galactosidase assay

Overnight cultures of the strains to be tested were diluted 1:50 in 5 ml BHI and additional compounds were added if necessary. The culture was shaken with 250 rpm at 25-37°C until an OD_{600} of 0.6-0.8. After centrifugation (11000 x g, 5 min) the pellet was washed in 600 µl ddH_2O and the cells were resuspended in 1200 µl PBS + 0.15% (v/v) mercaptoethanol. Cells were lysed by sonification for 30 min in total, where a 20 s sonification step at 40% power output was followed by a 10 s break. After centrifugation (11000 x g, 5 min), 50 µl of the supernatant was mixed with 950 µl 1x Roti®-Nanoquant solution (Roth) and protein concentration measured according to chapter 2.6.2 with 50 µl buffer W mixed with 950 µl Roti®-Nanoquant solution as blank value. 1 ml of the supernatant was transferred into a new tube and incubated at 30°C for 10 min. Afterwards, 200 µl of a 4 mg/ml o-nitrophenyl-β-D-galactopyranosid (ONPG) solution

in PBS was added to the tubes. The reaction was mixed by shaking, incubated at 30°C for 10-15 min and stopped by addition of 500 µl 1 M Na_2CO_3. Absorption was measured at λ=420 nm in a 1 ml plastic cuvette using the BioSpectrometer® basic photometer (Eppendorf). β-galactosidase activity was calculated using the following formula, where *t* is the incubation time in min and *c* the protein concentration in µg/µl.

$$1\ MU = 1000 * \frac{OD_{420}}{t * c}$$

PBS	137 mM NaCl
	2.7 mM KCl
	10 mM phosphate buffer, pH 7.4

2.7 Microbiological methods

2.7.1 Screen for promoter induction

Strains carrying the promoter fragment of an MDR transporter operon fused to *lacZ* were screened for induction of the individual promoter. For this, 200 ml of BHI broth was mixed with 200 µl of an overnight culture of the strain to be screened and 400 µl X-Gal stock solution. To this mixture, 200 ml BHI agar, which was cooled to ~50°C was added, mixed well and poured into 14x14 cm agar plates. After solidification of the agar, 1 µl of a 0.033 M solution of the substance to be tested (dissolved in DMSO) was spotted on top of the agar. Plates were incubated over night at 37°C and on the next day analyzed for blue coloring. The library used was part of the Natural Compound Library from the German Centre for Infection Research (DZIF) and contained 681 secondary metabolites from streptomycetes, myxobacteria and fungi.

2.7.2 Growth curves for analysis of minimal inhibitory concentrations (MICs)

Growth curves were used for the determination of minimal inhibitory concentrations (MICs). For this, an overnight culture was diluted to an OD_{600} of 0.1 and wells of a Cellstar® 96 well cell culture plate with flat bottom (Greiner Bio-One) were loaded with 100 µl BHI medium containing twice the concentration of the substance to be tested. 100 µl of the diluted culture was added to each well. The plate was then put into a Multiskan Sky or Multiskan Go Microplate Spectrophotometer (Thermo Fisher Scientific) and the OD_{600} measured with a shaking frequency of 10 s, followed by a 20 s break at 30-42°C in 5 min intervals over the course of 10-40 h. The MIC was defined as the lowest concentration of the agent used, where no bacterial growth could be measured after a certain time usually after 10 h or 20 h. MICs were determined via growth curves or by static incubation at 30°C, 37°C or 42°C. In all cases, the strain to be tested was inoculated to an OD of 0.1 and then added to double the amounts of the antibiotic in a 1:1 (v/v) ratio. In case of static incubation, just the turbitidy of the tube was evaluated.

2.7.3 Isolation of tartrolon B suppressors

To obtain tartrolon B resistant suppressors, the strains of interest were inoculated to a final OD_{600} of 0.05 in BHI broth containing a tartrolon B concentration equal to the MIC for each strain. The strains were grown at 37°C for at least 24 h in a Multiskan Sky or Multiskan Go Microplate Spectrophotometer (Thermo Fisher Scientific). If growth was obtained after 20 h or more, the culture was diluted to a factor of 10^{-8} and 200 µl plated onto BHI agar plates (which contained X-Gal in case of LMTE19). The plate was incubated at 37°C overnight and analyzed regarding their cell size and for blue coloring (LMTE19) on the next day. Normal sized and small colonies were streaked out on new BHI plates and incubated over night at 37°C. The next

day, an over-night culture was done using a single colony. The MIC of this culture was determined via growth curves at 37°C. If the MIC was increased compared to the wild type, the culture was stored as a glycerol stock culture and cell material used for whole genome sequencing.

2.7.4 Infection experiments

The intracellular replication rate of selected *L. monocytogenes* strains was tested using J774.A1 mouse ascites macrophages (ATCC). 3 x 10^5 macrophages were placed into a 24-well plate and cultivated in 1 ml high glucose DMEM medium (4.5 g/l glucose, 110 mg/l sodium pyruvate, and 584 mg/l l-glutamine) with 10% fetal calf serum (FCS) at 37°C in a 5% CO_2 atmosphere. The respective *L. monocytogenes* strains were grown overnight at 37°C in BHI broth, before being diluted to an OD_{600} of 0.2. 20 µl of this diluted culture was mixed with 2 ml DMEM not containing FCS. The medium for the macrophages was changed to 1 ml DMEM medium containing no FCS and 50 µl of the diluted bacterial culture added. The suspension was centrifuged (5 min, 800 g) and incubated for 1 h at 37°C, 5% CO_2. Gentamycin was added in a final concentration of 40 µg/ml and the suspension incubated for 1 h at 37°C, 5% CO_2. The wells were washed once in PBS buffer, before being covered with DMEM containing no FCS and 10 µg/ml gentamycin. The macrophages were lysed at a given timepoint. For this, the macrophages were washed once in PBS buffer, before being incubated with PBS buffer containing 0.1% Triton X-100 for 10 min. This suspension was diluted accordingly and plated on BHI plates. After incubation of the plates over night at 37°C, bacterial cell numbers were counted.

DMEM	4.5 g/l glucose 110 mg/l sodium pyruvate 584 mg/l l-glutamine

PBS	137 mM NaCl 2.7 mM KCl 10 mM phosphate buffer, pH 7.4

2.8 Statistical evaluation of data

Levels of significance were determined using a standard *t*-test assuming an equilateral distribution of a homoscedastic sequence of variables. The *P*-values obtained from this *t*-test were additionally weighted using the Bonferroni-Holm correction. Using this method, the lowest *P*-value is being multiplied with the number of samples used in the experiment, while the second lowest value is being multiplied with the same factor -1, until the highest *P*-value is multiplied by 1. Values which remained under the threshold of $P<0.05$ were considered as statistically significant.

2.9 Software

Processing of genome sequencing data was done in-house by the department of MF1 and evaluation performed with Geneious Prime® 2021.2.2. Sanger sequencing reactions were evaluated using CloneManager 9 Professional.

Modeling of tartrolon A and tartrolon B structures was done using the LEA3D software (Douguet *et al.*, 2005) provided on chemoinfo.ipmc.cnrs.fr/LEA3D/drawonline.html. On this website, the structures of tartrolon A and tartrolon B were drawn using the JSME structure editor (Bienfait & Ertl, 2013), where a 3D structure of the molecule was calculated using the RDKit-software. Afterwards, the coordinates of the molecules were exported as a .pdb file and analyzed using the PyMOL™ software (Version 1.7.x) (DeLano, 2002).

3 Results

3.1 Screening of potential ABC-type MDR transporters for its substrates

3.1.1 *In silico* identification of ABC-type MDR transporters

In order to identify potential MDR transporters, the TransportDB 2.0 software (Elbourne *et al.*, 2017) was used. The database takes well-known databases, such as RefSeq, COG and the Transporter Classification Database into account, to find ABC transporters in the EGD-e genome and classifies each transporter into a specific functional group. This revealed 172 ABC transporter genes, out of which 11 transporter genes were annotated as multidrug resistance (MDR) transporter genes. Furthermore, 14 transporters were found to have a high similarity to *Lactococcus lactis* LmrCD, a transporter that exports daunorubicin, an anthracycline produced by streptomyces (Lubelski *et al.*, 2006). Both of these ABC transporter classes were considered as potential drug exporters and should be investigated further. Transporters already characterized in previous studies were excluded in this work, leaving 20 ABC-type MDR transporters encoded within 18 operons to be analyzed for their relevance in transport of antimicrobial substances. The organization of each operon is summarized in Table 3-1. In a previous work, the transcription levels of these operons were quantified in transcripts per million (Hauf *et al.*, 2019), showing that most operons are tightly repressed – some of them by repressor proteins encoded in their own operon, suggesting a possible induction under certain conditions such as contact with small molecules including antibiotics.

Table 3-1: Overview of uncharacterized genes encoding for ABC transporters, which could potentially encode for transporters involved in compound secretion.

ATPase	permease	class	operon	transcripts per million
	lmo0107	multidrug?	*lmo0108 lmo0107*	2
	lmo0108	multidrug?	*lmo0108 lmo0107*	2
lmo0194	*lmo0195*	efflux (antimicrobial peptide?)	*lmo0193 lmo0194 lmo0195*	50
	lmo0607	multidrug	*lmo0606 (marR) lmo0607 lmo0608*	51
lmo0667	*lmo0668*	daunorubicin	No operon detected	60
lmo0742	*lmo0743*	multidrug?	*lmo0741 (gntR) lmo0742 lmo0743 lmo0744*	5
	lmo0744	macrolide?	*lmo0741 (gntR) lmo0742 lmo0743 lmo0744*	2
lmo0923	*lmo0925*	multidrug	*lmo0923 lmo0924 lmo0925 lmo0926 (tetR)*	30
lmo0986	*lmo0987*	daunorubicin	No operon detected	4
lmo1636	*lmo1637*	multidrug	*lmo1635 lmo1636 lmo1637*	178
	lmo1652	multidrug	*lmo1652 lmo1651 lmo1650 lmo1649 lmo1648*	23
lmo1724	*lmo1723*	daunorubicin	*lmo1725 (gntR) lmo1724 lmo1723*	22
lmo1964	*lmo1963*	daunorubicin	*lmo1964 lmo1963 lmo1962 (tetR)*	15
lmo2215	*lmo2214*	daunorubicin	*lmo2215 lmo2214*	97
lmo2227	*lmo2226*	daunorubicin	*lmo2228 lmo2227 lmo2226*	14
lmo2240	*lmo2239*	daunorubicin	*lmo2241 (mngR) lmo2240 lmo2239*	70
lmo2372	*lmo2371*	export?	*lmo2371 lmo2372*	
	lmo2745	multidrug	monocistronic	50
	lmo2751	multidrug	*lmo2751 lmo2752*	38
lmo2769	*lmo2768*	multidrug	*lmo2769 lmo2768 lmo2767 lmo2766 (eslR)*	30

3.1.2 Fusion of promoter regions to *lacZ*

Genes involved in detoxification of antimicrobial compounds are often induced upon exposure to these compounds. This principle can be exploited to identify genes required for compound detoxification. Genes encoding for alternative sigma factors, DNA gyrases or topoisomerases have already been shown to be inducible upon contact with certain antibiotics (Urban *et al.*, 2007, Gutierrez *et al.*, 2013), but this principle can also be suitable to assign ABC transporters to their specific substrates (Mascher *et al.*, 2004, Rietkötter *et al.*, 2008). Exploitation of this principle is also established in *L. monocytogenes*, where the aurantimycin A-mediated induction of the promoter controlling the *lieAB* transporter genes has revealed the function of the LieAB transporter as an exporter of this depsipeptide (Hauf *et al.*, 2019).

To monitor induction, the promoter of interest is fused to a reporter gene, most commonly *E. coli lacZ*, which cleaves lactose into its monosaccharides galactose and glucose. This reaction can be visualized by substituting lactose with 5-bromo-4-chloro-3-indolyl-β-D-galactopyranoside (X-Gal) or *o*-nitrophenyl-β-D-galactopyranoside (ONPG), which is cleaved to galactose and either a blue colored indigo dye or *o*-nitrophenol, respectively (Horwitz *et al.*, 1964, Miller, 1972, Kiernan, 2007). To screen promoters controlling the operons listed in Table 3-1 for induction, corresponding promoter-*lacZ* fusions were generated in a pIMK-based plasmid carrying a promoter-less *lacZ* gene (Monk *et al.*, 2008). For the promoter fragment, 400 bp upstream of the start codon of the first gene in the operon was estimated to be sufficient to include all regulatory elements. The plasmid was integrated into the EGD-e genome at the *attB* $tRNA^{Arg}$ locus and the promoter activity was measured by growing the resulting strains to mid-log phase followed by a β-galactosidase assay using ONPG as a substrate. Promoters were sorted according to their activity and strains carrying the promoter-less *lacZ* (LMSH16), the P_{lieA}-*lacZ* fusion (LMSH5) and the P_{lieA}-*lacZ* fusion in a Δ*lftR* background (LMSH98) were

included as negative and positive controls, respectively. The activity for all promoters is represented in Miller Units (MU) in Fig. 3-1. All promoters showed an activity well below the fully induced *lieA* promoter (8513±1507 MU), with the lowest *lacZ* activity measured for the strain carrying the $P_{lmo0742}$-*lacZ* fusion (14±2.6 MU) barely being higher than promoter-less *lacZ* (12,6±3.4 MU) and the most active promoter ($P_{lmo2215}$; 356±63 MU) still having an activity, which is over 20-fold lower than derepressed P_{lieAB}. These observations undermined the assumption, that all promoters have the potential to be induced when exposed to the right substance.

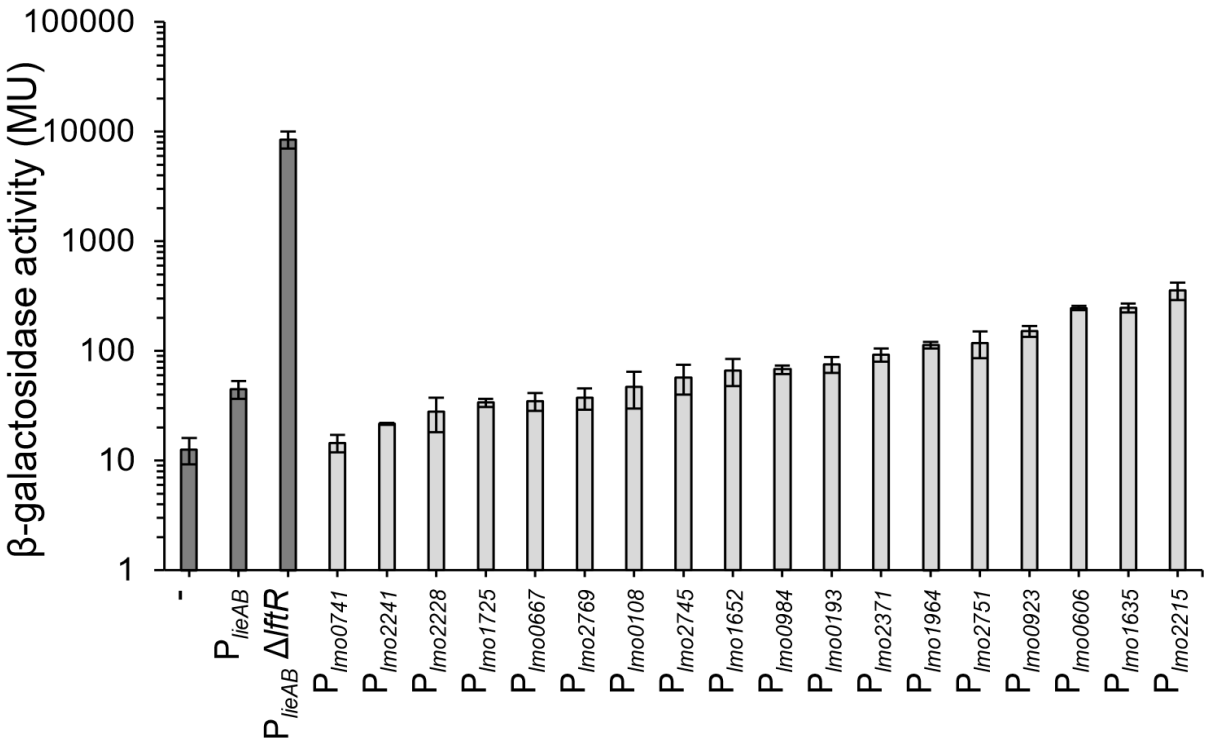

Figure 3-1: Activity of promoters controlling the expression of potential MDR transporters. Strains carrying promoter-*lacZ* fusions were grown at 37°C until mid-log phase and harvested. After cell lysis, the crude extract was used to quantify promoter strength using an ONPG β-Galactosidase assay in Miller Units (MU). As controls, strains with promoter-less *lacZ* (LMSH16), P_{lieAB}-*lacZ* (LMSH5) and P_{lieAB}-*lacZ* fusion in a Δ*lftR* background (LMSH98) were used. The experiment was done in three replicates and average values with their corresponding standard deviations were calculated.

3.1.3 Testing of commonly used antibiotics for induction of promoters of MDR transporter genes

As a first screening approach, antibiotics commonly used in clinical applications, as food additives or in veterinary medicine were tested for their ability to induce any of the promoters listed in Table 3-1. The antibiotics were classified according to their mode of action and source organism and are listed in Table 3-2. Most antibiotics were of natural origin, with the majority being secreted by *Streptomyces* species. Strains carrying promoter-*lacZ* fusions were poured into BHI agar containing X-Gal, a small volume of each substance was spotted on top of the agar and the plate was incubated at 37°C overnight. However, no antibiotic was able to induce any of the tested promoters.

Table 3-2: Antibiotics used for screening of promoter induction. Additionally, the origin, substance class and target of each antibiotic is listed, as well as its ability to induce any of the promoters.

compound	substance class	induction	source
inhibition of cell wall biosynthesis			
penicillin G	β-lactam	--	*Penicillium*
vancomycin	glycopeptide	--	*Streptomyces orientalis (*Brigham & Pittenger, 1956)
moenomycin	glycopeptide	--	*Streptomyces* (Subramaniam-Niehaus *et al.*, 1997)
bacitracin	lantibiotic	--	*Bacillus licheniformis* (Haavik, 1974)
targocil	synthetic	--	synthetic
ceftriaxon	β-lactam	--	synthetic
fosfomycin	phosphonic antibiotic	--	*Streptomyces fradiae* (Hendlin *et al.*, 1969)
cycloserine	D-alanine analogue	--	*Streptomyces garyphalus* (Svensson, 1982)
tunicamycin	nucleoside antibiotic	--	*Streptomyces* (Takatsuki *et al.*, 1971)
inhibition of ribosome activity			
spiramycin	macrolide		*Streptomyces ambofaciens* (Abou-Zeid *et al.*, 1980)
tetracyclin	polyketide	--	*Streptomyces aureofaciens* (Darken *et al.*, 1960)
kanamycin	aminoglycosides	--	*Streptomyces kanamyceticus* (Okami *et al.*, 1959)
chloramphenicol	amphenicol-class antibacterial	--	*Streptomyces venequelae* (Ehrlich *et al.*, 1948)

erythromycin	macrolide	--	*Streptomyces erythreus* (Weber *et al.*, 1985)
josamycin	macrolide	--	*Streptomyces narbonensis* (Eiki *et al.*, 1988)
tylosin	macrolide	--	*Streptomyces fradiae* (Seno *et al.*, 1977)
inhibition of cell division			
PC190723	FtsZ inhibitor	--	synthetic

3.1.4 Tartrolon B induces activity of the $P_{lmo1964}$ promoter

The antibiotics tested above were of great interest because of their widespread medical and agricultural usage. However, there are many more toxic substances to which *L. monocytogenes* is constantly being exposed to in its environmental habitat. To test more naturally occurring antibiotics for their ability to induce promoters, the natural compound library of the German Centre for Infection Research (DZIF) was screened. This library contains 681 compounds, which are being produced by *Streptomyces* (340 compounds), *Myxobacteria* (253 compounds) and *fungi* (88 compounds). Each compound was diluted to a concentration of 0.03 mM in DMSO. Using the same method as described in chapter 3.1.3, each strain carrying a promoter-*lacZ* fusion was tested for its induction by a compound included in this screen.

After incubation of the agar plate at 37°C overnight, a blue colored circle was observed upon exposure of the strain carrying the $P_{lmo1964}$-*lacZ* fusion to tartrolon B (Fig. 3-2A). As a control, the induction of the promoter by the related macrodiolides tartrolon A and boromycin was analyzed. However, the blue circle caused by exposure of this strain to tartrolon A was very weak and completely absent when boromycin was used. The tartrolons are a group of macrodiolides which are being secreted by the myxobacterium *Sorangium cellulosum* to battle competitors (Irschik *et al.*, 1995). Tartrolon A and tartrolon B are structurally similar, the only difference is the bound boron atom in the centre of tartrolon B (Fig. 3-2B). Boromycin is

another naturally occuring, boron containing macrodiolide, secreted by *Streptomyces antibioticus* (de Carvalho *et al.*, 2022).

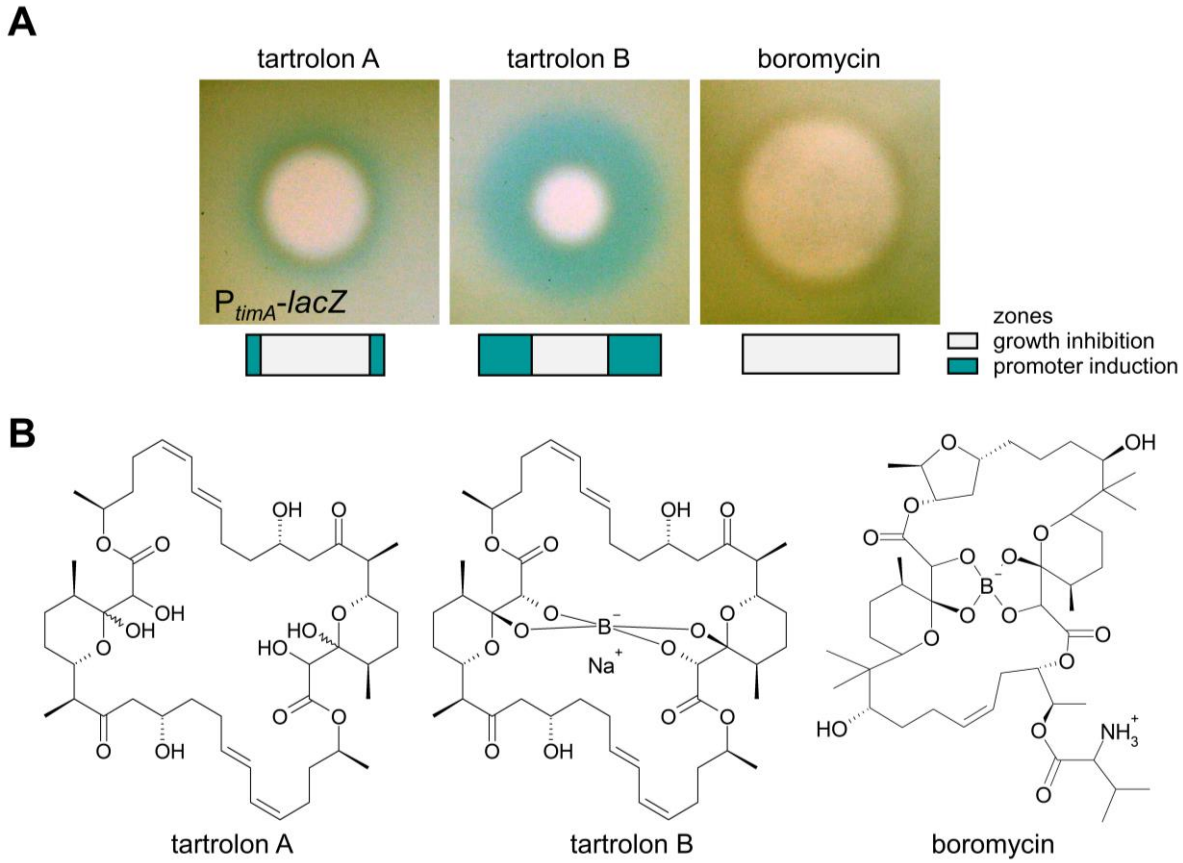

Figure 3-2: Induction of $P_{lmo1964}$-*lacZ* by tartrolon B. (A) Visualization of $P_{lmo1964}$ induction using an agar diffusion assay. Strain LMTE19 carrying the $P_{lmo1964}$-*lacZ* fusion was diluted 1:2000 in warm 0.5x BHI agar containing 50 µg/ml X-Gal and poured into an agar plate. After cooling down, 1 µl of 2.5 mg/ml of each substance was spotted on top of the agar and the plate incubated at 37°C overnight. **(B)** chemical structures of tartrolon A, tartrolon B and boromycin (from left to right)

The promoter induced by tartrolon B controls the expression of three genes (*lmo1962-lmo1964*), and the corresponding proteins are annotated as an ATPase domain-containing protein (Lmo1964), a permease (Lmo1963), and a protein of the tetracycline repressor family (Lmo1962). The genomic arrangement of the operon is shown in Fig. 3-3. Thus, the putative MDR transporter is being formed by an interaction of Lmo1964 and Lmo1963. No gene in this operon has yet been assigned with a function, so they have been termed tartrolon-inducible MDR transporter genes (*tim*). The ATPase (Lmo1964) will be referred to as TimA, the

permease (Lmo1963) as TimB and the repressor protein (Lmo1962) as TimR. As *timA* is the first gene in this operon, the promoter controlling the expression of these genes will be renamed to P_{timA}.

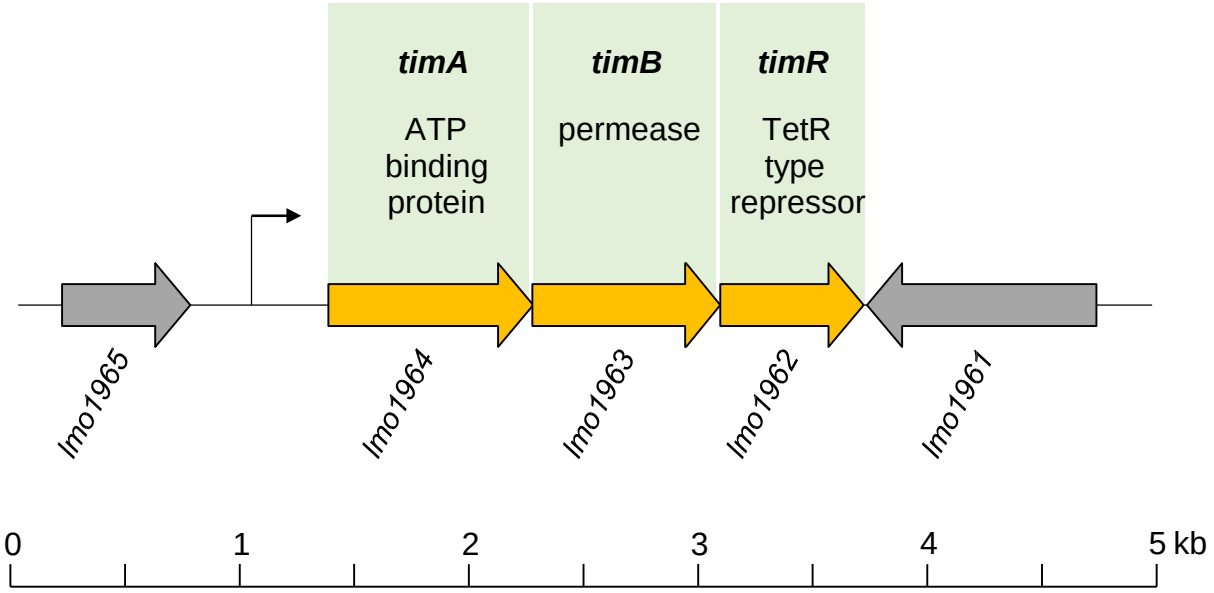

Figure 3-3: Genomic arrangement of the *timABR* locus of *L. monocytogenes* EGD-e. The operon contains thee genes and blast algorithms assigned Lmo1964 (TimA) as an ATP binding protein, Lmo1963 (TimB) as a permease and Lmo1962 (TimR) as a TetR-like repressor protein.

3.1.5 Quantification of P_{timA} induction by macrodiolides

Induction of P_{timA} by tartrolon B appeared weak on agar plates, even when using twice the amount of X-Gal used in the screen. To quantify the induction ratio of P_{timA} by tartrolon B, the strain carrying the P_{timA}-*lacZ* fusion was inoculated with increasing amounts of tartrolon A, tartrolon B and boromycin concentrations up to a concentration of 25 ng/ml to an OD_{600} of 0.1. Cells were grown at 37°C to mid-log phase, lysed by sonification and the β-galactosidase activity of the crude extract was measured using ONPG as substrate. Strains carrying promoter-less *lacZ* (LMSH16) and a Δ*lftR* P_{lieA}-*lacZ* strain (LMSH98) were used as negative and positive controls, respectively. Growing the strain carrying P_{timA}-*lacZ* in a concentration of 25 ng/ml tartrolon B increased the activity of the *timA* promoter 3.1-fold from 90±15 MU to 279±21 MU,

which was only a minor increase compared to the 2.8-fold induction rate observed when growing in presence of 10 ng/ml tartrolon B (255±26 MU, Fig. 3-4), suggesting that maximum promoter induction was close to being reached using 25 ng/ml tartrolon B. No significant promoter induction of P_{timA} was observed when using tartrolon A or boromycin, matching the observations made in the disc diffusion assay previously.

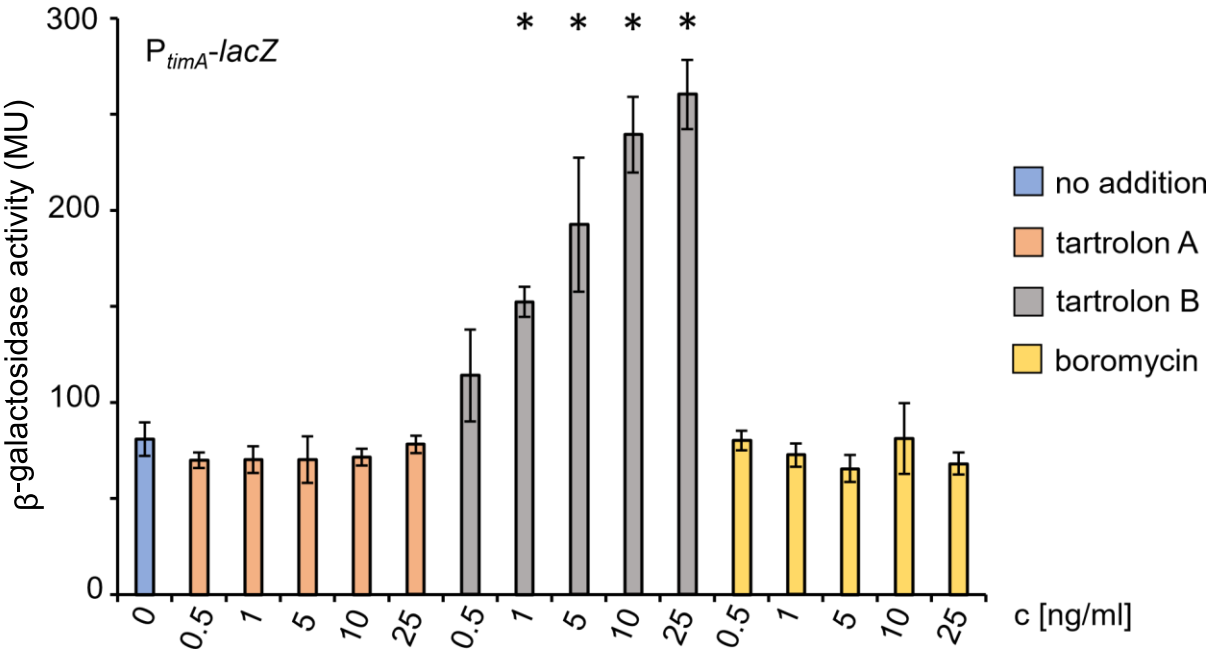

Figure 3-4: Quantification of P_{timA} induction by tartrolon A, tartrolon B and boromycin. An ONPG-based β-galactosidase assay was performed using a strain carrying P_{timA}-*lacZ* (LMTE19). The strain was incubated with varying amounts of tartrolon A, tartrolon B and boromycin and grown at 25°C until mid-log phase, before being harvested and lysed by sonification. Afterwards, the supernatant was used for quantification. The experiment was performed in triplicates with the average values and resulting standard deviations shown. Asterisks indicate a statistical significance using a *t*-test with Bonferroni-Holm correction with $P<0.05$.

3.1.6 Characterization of the TimAB transporter

The induction of P_{timA} by tartrolon B seen in disc diffusion and β-galactosidase assays suggested that the *timAB* genes encode for a tartrolon B transporter responsible for detoxifying the antibiotic by transporting it to the outside of the cell. As a conclusion, cells lacking *timAB* should become sensitive to tartrolon B, as the antibiotic can no longer be detoxified. In contrast, cells with a higher *timAB* expression level should be able to cope with tartrolon B more effectively and therefore become resistant to the macrodiolide. To test these hypotheses, knockout strains lacking *timAB* (LMTE34) and *timR* (LMTE37) - the putative repressor protein binding to P_{timA} - were generated and the minimal inhibitory concentrations (MICs) for tartrolon A, B and boromycin for these strains were determined at 37°C. The tartrolon A MIC was 32-fold decreased in the Δ*timAB* mutant (0.062±0 µg/ml) compared to the wild type (2±0 µg/ml) and the strain was ~200-fold more susceptible to tartrolon B (MIC=0.009±0.005 µg/ml for Δ*timAB* compared to 1.7±0.6 µg/ml for the wild type). Deletion of *timR* resulted in a strain more resistant to tartrolon B (MIC=4±0 µg/ml). However, the mutant was unaffected in its tartrolon A resistance. Neither mutant was affected in its boromycin resistance, as their MIC matched the one determined for the wild type at 0.25±0 µg/ml (Fig. 3-5A).

As a control experiment, the Δ*timAB* and the Δ*timR* mutant strains were complemented with pIMK derivates that bring *timAB* and *timR* under control of the *lacO* operator and the *lac* repressor LacI, so that gene expression can be induced by the lactose-analogon IPTG. Hence, these strains carry an ectopic, inducible copy of their deleted genes and just like other strains carrying a similar genotype will be referred to as strains carrying i*timAB* (LMTE51) or i*timR*, (LMTE52) respectively. These strains were tested similarly for their ability to restore tartrolon resistance to wild type levels in presence of 1 mM IPTG. As expected, the tartrolon A and tartrolon B MICs for i*timAB* and i*timR* were comparable in presence of IPTG to the MIC

determined for the wild type, while these strains showed similar phenotypes to their parental ones in absence of IPTG (Fig. 3-5A).

These experiments suggested, that *timAB* is essential in mediating tartrolon resistance. However, further evidence was needed to show that *timAB* is sufficient in mediating this resistance without any additional components. This could be proven by cloning *timAB* into pSG1154 - a vector that integrates into the *amyE* locus of *Bacillus subtilis* and contains a xylose-inducible promoter. Integration of this plasmid into the *amyE* locus results in a loss of AmyE amylase activity (Lewis & Marston, 1999). After transformation of *B. subtilis* 168 with this plasmid, the amylase activity of individual colonies was tested by streaking out onto an LB agar plate containing ampicillin and starch at 37°C overnight. The plate was incubated with iodine, where a purple coloration of strains indicated an inactive *amyE* locus. One of these strains was picked and used for further experiments (BSTE1).

The tartrolon A, tartrolon B and boromycin MICs for this strain in the presence and absence of xylose were determined on the basis of growth curves with varying concentrations of each antibiotic at 37°C (Fig 3-5B). The tartrolon B MIC of *B. subtilis* was determined at 0.7±0.2 µg/ml for tartrolon A and tartrolon B, while the strain expressing *timAB* showed a 15-fold increased MIC for both macrodiolides of 10.7±4.6 µg/ml when xylose was added for *timAB* induction. The boromycin MIC was not significantly affected in the strain overexpressing *timAB*. This confirmed previous findings, according to which TimAB was described as an exporter, which is specific for tartrolons A and B, but which is unable to export structurally related substrates such as boromycin.

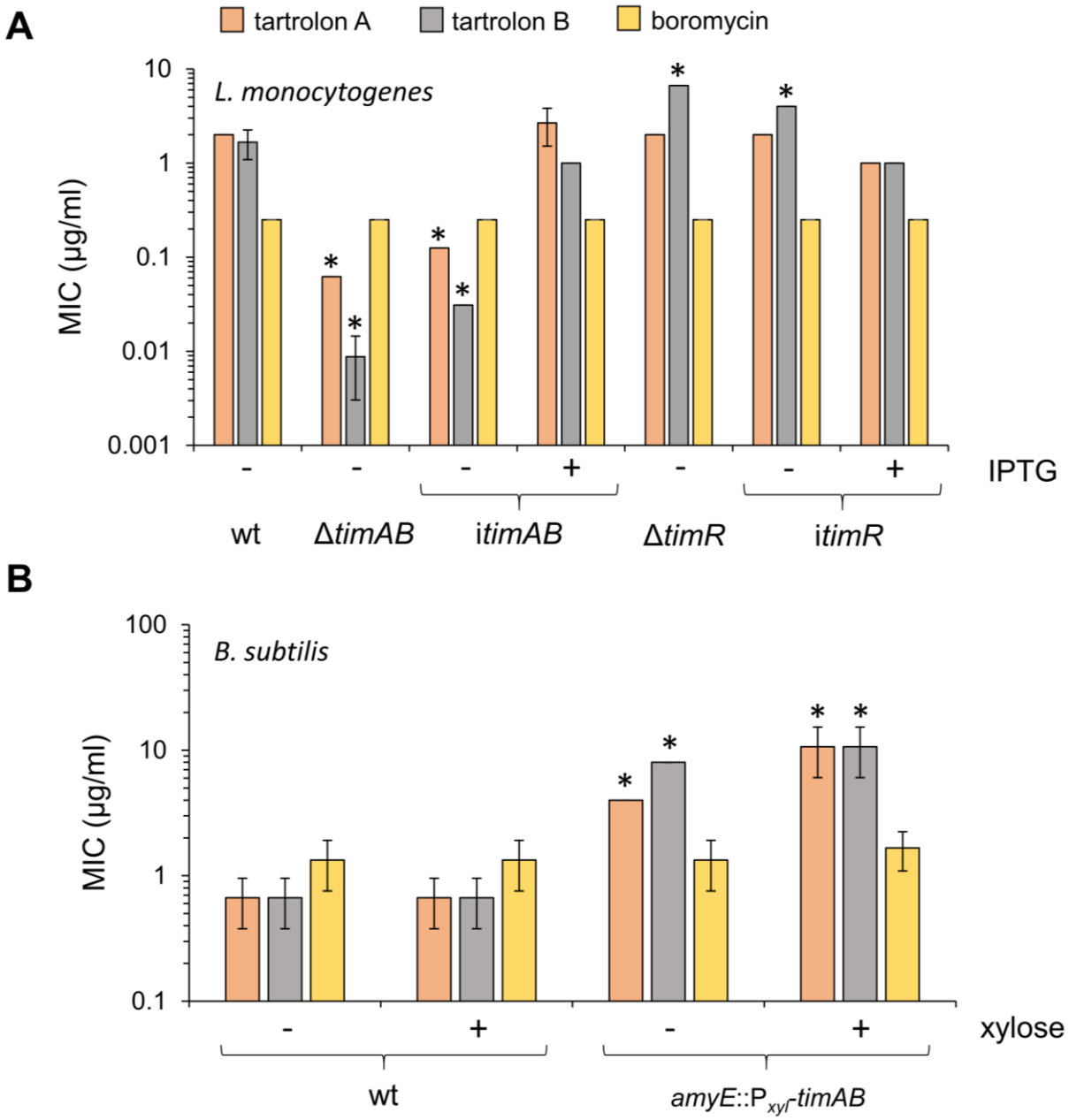

Figure 3-5: Determination of tartrolon A, tartrolon B and boromycin MICs of *L. monocytogenes* and *B. subtilis* strains carrying different *timABR* constructs. Each strain was grown at 37°C in varying concentrations of each compound and the MIC determined. **(A)** Contribution of the *timABR* genes to resistance against all three macrodiolides. Knockout mutants lacking *timAB* (LMTE34) or *timR* (LMTE37) were complemented with an inducible copy of *timAB* (LMTE51) and *timR* (LMTE52), respectively and grown in BHI broth ± 1 mM IPTG. **(B)** Resistance levels of *B. subtilis* 168 compared to BSTE1 (*amyE*::P_{xyl}-*timAB*). *B. subtilis* strains were grown in LB broth ±0.5% xylose. Average values and standard deviations from three replicates are shown. Statistically significant values were determined using the *t*-test with Bonferroni-Holm correction and are indicated by the asterisks ($P<0.05$).

3.1.7 Analysis of TimR binding to the P_{timA} promoter

At this point, first insights into the transport of tartrolon B by *timAB* and its specificity for the antibiotic were obtained. However, the function of the third gene in the *timABR* operon, *timR* was not well understood. TimR is annotated as a TetR-like repressor protein and in chapter 3.1.6, a strain lacking *timR* was described as being more resistant to tartrolon B, suggesting a possible binding of this repressor to the *timA* operator sequence.

The effect of TimR on *timABR* expression was investigated by introduction of the P_{timA}-*lacZ* reporter plasmid into a Δ*timR* background (LMTE50) and measurement of the β-galactosidase activity of this strain in comparison to P_{timA}-*lacZ* in the wild type background (Fig. 3-6A). In this experiment, LMSH16 (promoter-less *lacZ*) and LMSH98 (Δ*lftR* P_{lieA}-*lacZ*) were used as controls. Compared to the β-galactosidase activity of the P_{timA}-*lacZ* fusion in the wild type background (90±15 MU), the activity was elevated 4.7-fold to 425±58 MU upon deletion of *timR* (Fig. 3-6A). This suggests, that the MIC increase described for the Δ*timR* mutant is due to an increased P_{timA} activity caused by the absence of the repressor protein.

The binding of TimR to P_{timA} was also analyzed *in vitro* using an electrophoretic mobility shift assay (EMSA). For this assay, the *timA*-promoter and TimR-Strep were purified and TimR-Strep was titrated to a constant amount of P_{timA}. This titration was performed in the absence and presence of tartrolon B. The possible binding of TimR-Strep to its promoter was visualized by polyacrylamide gel electrophoresis and ethidium bromide staining (Fig. 3-6B). Upon titration of the repressor protein, the lowest band representing the unbound *timA*-promoter shifts towards two higher molecular weight complexes, with the higher band being favored at higher TimR-Strep concentrations. This shift was not observed in the presence of tartrolon B, suggesting a direct binding of tartrolon B to either P_{timA} or TimR, which prevents binding of TimR to the promoter fragment.

In a further EMSA experiment, the ability of tartrolon A and boromycin to prevent the formation of a P_{timA}:TimR complex was tested in a similar manner as described above for tartrolon B (Fig. 3-6C). In this experiment, the *timA*-promoter was used as a control in its unbound state and in complex with TimR. The repressor:promoter complex did not dissociate in the presence of tartrolon A or boromycin, suggesting that neither of these two macrodiolides

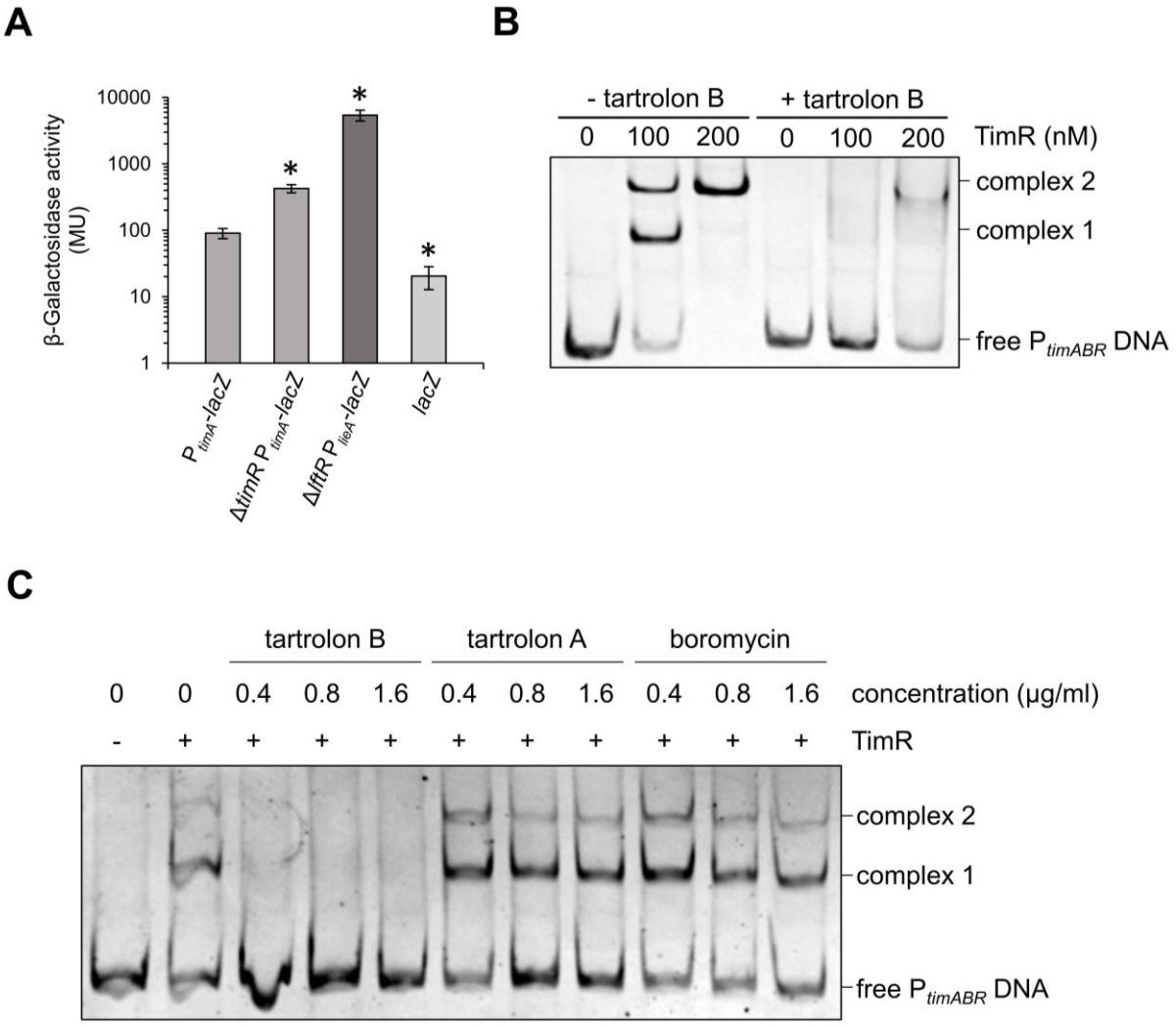

Figure 3-6: Studies investigating the interaction between P_{timA} and TimR. (A) ONPG-based β-galactosidase assay of strains LMTE19 (P_{timA}-*lacZ*) and LMTE50 (Δ*timR* P_{timA}-*lacZ*). Strains LMSH6 (promoter-less *lacZ*) and LMSH98 (Δ*lftR* P_{lieA}-*lacZ*) served as negative and positive controls, respectively. Strains were inoculated in BHI broth to an OD_{600} of 0.1 and grown at 37°C until mid-log phase. After harvesting and lysis, the supernatant was used for measurement of β-galactosidase activity. The assay was measured three times in biological replicates and average values and standard deviations are shown. Asterisks mark statistical significances as determined by the *t*-test using the Bonferroni-Holm correction ($P<0.05$). **(B)** Polyacrylamide gel for analysis of TimR binding to P_{timA}. TimR was titrated in the stated amounts to 32 nM P_{timA} ± 1.25 µg/ml tartrolon B. The reactions were left at room temperature for 5 min and the gel was loaded with the entire volume. Complexes representing bound and unbound promoter fragments are indicated. **(C)** Polyacrylamide gel analysing the specificity of tartrolon B in promoter de-repression. In each lane, 32 nM P_{timA} and 100 nM TimR was used and the respective antibiotics titrated in the stated concentrations. Signals representing bound and unbound promoter fragments are indicated.

is able to disrupt the interaction of TimR with P_{timA}, which is in good agreement with the fact, that these antibiotics were unable to induce the promoter *in vivo*.

These experiments presented insights into the mechanism of tartrolon B-mediated induction of the *timABR*-promoter. This mechanism revolves around the macrodiolide binding to TimR. This binding prevents the formation of a P_{timA}:TimR complex, which leads to P_{timA} induction and higher TimAB levels in the cell, mediating tartrolon resistance.

3.1.8 Tartrolon B susceptibility of other *Listeria* species

L. monocytogenes belongs to the genus of *Listeria*, which it shares with other *Listeria sensu stricto* spp. such as *L. seeligeri*, *L. inoccua* or *L. ivanovii*. The *timABR* genes are highly conserved within these *Listeria* spp. However, there are several *Listeria sensu lato* species that lack the *timABR* genes, mainly the *Mesolisteria* species *L. aquatica*, *L. fleischmanii* and *L. floridensis* and the *Murraya* species *L. grayi*. The genomic loci upstream and downstream of the *timABR* operon of all the mentioned *Listeria* species are summarized in (Fig. 3-7A). Since the *Mesolisteria* and *Murraya* contain *Listeria* species lacking the *timABR* genes, it would be fitting if these strains were sensitive to tartrolon B. This hypothesis was tested by determining the tartrolon B MICs for each strain by generating growth curves in different tartrolon B concentrations at 37°C (Fig. 3-7B). The MICs for tartrolon B did not vary too much within the *Listeria sensu stricto* species, with only the MIC for *L. innocua* at 6.7±2.3 µg/ml being slightly higher than the one for *L. monocytogenes* (MIC=1.3±0.6 µg/ml). In keeping with the model of species requiring *timAB* for tartrolon B resistance was the observation that *L. grayi* was found to be highly sensitive to the macrodiolide (MIC=0.004±0.002). However, despite the absence of the *timAB* genes, all *Mesolisteria* were resistant to tartrolon B, with the MIC for *L. floridensis* at 2.3±1.5 µg/ml being in the range of *L. monocytogenes*. An MIC could not be determined for *L. aquatica* and *L. fleischmanii*, as they were almost completely unaffected by the antibiotic

even when exposed to high concentrations of 16 µg/ml (Fig. 3-7C). This could be caused by an alternated membrane permeability in *Mesolisteria*, which leads to tartrolon B being unable to freely diffuse into the cell, or by a detoxification mechanism that is independent of *timABR*.

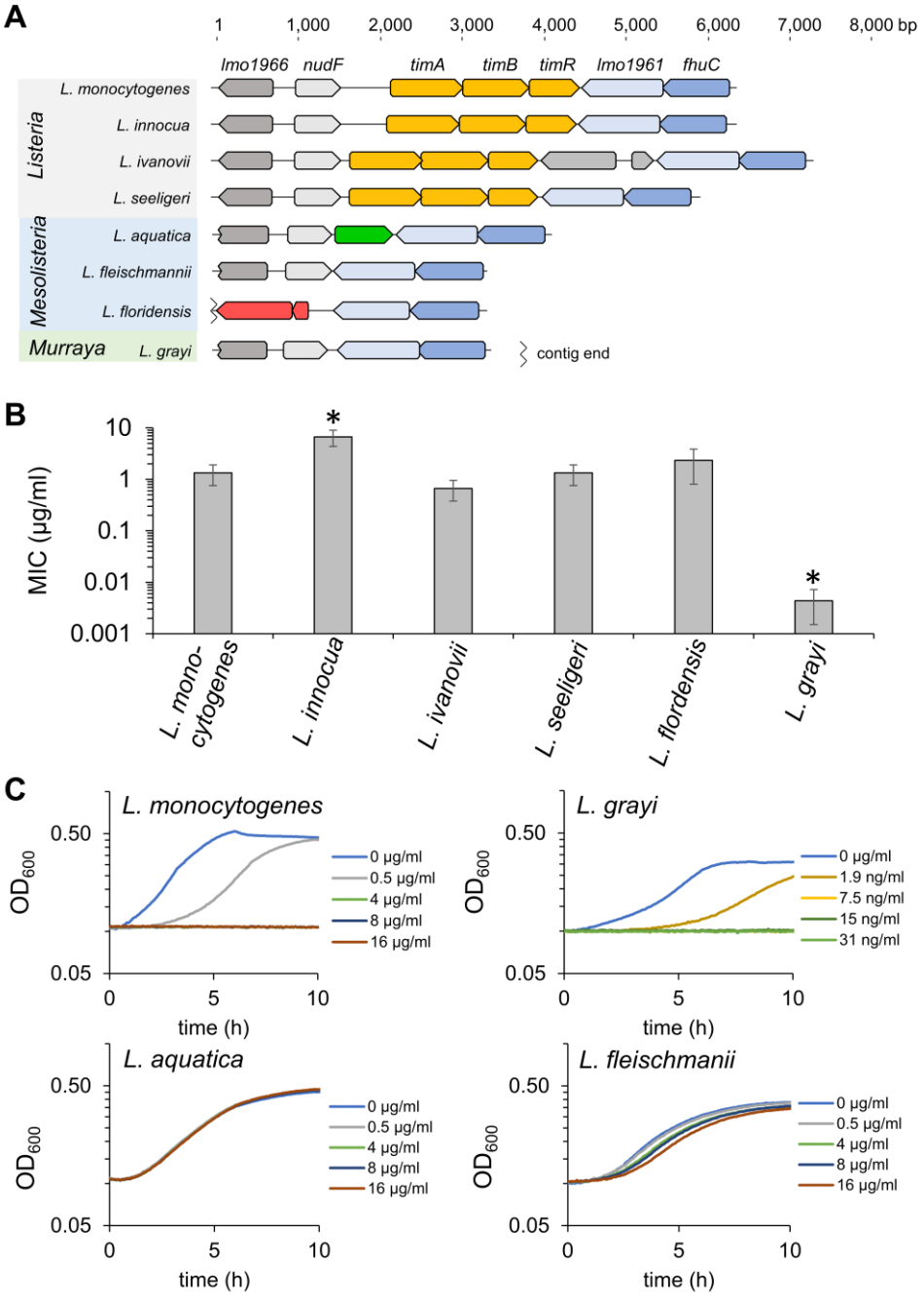

Figure 3-7: Analysis of tartrolon B resistance in *Listeria sensu stricto* and *sensu lato* species. (A) Genomic alignment of the *timABR* locus of different species belonging to the *Listeria*, *Mesolisteria* or *Murraya* clades. **(B)** Tartrolon B MICs for the *Listeria* species introduced in (A). All species were inoculated at an OD_{600} of 0.1 and grown in BHI broth at 37°C. The experiment was repeated three times and average values and standard deviations shown. Statistical significance is indicated by the asterisks using the Bonferroni-Holm method (P<0.05). **(C)** Growth curves of *L. monocytogenes*, *L. grayi*, *L. aquatica* and *L. fleischmanii* in different tartrolon B concentrations.

3.2 Mode of action of tartrolon B

Tartrolon B is structurally related to boromycin - both antibiotics being boron-containing macrodiolides with similar molecular masses. It is also known that both boromycin and tartrolon B are only active against gram-positive bacteria (Irschik *et al.*, 1995, Moreira *et al.*, 2016). Boromycin is a known potassium ionophore, which causes a deficiency of the potassium ion inside the cell, leading to a dysregulation of membrane potential, pH, and ribosome activity (Rozov *et al.*, 2019, Sweet *et al.*, 2021). However, the lack of potassium in cells treated with boromycin can be overcome by supplying the media with high levels of potassium salts (Moreira *et al.*, 2016). In such a medium, the antibiotic loses its toxic activity and bacterial strains become resistant.

To test tartrolon B for a possible similar ionophore activity, the MICs for both tartrolon B and boromycin were analyzed by inoculation of the wild type in BHI medium containing 250 mM potassium chloride and sodium chloride for control (Fig. 3-8A). In the presence of potassium chloride, the boromycin MIC for the wild type (0.4±0.1 µg/ml) increased ~150-fold to 85±37 µg/ml and the tartrolon B MIC increased 32-fold from 2±0 µg/ml in absence of potassium chloride to 64±0 µg/ml in its presence. This suggests that both antibiotics do indeed share the same function as potassium ionophores. In contrast, the MICs for both antibiotics decreased slightly when the media was supplemented with sodium chloride instead (4-fold lower for boromycin; 2-fold lower for tartrolon B), which might be caused by an unspecific binding of both macrodiolides to sodium.

These observations made it seem likely that tartrolon B causes a potassium deficiency in wild type cells, leading to their inability to grow in presence of tartrolon B. In such a scenario, potassium importers should increase in importance, since they may be able to counteract the membrane depolarization caused by the antibiotic by constantly pumping potassium into the

cell. Consequently, strains lacking some of these transporters should become sensitive to both tartrolon B and boromycin.

Several potassium transporters are known in *Listeria monocytogenes*, namely KimA, the KdpABCDE transporter system and KtrCD (Gibhardt *et al.*, 2019). Strains lacking each of these importers were tested regarding their resistance level for tartrolon B and boromycin via growth curves at 37°C (Fig. 3-8B). However, only the Δ*ktrD* strain showed an increased susceptibility for both macrolides, as the tartrolon B MIC was decreased 2-fold, and the boromycin MIC was 3-fold lower than for the wild type. The other two strains (Δ*kimA* and Δ*kdpABCDE*) were not sensitive to either drug. The sensitivity of the Δ*ktrD* strain did however validate the hypothesis that tartrolon B acts as a potassium ionophore.

An important factor in cell signaling is the second messenger molecule cyclic di-adenosine monophosphate (c-di-AMP). It is involved in various cellular processes such as osmotic stress, DNA repair mechanisms, but also potassium transport (Commichau *et al.*, 2018, Zarrella & Bai, 2020) and its level is tightly regulated by many proteins: The essential diadenylate cyclase CdaA is responsible for the production of c-di-AMP and is being regulated by the repressor protein CdaR. Also, c-di-AMP can be degraded by phosphodiesterases such as PgpH and PdeA (Schwedt *et al.*, 2023). Strains lacking each of these genes were tested for their resistance to tartrolon B by monitoring their growth at 37°C in various concentrations of the antibiotic (Fig. 3-8C). Since *cdaA* is essential, an IPTG-inducible *cdaA* depletion mutant was used in this experiment. While the strain carrying i*cdaA* was not affected in its tartrolon B resistance, only minor effects were observed in the Δ*cdaR* and the Δ*pgpH* Δ*pdeA* mutants, as the tartrolon B MIC for these strains was two-fold decreased to 1±0 µg/ml compared to the MIC for the wild type at 2±0 µg/ml. This may be due to the higher c-di-AMP levels present in both Δ*cdaR* and

Δ*pgpH* Δ*pdeA*, since c-di-AMP has been shown to inactivate potassium importers (Wang *et al.*, 2022).

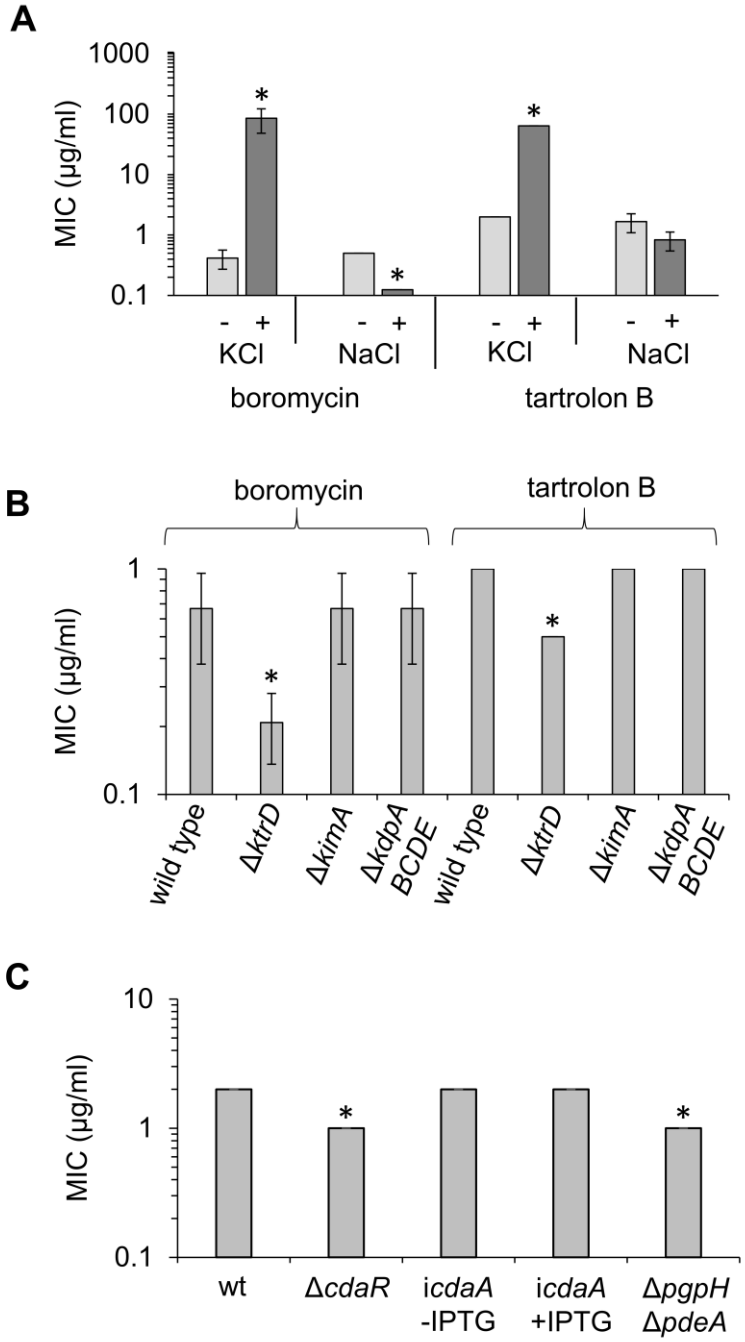

Figure 3-8: Mode of action analysis of tartrolon B. All strains shown were diluted to an OD_{600} of 0.05 and the MICs determined at 37°C using a series of dilutions of the respective drug. Each experiment was repeated twice and average values and standard deviations are shown. Asterisks mark statistically significant differences using a *t*-test followed by a Bonferroni-Holm correction ($P<0.05$). **(A)** Tartrolon B MICs for the wild type grown in presence of potassium chloride and sodium chloride. Wild type cells were inoculated in BHI medium containing no salt (light gray bars) or 250 mM potassium chloride or sodium chloride (dark grey bars). **(B)** Boromycin and tartrolon B MICs of *L. monocytogenes* strains lacking potassium importers. **(C)** Tartrolon B MICs for strains with a disturbed c-di-AMP metabolism.

3.3 The role of ClpP2 in tartrolon B resistance

3.3.1 Tartrolon B suppressor screen

In the previous chapters, mechanisms involved in the TimAB-mediated detoxification of tartrolon B were examined, and the mode of action of tartrolon B as a potassium ionophore was assigned. To identify novel genes involved in potassium homeostasis or other unknown pathways that might be disturbed by the antibiotic, the strain carrying the P_{timA}-*lacZ* fusion (LMTE19) was inoculated with the previously determined tartrolon B MIC for the wild type at 2 µg/ml. This strain was chosen over the wild type to quickly identify suppressors with an increased P_{timA} activity, which were not of interest in this context. After >40 h of incubation at 37°C, growth of strain LMTE19 was observed despite the presence of tartrolon B, and the culture was plated on BHI X-Gal plates without tartrolon B with the parental strain also grown without tartrolon B as a control and grown over night at 37°C. The next day, the colonies were analyzed, but no distinction regarding the coloring could be made in clones grown in the presence of tartrolon B to the parental strain grown in absence of the antibiotic. However, after incubation of LMTE19 and the wild type at high tartrolon B concentrations and subsequent plating of the culture, up to 50% of the clones were smaller than clones from their respective parental strain. Clones with normal colony size as well as small clones were isolated and tested for growth in the absence and presence of 1 µg/ml tartrolon B (Fig. 3-9).

Smaller colonies showed a significant growth deficit in standard BHI medium, but were unaffected when grown in presence of 1 µg/ml tartrolon B. Clones with normal colony size showed a normal growth rate in the absence of tartrolon B, but were mostly unable to grow within the first 15 h after inoculation with the macrodiolide, matching the phenotype of the parental strain (data not shown). This suppressor experiment was repeated twice with the wild

type, showing similar results regarding the ratio of smaller and normal-sized colonies, as well as their resistance properties.

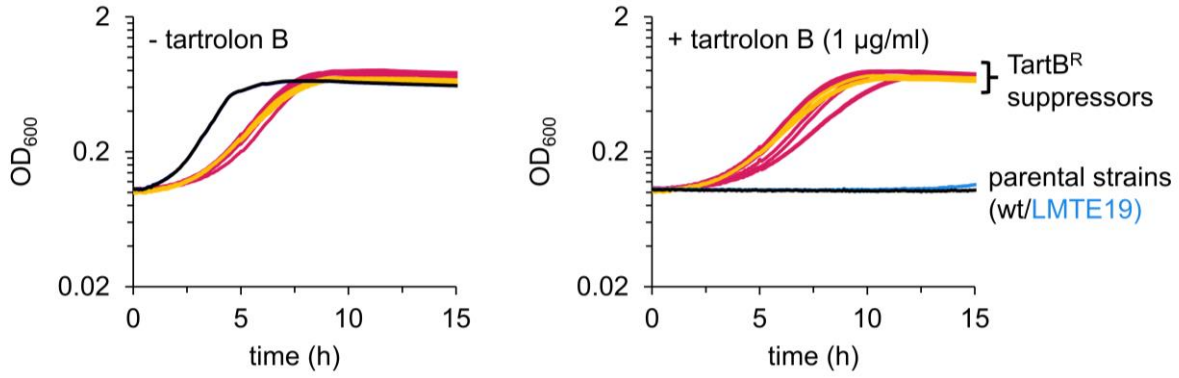

Figure 3-9: Growth of tartrolon suppressors with small colony phenotype in the absence and presence of 1 µg/ml tartrolon B. Smaller colonies were isolated from wild type and P_{timA}-*lacZ* (LMTE19) by inoculating these strains in the presence of 2 µg/ml tartrolon B for >20 h before plating the culture onto BHI plates and incubation at 37°C overnight. As controls, the parental strains were included in this experiment. Growth curves of strains carrying a *clpP2* E9K allele are shown in pink, and strains carrying a *clpP2* T90I allele shown in yellow.

3.3.2 Mutations in the *timABR*-locus and in the *clpP2* gene mediate resistance against tartrolon B

In order to identify the mutations responsible for the resistance gain of the smaller colonies, their genomes were sequenced. It is noteworthy, that in each experiment, the mutations obtained for individual clones were all identical. In the screen using the strain carrying P_{timA}-*lacZ*, a single nucleotide polymorphism (SNP) was identified in the *clpP2* gene (*lmo2468*), leading to the exchange of glutamic acid 9 to a lysine (E9K) in ClpP2. ClpP2 is a caseinolytic protease responsible for the degradation of many cellular proteins (Balogh *et al.*, 2022). In the two suppressor screens, in which the wild type was used, this exact same SNP was observed again, with the other mutation identified being another SNP in *clpP2*, leading in the exchange of threonine 90 to an isoleucine (T90I). The growth deficits of strains carrying either one of these mutations are shown in Fig. 3-9 (pink: strains carrying *clpP2* E9K; yellow: strains carrying *clpP2* T90I) and were comparable to each other.

The tartrolon B MICs for a *clpP2* E9K and *clpP2* T90I strain were determined via growth curves at 37°C (Fig. 3-10A). These SNPs resulted in a highly resistant strain with a tartrolon B MIC of 64±0 µg/ml - a MIC eight times higher than the one observed for the Δ*timR* strain determined in previous experiments (MIC=8±0 µg/ml). It was therefore plausible, that mutations in *clpP2* would lead to the highest levels of resistance a strain could acquire, making it difficult to find other factors affecting tartrolon B resistance using this experimental setup.

While all other normal-sized clones were not resistant to tartrolon B, one clone was found, for which the tartrolon B MIC was increased to 8±0 µg/ml compared to 2±0 µg/ml in the wild type (Fig. 3-10B). Genome sequencing of this suppressor revealed a frame shift mutation in *timR* (LMTE65), in which the 604th nucleotide in *timR* is deleted. This frame shift results in TimR having a non-natural C-terminal region starting from K202, which is also elongated by 6 additional amino acids (Fig. 3-10C). The observed increase in resistance in this strain suggests that this frame shift leads to the inactivation of TimR, and therefore the strain having a Δ*timR* phenotype.

In order to isolate suppressors outside of *clpP2* in a higher frequency, a second, IPTG-inducible copy of the *clpP2* gene was introduced into the wild type genome, so that *clpP2* needed be mutated in both copies to mediate tartrolon B resistance, which was way less likely than in the wild type background. Using this strain, the suppressor screen was repeated in the presence of IPTG. Growth was observed 24 h after inoculation in presence of 2 µg/ml tartrolon B and this culture was plated on BHI plates. After overnight incubation at 37°C, all colonies showed a wild type-like cell morphology. The resistance level of these suppressors against tartrolon B was increased 2-fold (MIC=4±0 µg/ml) compared to the wild type (MIC=1.7±0.6 µg/ml) (Fig. 3-10B). Genome sequencing of three clones (LMTE91-LMTE93) revealed identical SNPs in P_{timA} 14 nucleotides upstream of *timA* and right next to the ribosome binding site, suggesting a

higher P_{timA} activity as the reason for tartrolon B resistance (Fig. 3-10C). No suppressors outside of *clpP2* or the *timABR* region could be isolated in these experiments, which led to the assumption that tartrolon B resistance is mainly mediated by these two factors.

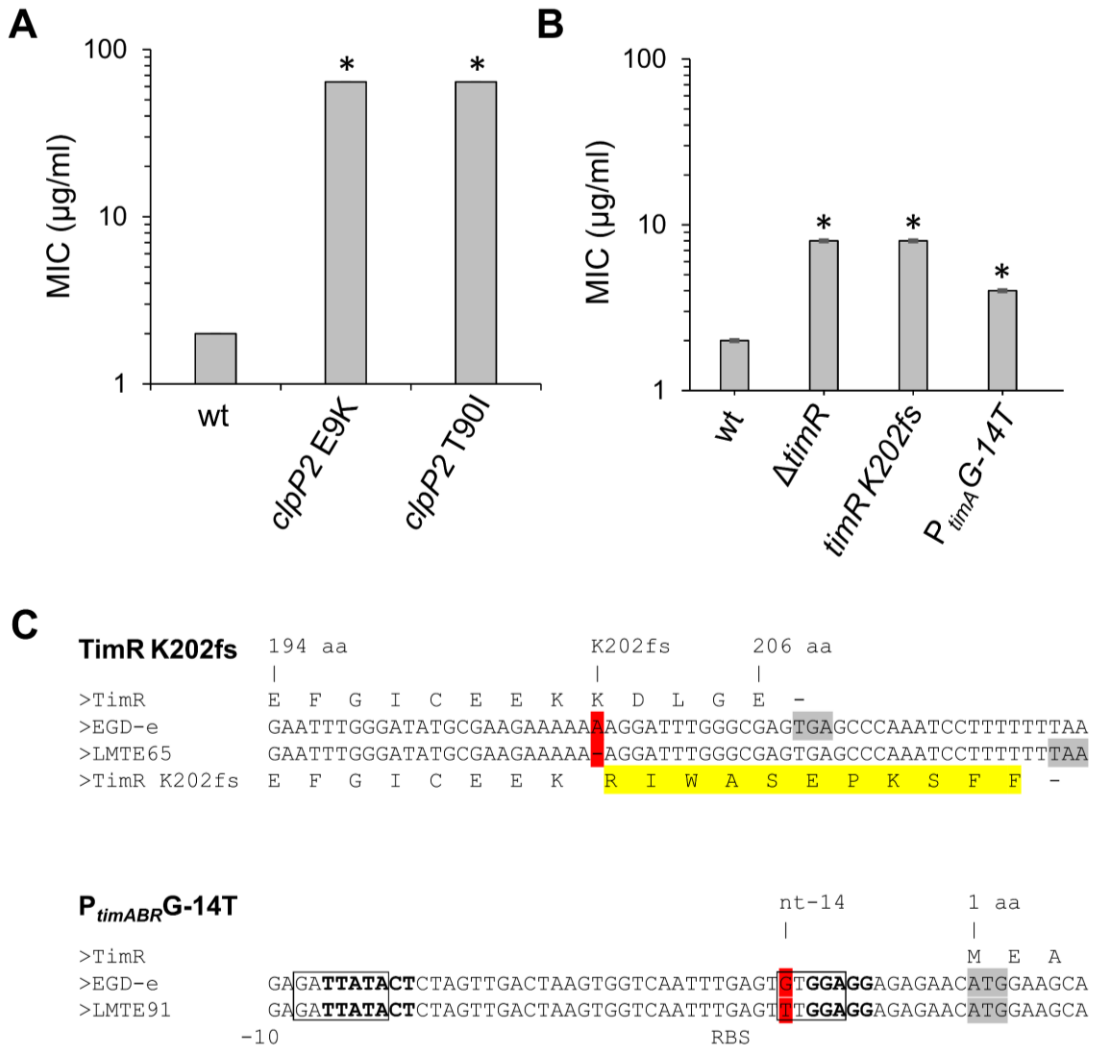

Figure 3-10: Identification of tartrolon B resistant suppressor mutants. (A) Determination of the tartrolon B MICs for two smaller colonies, which carried SNPs in *clpP2*. Strains were diluted to an OD_{600} of 0.05 and grown in a series of tartrolon B dilutions in BHI medium. The experiment was performed three times, with the MICs in each experiment being identical. Asterisks mark statistically significant differences as determined by a *t*-test and a Bonferroni-Holm correction ($P<0.05$). **(B)** Tartrolon B MICs of normal-sized colonies carrying mutations in *timR* and P_{timA}. Strains were grown starting from an OD_{600} of 0.05 in various tartrolon B concentrations. Three replicates were prepared, with all of them yielding the same MICs for each strain. Statistical significances are indicated with the asterisks. **(C)** Sequence alignment of the suppressor strains characterized in (B). The mutations identified are marked in red, and the additional sequence of TimR in LMTE65 is highlighted in yellow.

3.3.3 Generation and characterization of a Δ*clpP2* mutant

Since the most frequent suppressors found in the tartrolon B suppressor screen carried mutations in *clpP2*, which out of all suppressors also showed the largest resistance gain, the generation of a Δ*clpP2* mutant was mandatory. A *clpP2* mutant in *L. monocytogenes* has recently been described (Balogh *et al.*, 2022). The importance of ClpP2 increases with temperature, as heat leads to a higher rate of protein misfolding and hence the need for their degradation, which is the cause for increased *clpP2* expression in heat shocked gram-positive cells (Krüger *et al.*, 2001). In good agreement with this, a Δ*clpP2* mutant could only be generated when using the pMAD derivate pMinimad, which allows plasmid excision at room temperature (Patrick & Kearns, 2008). The Δ*clpP2* strain was confirmed by PCR controlling for both the gene deletion and plasmid absence (Fig. 3-11A). The primers used to check the deletion of *clpP2* create a product of 1.8 kbp when *clpP2* is present, and a 1.3 kbp product in absence of the gene, which was in good agreement with the bands observed in the gel. The genome of the Δ*clpP2* mutant was sequenced, and no second site mutations could be identified. Clones lacking the plasmid and *clpP2* were significantly smaller when streaked out on BHI agar.

Before using the Δ*clpP2* mutant (LMTE80) in experiments revolving around tartrolon B, the strain was analyzed regarding known features of this mutant in other organisms. Firstly, the ability to grow at elevated temperatures was tested, a feature that is absent in a *B. subtilis* Δ*clpP* mutant (Msadek *et al.*, 1998). Strains EGD-e, LMTE80 (Δ*clpP2*), LMTE38 (*clpP2* E9K) and LMTE74 (*clpP2* T90I) were inoculated to an OD_{600} of 0.05 and incubated at 37°C and 42°C for 24 h (Fig. 3-11B-C). While both strains carrying SNPs in *clpP2* had little effect on their growth rate at 37°C, they were barely able to grow when the temperature was switched to 42°C.

The growth rate of the Δ*clpP2* mutant was severely affected at 37°C, with the strain being unable to grow at 42°C.

As a control for the correctness of the mutant, an ectopic, IPTG-inducible copy of *clpP2* was introduced into the Δ*clpP2* background and tested for its ability to complement the lack of growth of the Δ*clpP2* mutant at 42°C (Fig. 3-11D). While the i*clpP2* strain showed a similar inability to grow at 42°C as the Δ*clpP2* mutant without IPTG, addition of IPTG partially complemented the growth deficit associated with the lack of *clpP2* expression observed in the absence of IPTG, however the IPTG-dependent effect on the growth was significant.

Suppressor strains carrying mutations in *clpP2* as well as the Δ*clpP2* mutant were tested for their ability to infect mammalian cells in a J774 mouse macrophage infection model, as multiple reports investigating a *clpP2* deletion mutant in other species suggested a reduced ability to replicate in such an environment (Loughlin *et al.*, 2009, Knudsen *et al.*, 2013, Zhao *et al.*, 2016), and for *L. monocytogenes*, ClpP2 is required for growth inside mice liver cells (Gaillot *et al.*, 2001). Macrophages were infected with the wild type, the Δ*hly* mutant as a negative control, as well as the strains carrying the *clpP2* SNPs and a Δ*clpP2* deletion and the bacterial titer of each strain was determined (Fig. 3-11E). Consistent with the literature, where the essentiality of *clpP2* for intracellular replication is described (Gaillot *et al.*, 2000), the Δ*clpP2* mutant replicated six-fold only and hence ~5,5-fold slower than the wild type at (27-fold replication).

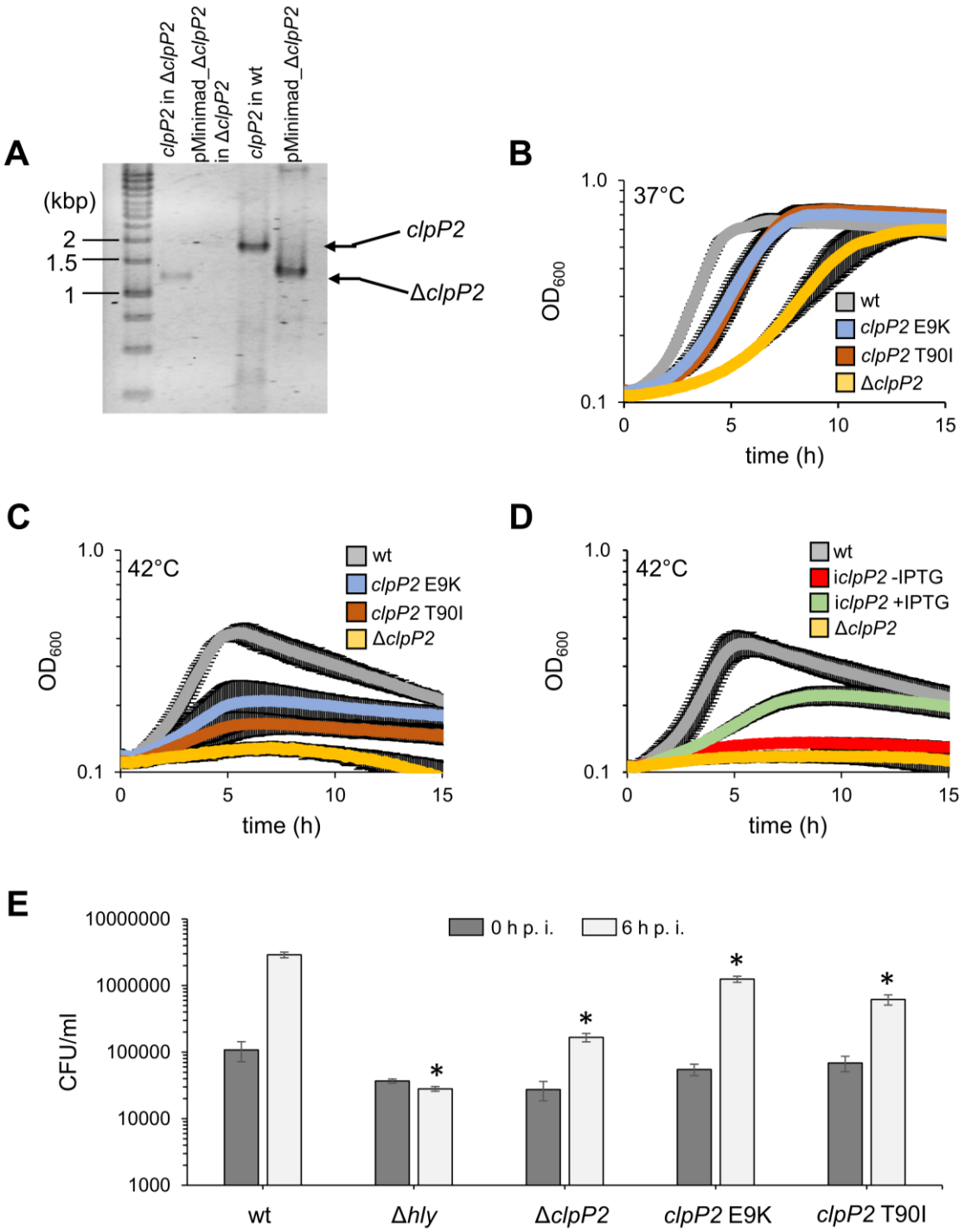

Figure 3-11: Characterization of a Δ*clpP2* mutant strain. (A) Agarose gel validating the deletion of the *clpP2* gene. Chromosomal DNA of the mutant strain was checked for absence of *clpP2* (lane 1) and for absence of the plasmid used for *clpP2* deletion (lane 2). As positive controls, wild type chromosomal DNA was used for the *clpP2* locus (lane 3) and pMinimad_Δ*clpP2* for functionality of the plasmid-specific PCR. **(B-C)** Growth curves of strains carrying *clpP2* E9K (LMTE38) and *clpP2* T90I mutations (LMTE74) as well as the Δ*clpP2* deletion (LMTE80) at 37°C **(B)** and 42°C **(C)**. Data was generated from three biological replicates and average values and standard deviations are shown. **(D)** Growth curves of the i*clpP2* mutant (LMTE90) at 42°C±1 mM IPTG with the wild type and Δ*clpP2* mutant used as controls. Growth curves were performed in three biological replicates and mean values and standard deviations are shown. **(E)** Infection of J774 macrophages with *clpP2* E9K, *clpP2* T90I and Δ*clpP2* mutant strains. Bacterial cell numbers were determined 0 h and 6 h post infection (p.i) as a biological triplicate from which average values standard deviations are shown. Asterisks indicate statistical differences calculated with a *t*-test and a Bonferroni-Holm correction ($P<0.05$).

3.3.4 Inactiviation of *clpP2* confers tartrolon resistance

In chapter 3.3.2, tartrolon B resistant suppressor strains carrying mutations in *clpP2* (E9K and T90I) were isolated. The tartrolon B resistance level of these two strains was identical, however the intramolecular distance between the respective Cα atoms of E9 and T90 within ClpP2 is ~25.4 Å with the intermolecular distance between adjacent ClpP2 monomers being ~23.8 Å (Fig. 3-12A) – distances too large to be part of a single interaction surface for tartrolon B which if disturbed would result in tartrolon B resistance. Tartrolon B only spans a distance of ~15.5 Å (data not shown). E9 is part of the electrostatic network of the ClpP2 amino terminus required for ATPase recruitment (Gatsogiannis *et al.*, 2019, Mabanglo *et al.*, 2019, Malik *et al.*, 2020). This suggests that substitution of this amino acid leads to ClpP2 inactivation, as the protease is no longer able to bind ATPases. T90 is not exposed on the ClpP2 surface and its function is rather unknown. However, the fact that the resistance levels of strains carrying E9K and T90I mutations are identical suggests that both substitutions have similar effects.

To analyze their effect on ClpP2 activity, the strains carrying these point mutations in *clpP2* were grown together with the *clpP2* and the *clpC* deletion mutants (LMJR138) to an OD_{600} of 0.8-1.0 and the crude extract analyzed by Western blotting using an antibody against MurA, which is known to be degraded by the ClpCP2 proteasome (Wamp *et al.*, 2020) and hence should accumulate if these mutants have a reduced ClpP2 activity (Fig. 3-12B). MurA levels were elevated in *clpP2* suppressor strains (2.5±0.15-fold for *clpP2* E9K and 2±0.4-fold for *clpP2* T90I) to a level comparable to the Δ*clpP2* and the Δ*clpC* mutant, which had a 2.6±0.1-fold (Δ*clpP2*) and a 2.3±0.4-fold (Δ*clpC*) increased MurA level (Fig. 3-12C). This strongly suggests that E9K and T90I act as inactivating mutations, which is in good agreement with the fact, that a Δ*clpP2* mutant is highly resistant to tartrolon B (MIC=128±0 µg/ml) – a level

comparable to the one determined for the suppressor strains in chapter 3.3.2 (MIC=64±0 µg/ml).

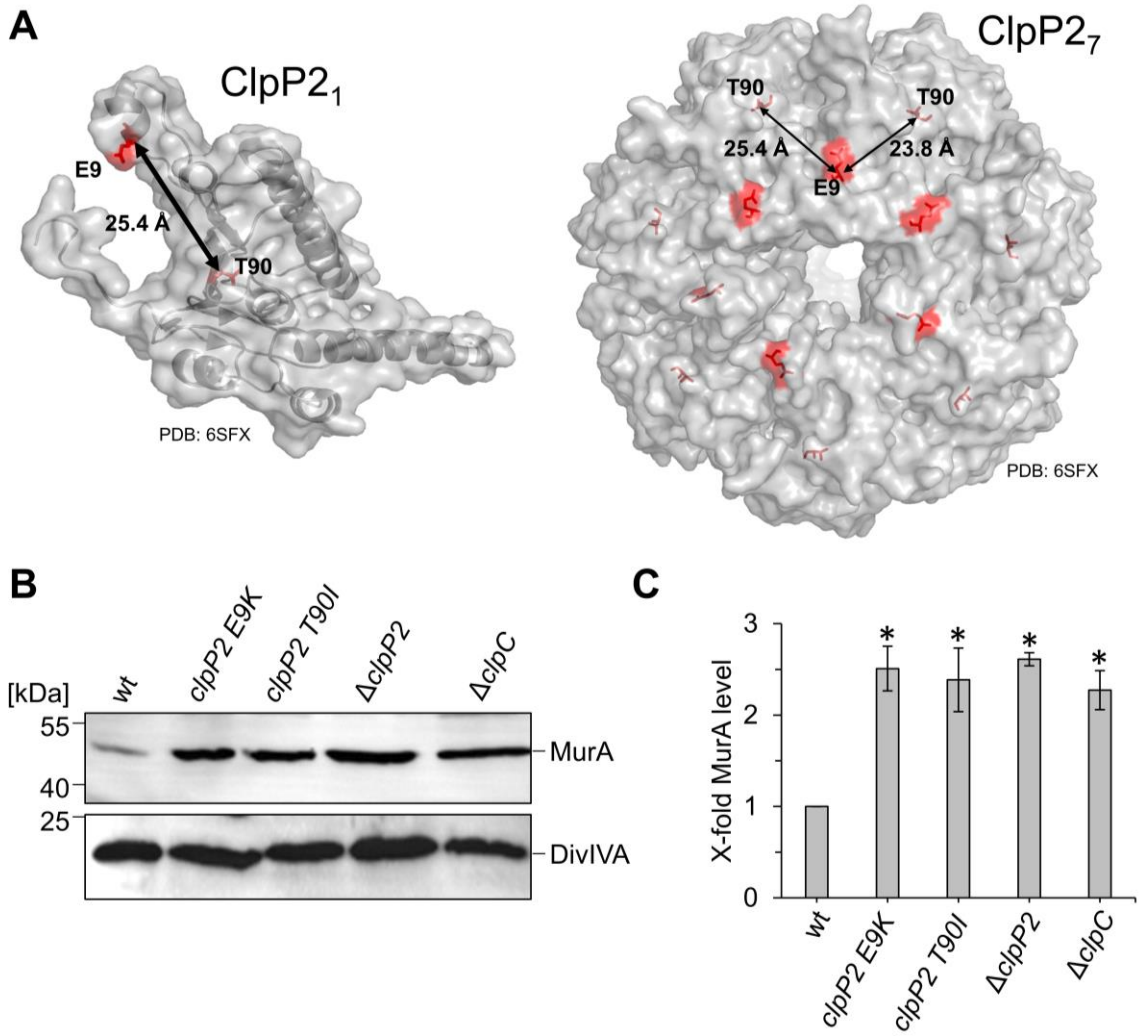

Figure 3-12: Analysis of the effect of the *clpP2* E9K and T90I mutations on ClpP2 activity. (A) Crystal structure of *L. monocytogenes* ClpP2 in its monomeric state (left) as well as the assembled heptameric protease complex (right). The E9 and T90 residues, which are mutated in the tartrolon B suppressor screen are highlighted in red and the intra- and intermolecular distances of their Cα-atoms are calculated. **(B)** Western blot showing levels of MurA in wild type and strains carrying *clpP2* E9K, *clpP2* T90I, Δ*clpP2* and Δ*clpC*. As a control, the DivIVA level was also analyzed. **(C)** Quantification of MurA levels relatively to the wild type. The western blot shown in (B) was performed three times and the band intensity for each strain was quantified using the ImageJ software. Statistical significances were calculated using a *t*-test and the Bonferroni-Holm correction and are indicated by the asterisks (P<0.05).

3.3.5 Tartrolon B does not alter ClpP2 activity

As described above, E9 and T90 are located too far apart in ClpP2 to form an interaction surface. However, it still seemed possible that tartrolon B could bind directly to ClpP2 and activate it – making inactivating mutations beneficial for balancing out the ClpP2 activity *in vivo*. Another argument supporting this hypothesis is the fact that acyldepsipeptides (ADEPs) have been shown to activate ClpP2 and frequently force E9 to mutate, causing this described balancing of ClpP2 activity. ADEP binds to ClpP2 and mimics ATPase-mediated activation of the protease, resulting in a constantly active ClpP2 and dysregulation of protein metabolism (Kirstein *et al.*, 2009, Mabanglo *et al.*, 2019).

This activation can be monitored *in vitro* by using a fluorescence-based assay with purified ClpP2 and N-succinyl-Leu-Tyr-7-amido-4-methylcoumarin as a fluorescent substrate. Upon ClpP2-mediated cleavage of the substrate, the cleaved 4-methylcoumarin can be detected by excitation at 380 nm and emission at 440 nm. ClpP2 can only cleave the substrate after being activated, as the substrate channel remains closed in its native state (Kirstein *et al.*, 2009). Purified ClpP2-Strep and ClpP2 E9K-Strep were incubated with varying amounts of tartrolon B and ADEP2 used as a positive control. Afterwards, the fluorescent substrate was added and its cleavage monitored for 3 h (Fig. 3-13A). An increase in fluorescence intensity was clearly observed when ADEP2 was titrated to constant levels of ClpP2 and to a lesser extent even when the inactive ClpP2 variant ClpP2 E9K was used. However, there was no increased substrate degradation visible when ClpP2 or ClpP2 E9K were incubated with tartrolon B. This suggests, that tartrolon B does not activate ClpP2 through direct binding to the protease and that the reason for tartrolon B resistance caused by ClpP2 inactivation is of a more complex nature.

This observation was also confirmed *in vivo*. Previous studies have shown that the activity of the *clpP2* promoter increases upon exposure of the host to elevated temperatures, as higher

levels of ClpP2 are needed for degradation of misfolded proteins caused by heat stress (Derre *et al.*, 1999). Consequently, ADEP2 should become more effective at higher temperatures, as it has been shown to disrupt the interaction between ATPases and ClpP2, leading to inactivation of the proteasome (Kirstein *et al.*, 2009). If the mode of action of ADEP2 and tartrolon B would be similar, *L. monocytogenes* should show an increased susceptibility to both of these antibiotics at higher temperatures. To investigate this theory, the wild type was analyzed for its ADEP2 and tartrolon B resistance levels at 30°C, 37°C and 42°C (Fig. 3-13B). While the MIC of ADEP2 was decreased 3-fold when switching from 30°C to 37°C

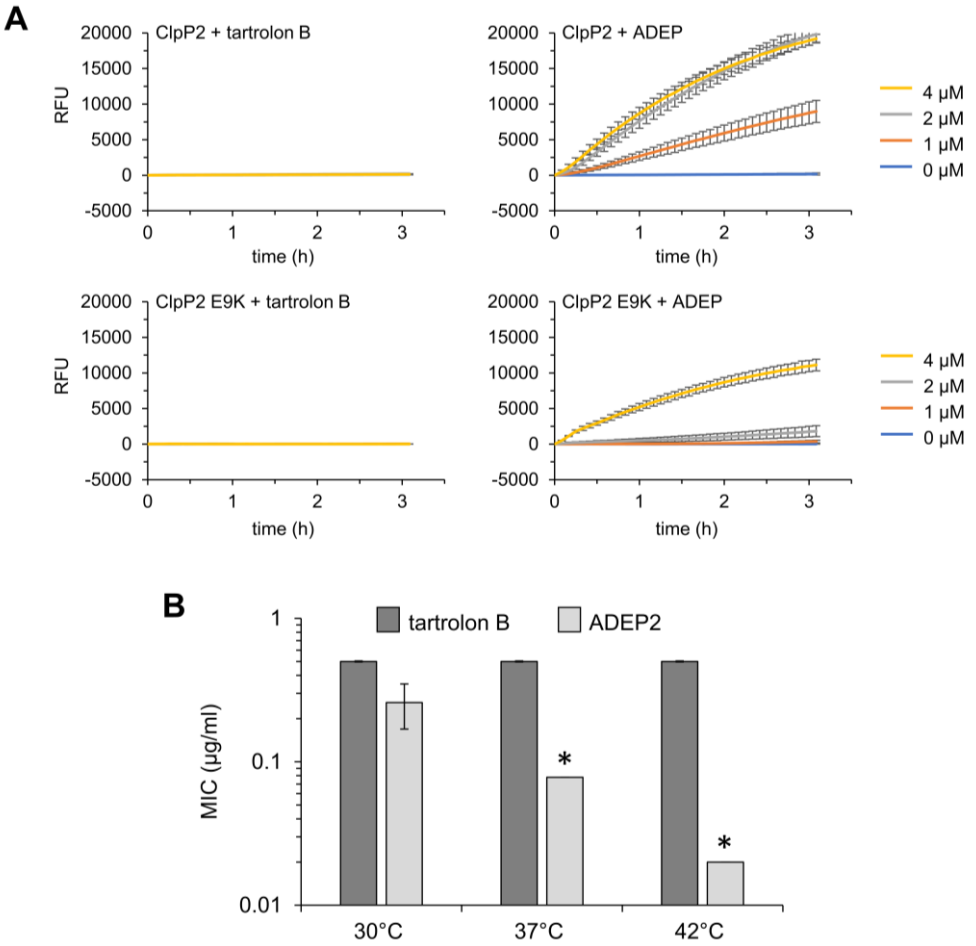

Figure 3-13: Studies investigating an interaction between tartrolon B and ClpP2. (A) N-succinyl-Leu-Tyr-7-amido-4-methylcoumarin based fluorescence assay comparing the tartrolon B and ADEP2 -mediated activation of ClpP2. Both drugs were mixed in the indicated concentrations with set amounts of ClpP2. After addition of the fluorescent substrate, the fluorescence intensity was measured by excitation at 380 nm and emission at 440 nm for 3 h. **(B)** MICs for the *L. monocytogenes* wild type for tartrolon B (dark gray) and ADEP2 (light gray) at 30°C, 37°C and 42°C. Three biological replicates were done and the average values and standard deviations calculated. Statistically significant differences are indicated by the asterisks using a *t*-test followed by a Bonferroni-Holm correction (P<0.05).

(0.259±0.09 µg/ml to 0.078±0 µg/ml) and further decreased 4-fold to a MIC of 0.02±0 µg/ml at 42°C, the resistance of the wild type against tartrolon B was unaffected by temperature changes. Overall, the data generated *in vitro* and *in vivo* undermined that tartrolon B and ADEP2 differ in their mechanisms of action and that tartrolon B likely does not bind to ClpP2.

3.3.6 A Δ*timAB* deletion is dominant over the tartrolon B hyper-resistance of the Δ*clpP2* mutant

Another reason for tartrolon B resistant strains carrying inactivating mutations in *clpP2* could be caused by the accumulation of a ClpP2 substrate in these strains, which is involved in the detoxification of the antibiotic. While trying to identify genes involved in tartrolon B resistance using suppressor screens, mutations leading to *clpP2* inactivation or elevated *timAB* expression levels were the two major suppressor groups impacting tartrolon B resistance. While deletion of *timAB* results in a highly sensitive strain, deletion of *clpP2* renders *L. monocytogenes* highly resistant to tartrolon B. However, when the strain carrying Δ*timAB* was incubated with tartrolon B concentrations above its MIC for 30 h, the strain was unable to acquire tartrolon B resistance by suppressor formation, suggesting that inactivating mutations in clpP2 only mediate tartrolon B resistance in the presence of *timAB* (Fig 3-14A).

To gain further insight into these mechanisms, a Δ*clpP2* Δ*timAB* mutant was created (LMTE95) and tested for its tartrolon B resistance level. The tartrolon B MIC for this strain was at 0.016±0.007 µg/ml, which was comparable to the MIC of 0.0125±0 µg/ml determined for the Δ*timAB* mutant (Fig. 3-14B). This demonstrated, that *clpP2* inactivation has an effect on tartrolon B resistance only in the presence of *timAB*.

To validate these data, an IPTG-inducible variant of *timAB*, in which TimA is fused to a C-terminal Strep-tag to facilitate TimA detection by Western blotting (i*timA-strep-timB*) was constructed and introduced into the Δ*clpP2* Δ*timAB* background. The tartrolon B resistance level was measured in the presence or absence of IPTG. In the absence of IPTG, this strain should have a tartrolon B MIC comparable to the one of the Δ*timAB* single and Δ*clpP2* Δ*timAB* double mutant, whereas in presence of IPTG, a Δ*clpP2* phenotype should be acquired due to

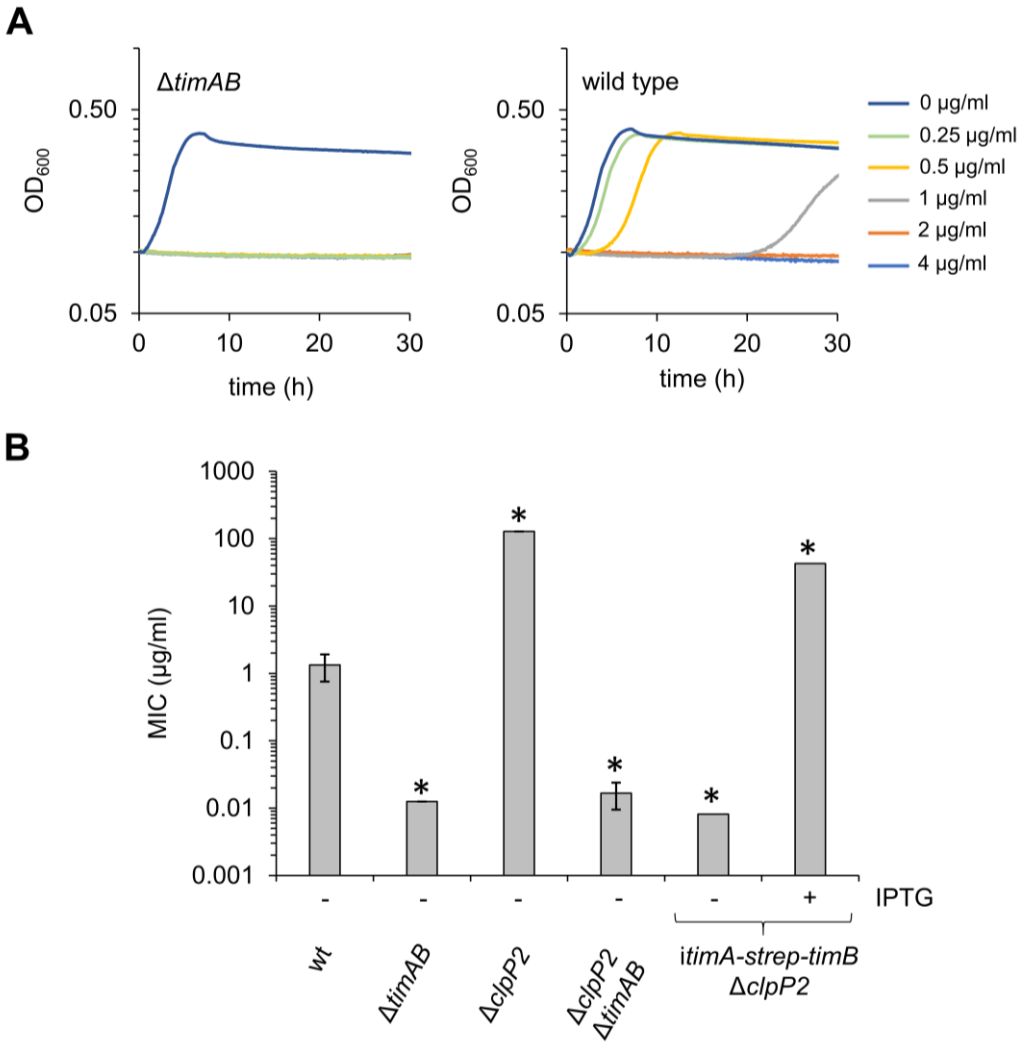

Figure 3-14: Analysis of the interplay between *timAB* and *clpP2* in regards to tartrolon B resistance. (A) Growth curves to test for the appearance of tartrolon B resistant suppressors in strain LMTE34 (Δ*timAB*). Wild type and LMTE34 were grown in the indicated amounts of tartrolon B for 30 h at 37°C. Suppressor formation was usually observed if the culture showed growth after >20 h. **(B)** Tartrolon B MICs for the *clpP2 timAB* double mutant strain. Strains LMTE34 (Δ*timAB*), LMTE80 (Δ*clpP2*), LMTE95 (Δ*clpP2* Δ*timAB*) and LMTE110 (i*timA-strep-timB* Δ*clpP2*) were inoculated to an OD_{600} of 0.1 and the tartrolon B MIC determined via a serial dilution assay. The experiment was performed three times and average values as well as standard deviations shown. Asterisks mark statistically significant changes as determined by a t-test followed by a Bonferroni-Holm correction ($P<0.05$).

the transcription of *timAB*. The results were in line with these expectations, as this strain was able to span the entire tartrolon B resistance range of *L. monocytogenes*. When grown without IPTG, the tartrolon B MIC determined for this strain was 0.008±0.006 µg/ml, therefore being in the same resistance range as the Δ*timAB* and of the Δ*clpP2* Δ*timAB* mutant. In the presence of IPTG, the resistance level increased ~5000-fold to levels comparable to the Δ*clpP2* strain (MIC=42±18 µg/ml) (Fig. 3-14B).

3.3.7 Role of potassium for tartrolon resistance of Δ*clpP2* and Δ*timAB* mutants

The gain of tartrolon B resistance in a Δ*clpP2* strain could be manifested in other beneficial traits that help the mutant survive against the antibiotic. The results obtained in the previous chapters suggest that tartrolon B acts as a potassium ionophore. Therefore, the resistance gain of a Δ*clpP2* strain could be caused by a mechanism that helps the mutant to cope with potassium deficiency.

A suitable experiment to test this theory is to determine the resistance level of the Δ*clpP2* strain to boromycin, since the mode of action of these two compounds appeared to be identical in previous experiments. The boromycin MIC for wild type and Δ*clpP2* was determined from growth curves in different concentrations of the antibiotic at 37°C (Fig. 3-15A). In contrast to the ~100-fold increase in resistance against tartrolon B, the Δ*clpP2* mutant was not significantly resistant to boromycin. These experiments suggested, that there is no linkage of a disrupted potassium homeostasis in the Δ*clpP2* mutant to its resistance gain against tartrolon B.

To further test the effect of potassium on the tartrolon B resistance level of a Δ*clpP2* mutant, BHI medium was supplemented with potassium chloride and the tartrolon B MIC of the mutant determined. As the main conclusion of the previous chapter was that deletion of *clpP2* mediates

resistance only in presence of *timAB*, the tartrolon B MICs of the Δ*timAB* and Δ*clpP2* Δ*timAB* mutants were also analyzed in dependence of potassium (Fig. 3-15B). Strains lacking *timAB* showed a high responsiveness to potassium independent of the presence of *clpP2*, as the tartrolon B MIC of the Δ*timAB* mutant in potassium-rich medium increased ~250-fold from 0.02±0.009 µg/ml to 5.3±2.3 µg/ml and the tartrolon B MIC of Δ*clpP2* Δ*timAB* in a similar margin from 0.03±0.009 µg/ml to 5.3±2.3 µg/ml. However, the Δ*clpP2* mutant was barely affected in its tartrolon B resistane level upon potassium supplementation, as the MIC for this mutant increased 2-fold from 106±37 µg/ml in absence to 256±0 µg/ml in presence of potassium. The general trend in this experiment was, that the tartrolon B resistance gain of a strain in presence of potassium was inversely correlated with its intrinsic resistance level in the absence of potassium.

Another point of interest regarding the potassium mediated resistance gain was the role of the *timAB* expression level. In a model where TimAB constantly exports tartrolon B, strains with elevated *timAB* expression should be less dependent on a potassium rich media as they are able to maintain a more stable membrane potential. To validate this hypothesis, a second IPTG-inducible copy of *timAB* was introduced into the wild type and the Δ*timR* background and the tartrolon B MIC in presence and absence of potassium chloride analyzed (Fig. 3-15C). As a first observation, the resistance levels and the responsiveness to potassium obtained when the strains were grown in absence of IPTG were similar to the ones of the wild type and the Δ*timR* mutant, respectively. In presence of IPTG, the effect of potassium on tartrolon B resistance level was diminished, as *timAB* overexpression in the wild type led to a ~5-fold higher MIC upon potassium supplementation, and the Δ*timR* P_{help}-*timAB* strain being even less responsive to the alkali metal, in which supplementation with potassium only resulted in a 2-fold increase in its tartrolon B MIC. In these experiments, another pattern is recognizable: The higher the level of TimAB in a strain, the lower the effect of potassium becomes in mediating tartrolon B

resistance. The high level of TimAB might also be the reason for the highly resistant phenotype of the Δ*clpP2* mutant, possibly due to TimAB being substrate of ClpP2, which would accumulate in a strain lacking the protease due to the lack of degradation.

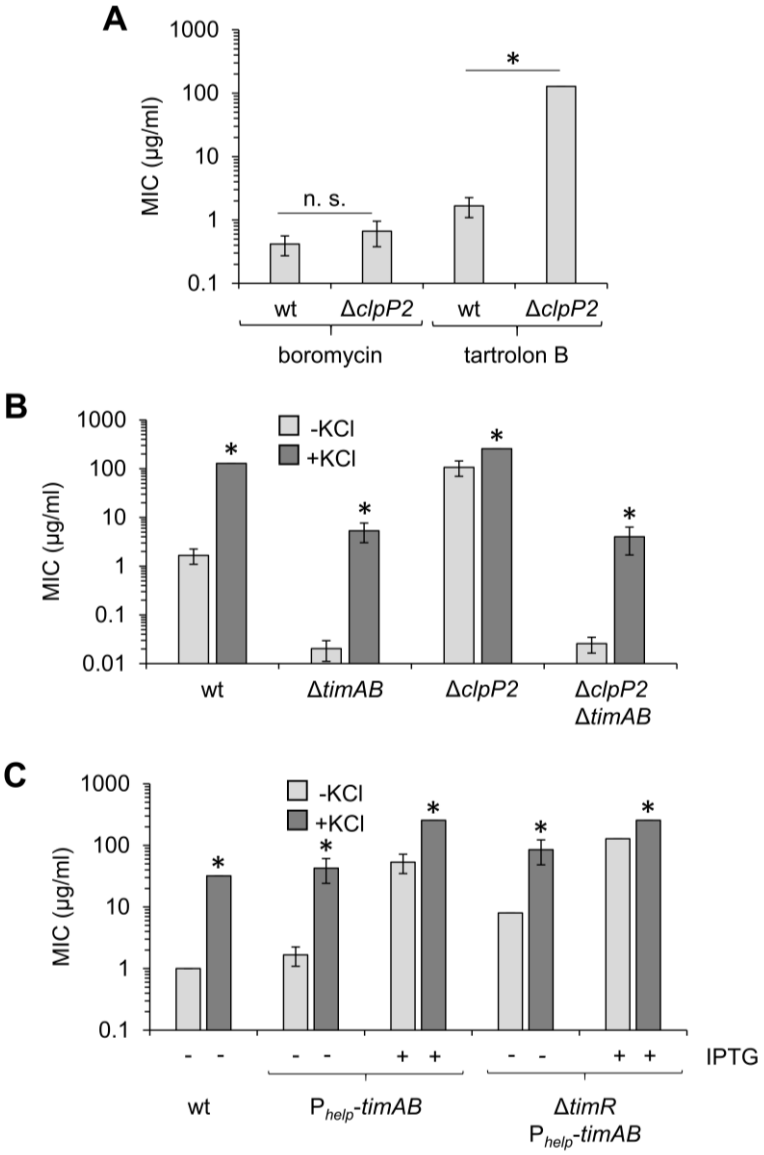

Figure 3-15: Effect of high potassium concentrations on the resistance level of selected *tim* and *clpP2* mutant strains. Strains were inoculated to an OD_{600} of 0.05 and the MICs determined by growth experiments at 37°C in serial dilutions of the respective antibiotic in BHI medium. **(A)** MICs of the Δ*clpP2* mutant to boromycin and tartrolon B.. **(B)** Tartrolon B resistance levels of strains Δ*timAB* (LMTE34), Δ*clpP2* (LMTE80) and Δ*clpP2* Δ*timAB* (LMTE95) upon supplementation of BHI medium with 250 mM KCl. **(C)** Effect of 250 mM potassium on tartrolon B resistance of strains overexpressing *timAB*. Strains containing a second IPTG-inducible *timAB* allele in the wild type (LMTE89) and in a Δ*timR* background (LMTE94) were analyzed for their tartrolon B resistance ±250 mM KCl.
All experiments were conducted in triplicates and average values and standard deviations are shown. Asterisks mark statistically significant differences as determined by a *t*-test and the Bonferroni-Holm correction (P<0.05).

3.3.8 Analysis of TimA levels

The *timAB* genes being dominant over *clpP2* with respect to tartrolon B resistance suggests that either TimA or TimB - or both - are ClpP2 substrates. In this model, the transporter would be constantly degraded by ClpP2, resulting in a moderate level in the cell. In the absence of a functional ClpP2, the transporter could not be degraded anymore and therefore accumulates, mediating high-level resistance to tartrolon B. This hypothesis was previously undermined by IPTG-dependent *timAB* expression in a Δ*timR* background, which matched the MIC of the Δ*clpP2* mutant at 128±0 µg/ml (see previous chapter). In addition, complementation of the Δ*clpP2* Δ*timAB* with an ectopic i*timA-strep-timB* copy rescued the phenotype of the Δ*clpP2* mutant. Since expression of the *timAB* genes are under control of the *lacO-lacI* system in this strain, and not under control of their native promoter, this suggests that the resistance gain of the Δ*clpP2* mutant is not caused by transcriptional activation of P_{timA}. Therefore, the resistance-gain of the Δ*clpP2* mutant could be caused by accumulation of the TimAB transporter, caused by a lack of degradation of TimAB by ClpP2.

To test the hypothesis of TimAB being a ClpP2 substrate, the strains carrying i*timA-strep-timB* (LMTE106) and i*timA-strep-timB* Δ*clpP2* (LMTE110) were used in a degradation assay. The Strep-tag fused to the C-terminus of TimA allowed monitoring of the protein by Western blotting using an antibody which binds to the Strep-tag. TimA seemed more likely to be a substrate of ClpP2 than TimB, since it represents the ATPase domain and is therefore soluble in the cytosol. In this context, a Δ*timAB* background appeared to be appropriate in order to eliminate slower degradation rates of the Strep-tagged protein caused by untagged TimA in a wild type scenario. Additionally, the wild type and the Δ*clpP2* mutant were used in this experiment to distinguish between TimA-Strep and non-specifically detectable proteins.

To analyze TimA-Strep degradation, the strains described were grown at 37°C to an OD_{600} of 0.8-1.0. Half of the culture was pelleted and stored at -20°C, while the other half was treated with chloramphenicol to stop protein translation. The strains were shaken for a further 90 min before being pelleted. The crude extracts of these strains were analyzed for their TimA-Strep levels by Western blotting using the wild type and Δ*clpP2* mutant as control strains (Fig. 3-16). As a control for the suitability of the assay, a second antibody against the known ClpP2 substrate MurA was used. If TimA was indeed a ClpP2 substrate, a degradation of the Strep-tagged protein should be observed in a Δ*timAB* background, but not in the Δ*clpP2* Δ*timAB* background.

A clear loss of the MurA band 90 min after translation stop was observed in the wild type background, whereas the MurA level remained constant when ClpP2 was lacking. Also, MurA accumulation could be seen in both strains lacking *clpP2*, validating the proper construction of these strains. However, the intensity of the TimA-Strep band remained unchanged even when ClpP2 was present. This suggests that TimA is not a ClpP2 substrate and that the increased TimAB activity - if present in a Δ*clpP2* background - is caused by a different mechanism. The same experiment was done using TimB-Strep, this protein was, however, not detectable, likely because of TimB being a transmembrane protein.

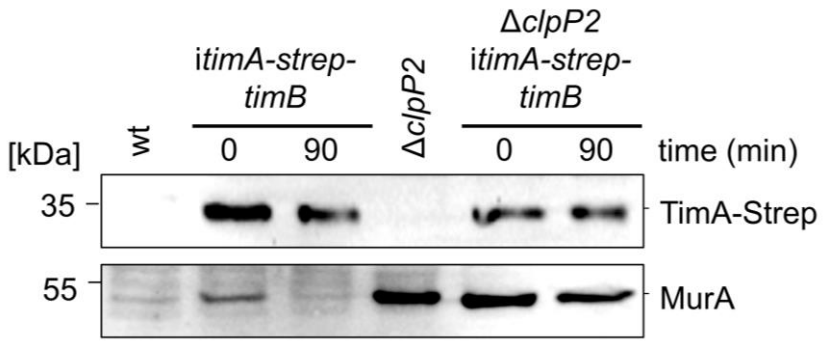

Figure 3-16: Western blot for the analysis of TimA-Strep degradation by ClpP2. The wild type and strains LMTE80 (Δ*clpP2),* LMTE106 (i*timA-strep-timB*) and LMTE110 (Δ*clpP2* i*timA-strep-timB*) were grown to mid-log phase, half of the culture harvested and 200 µg/ml chloramphenicol added to the other half. After incubation for a further 90 min, the cells were harvested and lysed by sonification. The crude extract was used to analyze the level of TimA-strep in each sample, with a parallel immunoblot using an α-MurA antibody as a control.

3.3.9 Determination of tartrolon B resistance levels in Clp ATPase mutants

Data from previous experiments suggested that the tartrolon resistance gain of a Δ*clpP2* mutant is caused by accumulation of a ClpP2 substrate involved in tartrolon detoxification. The fact that ClpP2 is only active when complexed with an ATPase which opens its proteolytic chamber is widely known (Katayama *et al.*, 1988, Frees *et al.*, 2007, Alexopoulos *et al.*, 2012). As a logical consequence, suppressor mutations inactivating the ATPase responsible for the proteolytic degradation of the said substrate should also become resistant to the antibiotic. However, despite numerous attempts, none of these suppressor mutations could ever be isolated. One explanation for this is, that the degradation of the substrate can be initiated independently of any ATPase, or that the ATPases are redundant. In such a scenario, multiple ATPases would have to be inactivated for a suppressor to become resistant, which is less likely than a single inactivating mutation in *clpP2*.

In *L. moncytogenes*, three ATPases are known, which interact directly with ClpP2 - namely ClpC, ClpE and ClpX (Derré *et al.*, 1999, Gatsogiannis *et al.*, 2019, Wamp *et al.*, 2020). Strains lacking one, two or all three of these ATPases were created and agarose gels used to confirm deletions, exemplarily shown in Fig. 3-17A. The size of the amplified ATPase-loci on the gel matched the theoretical sizes of the wild type or deletion loci in every mutant.

All of these ATPase mutant strains were tested for tartrolon B resistance by plotting growth curves at different tartrolon B concentrations (Fig. 3-17B). The single deletion mutants lacking *clpC* (MIC=1.6±0.6 µg/ml) and *clpE* (MIC=1±0 µg/ml) did not show a significantly increased tartrolon B resistance compared to the one determined for the wild type at 1±0 µg/ml, while the tartrolon B MIC for the Δ*clpX* mutant was slightly increased (MIC=2±0 µg/ml). A Δ*clpP2*-like resistance level of 42.7±18.5 µg/ml could only be reached upon deletion of both *clpX* and *clpC* (MIC=26.6±9.2 µg/ml), and as a logical consequence also in a Δ*clpCEX* triple mutant

(MIC=42.7±18.5 µg/ml). It is also noteworthy, that the Δ*clpC* mutant showed the biggest growth deficit out of all the three single deletion strains, whereas a Δ*clpP2* like growth deficit was only reached in the Δ*clpCX* and Δ*clpCEX* strains (data not shown).

At last, the genome of the strains carrying deletions in *clpX* were sequenced, since a Δ*clpX* mutant has not yet been described in *L. monocytogenes*. While the genome of the Δ*clpX* and Δ*clpCEX* mutants were free of unwanted second site mutations, the Δ*clpCX* mutant carried a 250 kbp genome duplication starting from the 23S rRNA encoding gene *lmor14* and ending with another 23S rRNA encoding gene (*lmor17*) (Fig. 3-17C). Hence, all genes ranging from *lmo2367* to *lmo2589* are present twice in the Δ*clpCX* genome. However, this mutant matched expectations regarding its clear growth deficit and tartrolon B resistance level. This led to the assumption, that the genome duplication has no major effect on the tartrolon B phenotype of the mutant, which is also validated by the fact, that the clean Δ*clpCEX* mutant strain shares the same growth deficit and tartrolon B resistance level as the Δ*clpCX* mutant strain.

These results suggest that the reason for tartrolon B resistance in a Δ*clpP2* strain is due to its lack of proteolytic degradation of (an) unknown substrate(s), which results in the accumulation of at least one protein, which mediates tartrolon B resistance and can be degraded by the ClpCP2 and ClpXP2 proteasomes.

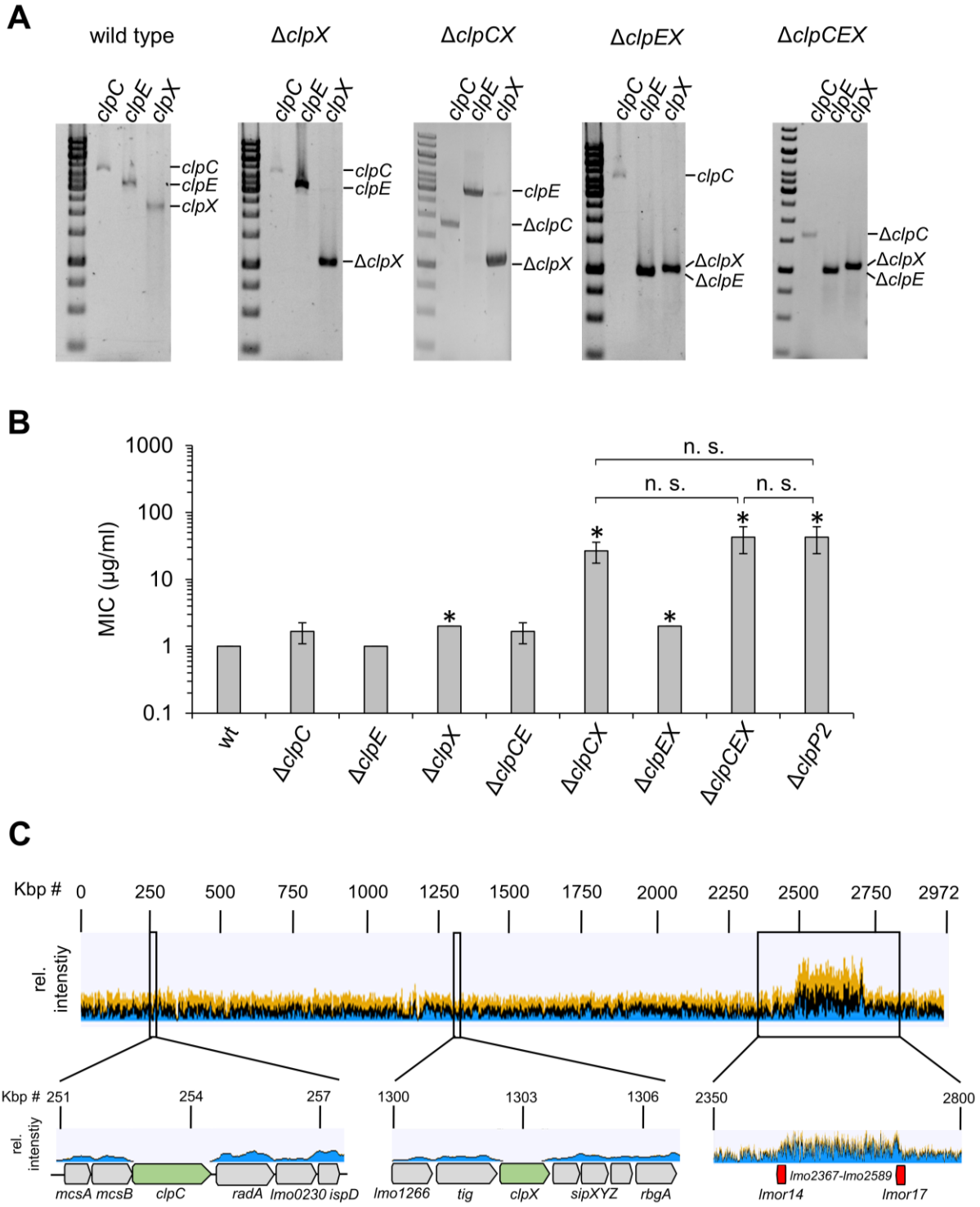

Figure 3-17: Generation and characterization of Clp ATPase mutants. (A) Agarose gels for validation of each *clpX* deletion strain. The presence of all three Clp ATPase genes was analyzed for each strain. Theoretical fragment sizes: *clpC*: 4.5 kb, *clpE*: 3.4 kb, *clpX*: 2.8 kb, Δ*clpC*: 1.7 kb, Δ*clpE*: 1 kb, Δ*clpX*: 1.1 kb. **(B)** Tartrolon B MICs for each Clp ATPase mutant at 37°C. The MICs were determined in triplicates and average values and standard deviations are shown. Asterisks mark statistically significant resistance levels using a *t*-test and the Bonferroni-Holm correction ($P<0.05$). **(C)** Genome sequence of the Δ*clpCX* mutant. The genomic loci around *clpC* and *clpX* as well as the region where genome duplication occurred are shown with the relative intensity of detected reads in the sequencing experiment.

3.3.10 The role of *spxA1* in tartrolon B resistance

Throughout the screening for tartrolon B resistant suppressor mutants, a single mutant (LMTE66) was isolated, which carried a frame shift in *ybjH* caused by the deletion of its 424th nucleotide, which on a protein level leads to the replacement of glutamic acid 143 by an isoleucine, followed by an immediate stop codon. YbjH therefore lacks the following 112 amino acids that occur in the natural protein sequence (Fig. 3-18A). This probably leads to inactivation of YjbH. To confirm this hypothesis, a Δ*ybjH* mutant was generated, and its tartrolon B MIC determined. The Δ*ybjH* strain showed the same two-fold increase in resistance as in the *ybjH* suppressor, consistent with the expectation, that the frame shift in *ybjH* inactivates the protein (Fig. 3-18B).

In *Bacillus subtilis*, YjbH has only one known function, which is to increase the ClpCP- and ClpXP-mediated degradation rate of Spx, a transcriptional regulator (Larsson *et al.*, 2007, Rojas-Tapias & Helmann, 2019). Spx is involved in the regulation of ~275 genes responsible for various cellular processes, such as responses to disulfide or cell wall stress, competence development, but also in detoxification of antibiotics (Nakano *et al.*, 2001, Larsson *et al.*, 2007, Runde *et al.*, 2014, Rojas-Tapias & Helmann, 2018, Rojas-Tapias & Helmann, 2019). It has been shown, that a *B. subtilis* Δ*clpP* mutant shows high levels of Spx, since degradation of the protein is absent (Nakano *et al.*, 2001, Rojas-Tapias & Helmann, 2019). Two paralogues of Spx (SpxA1 and SpxA2) are annotated in the *L. monocytogenes* genome, however, SpxA1 is the biologically active one (Whiteley *et al.*, 2017). Assuming the control of the Spx level by ClpP shown in *B. subtilis* can be applied to *L. monocytogenes* SpxA1 and ClpP2, respectively, accumulation of SpxA1 causing the activation of tartrolon resistance genes could be the reason for the resistance of a Δ*clpP2* mutant. In general, the SpxA1 level should correlate positively with tartrolon resistance - but only when TimAB is present.

Under standard growth conditions, *spxA1* is an essential gene in *L. monocytogenes* (Cesinger *et al.*, 2020). Hence, it was not possible to create a Δ*spxA1* deletion mutant and a strain carrying an IPTG inducible copy of *spxA1* was created instead. While the strain showed a wild type-like growth rate in the presence of IPTG, it only grew to a low OD_{600} in absence of IPTG (Fig. 3-18C). The strain was tested regarding its tartrolon B resistance level in the absence and presence of IPTG. If IPTG was absent, the tartrolon B MIC of the i*spxA1* strain was reduced 4-fold compared to wild type levels (Fig. 3-18D). This matched the hypothesis of the SpxA1 level correlating with tartrolon B resistance.

The impact of an IPTG-inducible *spxA1* copy regarding the tartrolon B MIC was also analyzed in the Δ*timAB* strain and the wild type. The resulting strains were tested regarding their tartrolon B MIC in absence and presence of IPTG and compared to the MIC of each parental strain, which lacks the *spxA1*-expressing plasmid. As a first observation, the slight growth deficit in the presence of IPTG of both strains has to be pointed out (Fig. 3-18E), which validates the proper function of the desired strains since *B. subtilis* strains overexpressing *spx* are also known to possess growth deficits (Larsson *et al.*, 2007). The tartrolon B resistance level increased two-fold in presence of IPTG in the wild type background from 2±0 µg/ml to 4±0 µg/ml, while no significant increase in the MIC of the Δ*timAB* mutant was observed. This further suggested, that an increased level of SpxA1 is only beneficial for tartrolon B resistance, if the *timAB* genes are present. However, the effects observed were only minor and a clear conclusion could not be drawn from this experiment alone.

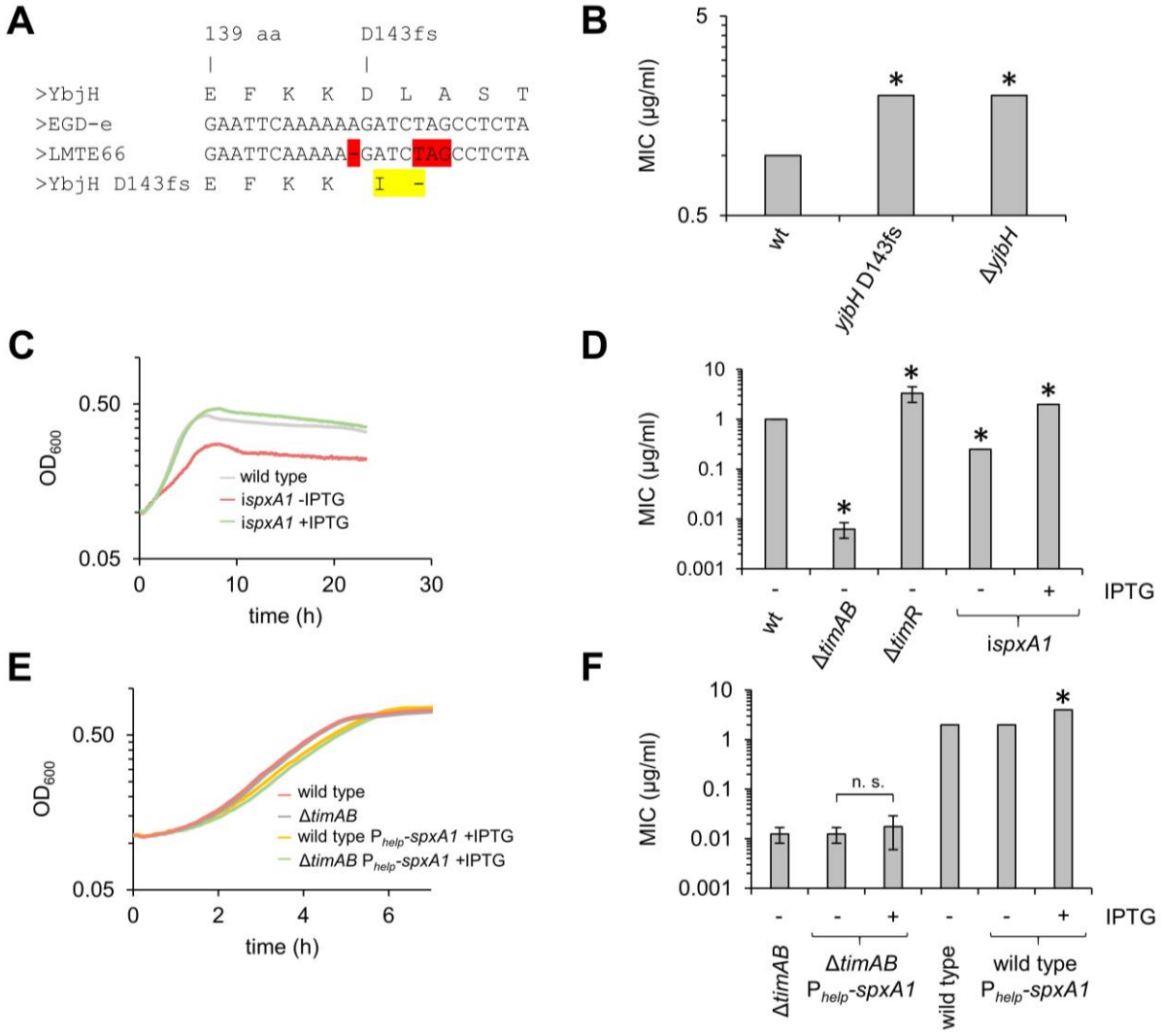

Figure 3-18: Impact of *spxA1* on tartrolon B resistance. (A) DNA and resulting protein sequence of a tartrolon B resistant suppressor carrying a frameshift in *yjbH*. The deleted base pair as well as the resulting premature stop codon are marked in red, and the altered protein sequence is marked in yellow. **(B)** Tartrolon B MICs of strains carrying the *yjbH* frameshift and a Δ*yjbH* deletion mutant in comparison to the wild type. **(C)** Growth curves of the i*spxA1* mutant strain ±IPTG compared to the wild type at 37°C. **(D)** Tartrolon B MICs of the i*spxA1* mutant ±IPTG. As controls Δ*timAB* and Δ*timR* strains as well as the and wild type were used. **(E)** Growth curves of strains overexpressing *spxA1* in the wild type and the Δ*timAB* background in comparison to their respective parental strains. **(F)** Tartrolon B MICs of strains overexpressing *spxA1* in the wild type and the Δ*timAB* background in comparison to their respective parental strains.
All experiments were conducted three times and average values as well as standard deviations are shown in case of the tartrolon B MICs. Asterisks mark statistically significant differences compared to the respective reference strains as determined by a *t*-test followed by the Bonferroni-Holm correction ($P<0.05$).

Since accumulation of SpxA1 is likely the reason for a *clpP2* mutant being highly resistant to tartrolon B, but a Δ*clpP2* Δ*timAB* mutant breaks this phenotype, the logical consequence is that SpxA1 accumulation only mediates tartrolon B resistance if *timAB* is present. This could be accomplished by three mechanisms: (1) SpxA1 could activate expression of the *timABR* operon, (2) SpxA1 activates the expression of another transcriptional activator, which then activates the *timABR* operon, or (3) SpxA1 activates the transcription of a gene encoding for a protein, which enhances the TimAB-mediated detoxification rate of tartrolon B.

3.4 Gallidermin induces the promoter of the *lmo0193-lmo0195* genes

Tartrolon B inducing the expression of the *timABR* genes was not the only hit obtained in the compound library screen described in chapter 3.1.4, as gallidermin, and to a lesser extend enduracidin were capable of inducing the genes of another uncharacterized ABC transporter (*lmo0194-lmo0195*) (Fig. 3-19A). Both antibiotics are antimicrobial peptides synthesized by *Staphylococcus gallinarum* (gallidermin) and *Streptomyces fungicidicus* (enduracidin) (Higashide *et al.*, 1968, Kellner *et al.*, 1988). These compounds belong to class A lantibiotics, therefore sharing the same mechanism of action as nisin or ramoplanin, which is the inhibition of cell wall biosynthesis by binding to the peptidoglycan precursor lipid II (Fang *et al.*, 2006, Panina *et al.*, 2021). This suggests, that the Lmo0194/0195 ABC transporter could be a transporter for lipid II targeting lantibiotics. In a similar manner to the TimAB experiments validating its capability to export tartrolon B, a Δ*lmo0194/lmo0195* deletion mutant was created and its MIC for gallidermin determined. However, the deletion mutant had no phenotype with respect to gallidermin resistance.

This could be due to the fact that several different MDR transporters are active in the wild type, all of which export gallidermin. In such a scenario, phenotypic differences would only manifest in strains lacking multiple, or all of these transporters. To identify closely related transporters, a multiple alignment was performed. The resulting phylogenetic tree encompassing the ATPase components for each ABC transporter identified in chapter 3.1.1 is shown in Fig. 3-19B. In this tree, Lmo0194 appeared to be homologous to the Lmo0744 and Lmo2372 ATPases. Pairwise alignment of Lmo0194 to either of these genes yielded a 63% homology (44% sequence identity) to Lmo0744 and a 59% homology (37% sequence identity) to Lmo2372.

At first, gallidermin and enduracidin were tested in their ability to induce the $P_{lmo0744}$-*lacZ* and $P_{lmo2371}$-*lacZ* reporter strains in a disc diffusion assay using the strain carrying the $P_{lmo0193}$-*lacZ* construct as positive control. While the induction of $P_{lmo0193}$-*lacZ* with gallidermin was barely visible, it was not able to induce the other two promoters (data not shown). Disregarding this observation, a Δ*lmo0194-lmo0195* Δ*lmo0744* Δ*lmo2371-lmo2372* triple mutant strain was created and its sensitivity to gallidermin analyzed. However, even this triple deletion strain showed no phenotypic differences compared to the wild type.

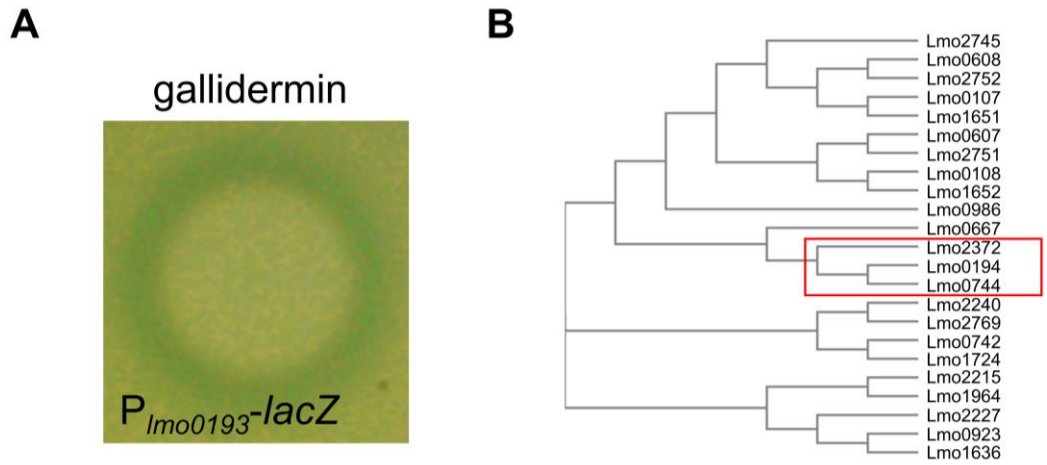

Figure 3-19: Analysis of gallidermin detoxification in *L. monocytogenes*. (A) Induction of $P_{lmo0193}$ by gallidermin. Strain $P_{lmo0193}$-*lacZ* was poured into warm BHI-agar containing 50 µg/ml X-Gal and 1µl gallidermin spotted on top of the plate. After incubation over night at 37°C, the induction circle shown was visible. **(B)** Phylogenetic tree of the ATPase proteins/domains for each MDR transporter identified in chapter 3.1.1. The ATPases clustering with Lmo0194 are marked in the red rectangle.

3.5 Analysis of LftR binding to the *lieAB* promoter

A previously characterized ABC-type MDR transporter was the LieAB transporter. This transporter functions as an exporter of aurantimycin, a depsipeptide secreted from *S. aurantiacus* (Hauf *et al.*, 2019). Expression of the *lieAB* genes is tightly repressed by LftR, and aurantimycin resistant clones isolated from a suppressor screen frequently carry mutations in *lftR*, the *lftR* promoter sequence or the *lieAB* ribosomal binding site. From this suppressor screen, two strains were isolated, which carried SNPs in *lftR*, with the first strain carrying a LftR G27S variant and the second strain carrying a LftR T46M variant. These LftR-variants were purified as a Strep-tagged protein and their ability to bind to the *lieAB* promoter was tested in an EMSA experiment using native LftR as a control. The three bands representing different LftR:P_{lieAB} complexes, which are established when using P_{lieAB} and wild type LftR were all missing when the G27S and T46M variants were used, suggesting that these amino acids are essential for LftR-binding to its operator sequence on the *lieAB* promoter (Fig. 3-20A).

To determine the binding site of LftR on the *lieAB* operator, stepwise truncations of the *lieAB* promoter fragment were fused to *lacZ* and the β-galactosidase activity in strains carrying these constructs measured in the absence and presence of subinhibitory concentrations of aurantimycin. A higher β-galactosidase activity in any of these strains in absence of aurantimycin would indicate a higher activity of the *lieAB* promoter caused by a weakened binding of LftR. In contrast, a lower β-galactosidase activity in any strain in the presence of aurantimycin would suggest, that crucial elements of the *lieAB* promoter needed for its induction were already truncated. Fig. 3-20B summarizes the β-galactosidase activity of each strain carrying the construct illustrated on the left in the absence and presence of aurantimycin. The β-galactosidase activity was not significantly affected when the promoter fragment was shortened from 315 to 122 base pairs, suggesting that no important regulatory elements are

present in this region. However, aurantimycin-mediated induction of the promoter was ~10-fold reduced if the promoter fragment was shortened from 122 to 97 base pairs. This result suggested that the nucleotides 1 to 122 contain critical elements for promoter activity.

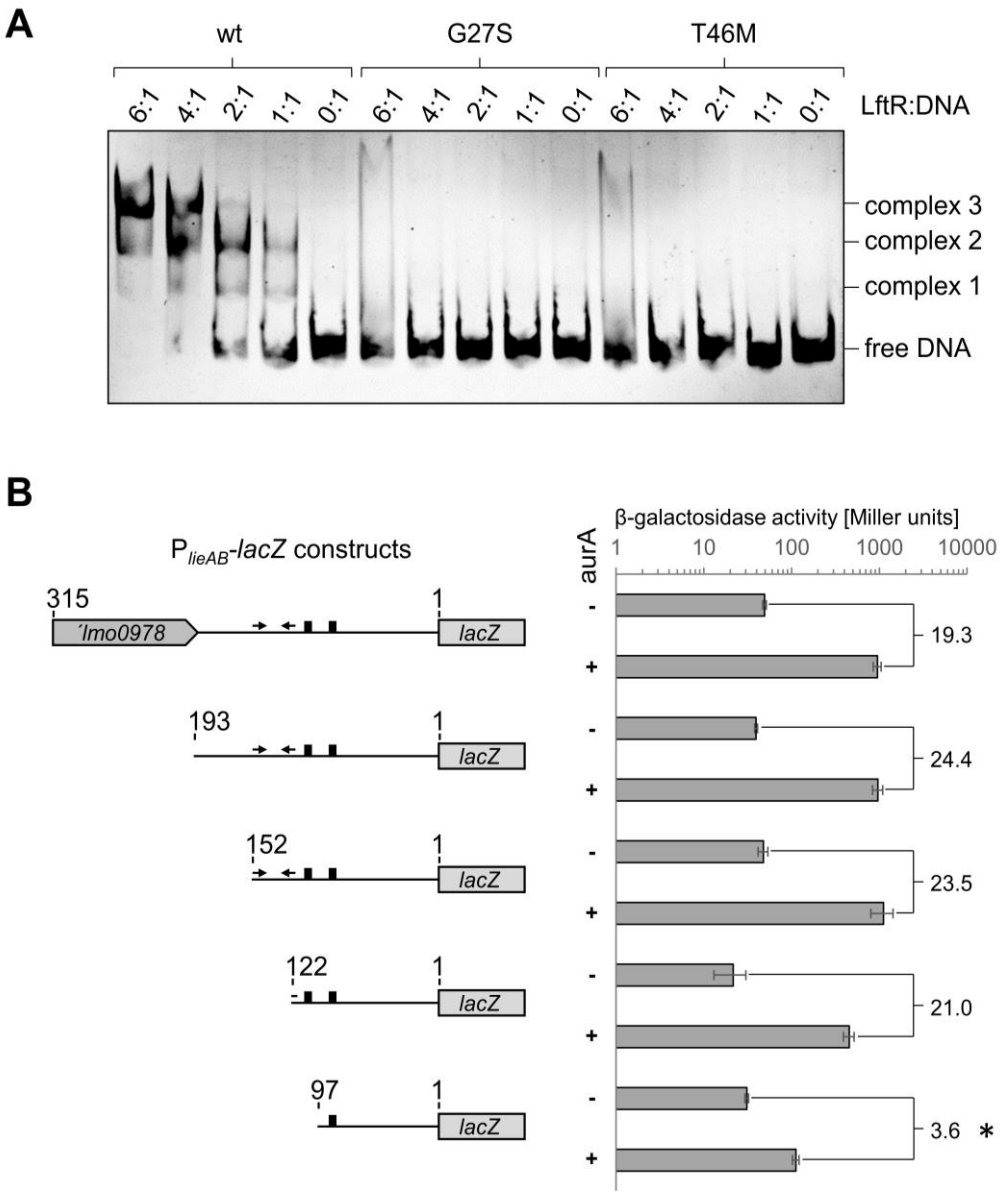

Figure 3-20: Studies investigating the binding of LftR to P_{lieAB}. (A) PA-gel for the analysis of the binding capabilities of LftR variants identified in an aurantimycin suppressor screen. The LftR proteins were mixed with the *lieAB* promoter fragment in the indicated molar ratios and the establishment of the described molecular complexes visualized by ethidium bromide staining. The experiment was performed three times showing similar results each time. **(B)** Quantification of β-galactosidase activity of the respective P_{lieAB}-*lacZ* constructs shown on the left. Strains carrying the respective *lacZ*-fusions were incubated at 37°C ±100 ng/µl aurantimycin A (aurA) until mid-log phase. After lysis, the β-galactosidase activity of each supernatant was determined. The experiment was conducted as a biological triplicate, and average values and standard deviations are shown. Statistically significant differences were determined using a *t*-test and are indicated as asterisks. As reference, the full-length fragment shown on top was used.

The reason for the weak induction of $P_{lieAB(1\text{-}97)}$ by aurantimycin is likely due to the -35 box consisting of nucleotides 105-111 not being present in this construct, which leads to promoter inactivation. A mutated LftR binding site would however be manifested in a highly active *lieAB* promoter. LftR is a PadR-type repressor protein recognizing inverted repeats which consist of a 4 to 9- bp long motifs that are separated by a 4- to 8-bp long spacer region (Nguyen *et al.*, 2011). A motif like this is present on P_{lieAB} (TTACTA-N_5-TAGTAA) and shown in red in Fig. 3-21A. Since the first repeat of this motif was part of the -10 box, mutating this repeat would likely cause promoter inactivation. Hence, the second putative repeat of this motif ranging from nucleotides 78 to 73 was mutated, however, this did not change the induction ratio of P_{lieAB}-*lacZ* (data not shown). This led to the conclusion that the binding site had to be further downstream on the promoter region. To identify the LftR binding site, the β-galactosidase activity of strains carrying systematic transversions (G↔C and A↔T) of 10 nucleotides ranging from the nucleotides 69 to 21 was measured in the absence of presence of aurantimycin. This led to the observation, that if the nucleotides 69-61 or 60-51 are transversed, the *lieAB* promoter is induced 12- and 31-fold in the absence of aurantimycin, respectively. However, aurantimycin was still able to induce these promoters 2- and 4-fold, respectively, with a measured β-galactosidase activity of 1.182±142 MU for $P_{lieAB(1\text{-}122)\ \text{transversion}\ 69\text{-}61}$ and 1.755±88 MU for $P_{lieAB(1\text{-}122)\ \text{transversion}\ 60\text{-}51}$ in presence of the depsipeptide, which is close to the fully induced promoter present in the Δ*lftR* mutant (1.938±218 MU). Transversion of nucleotides 51-40, 40-31 and 30-21 did not significantly alter the *lieAB* promoter activity (Fig. 3-21B). With this data, the LftR binding site on P_{lieAB} could be narrowed down to the nucleotides 69-51, and further studies suggested, that the LftR operator sequence on P_{lieAB} consists of the nucleotides 69 to 56 (data not shown).

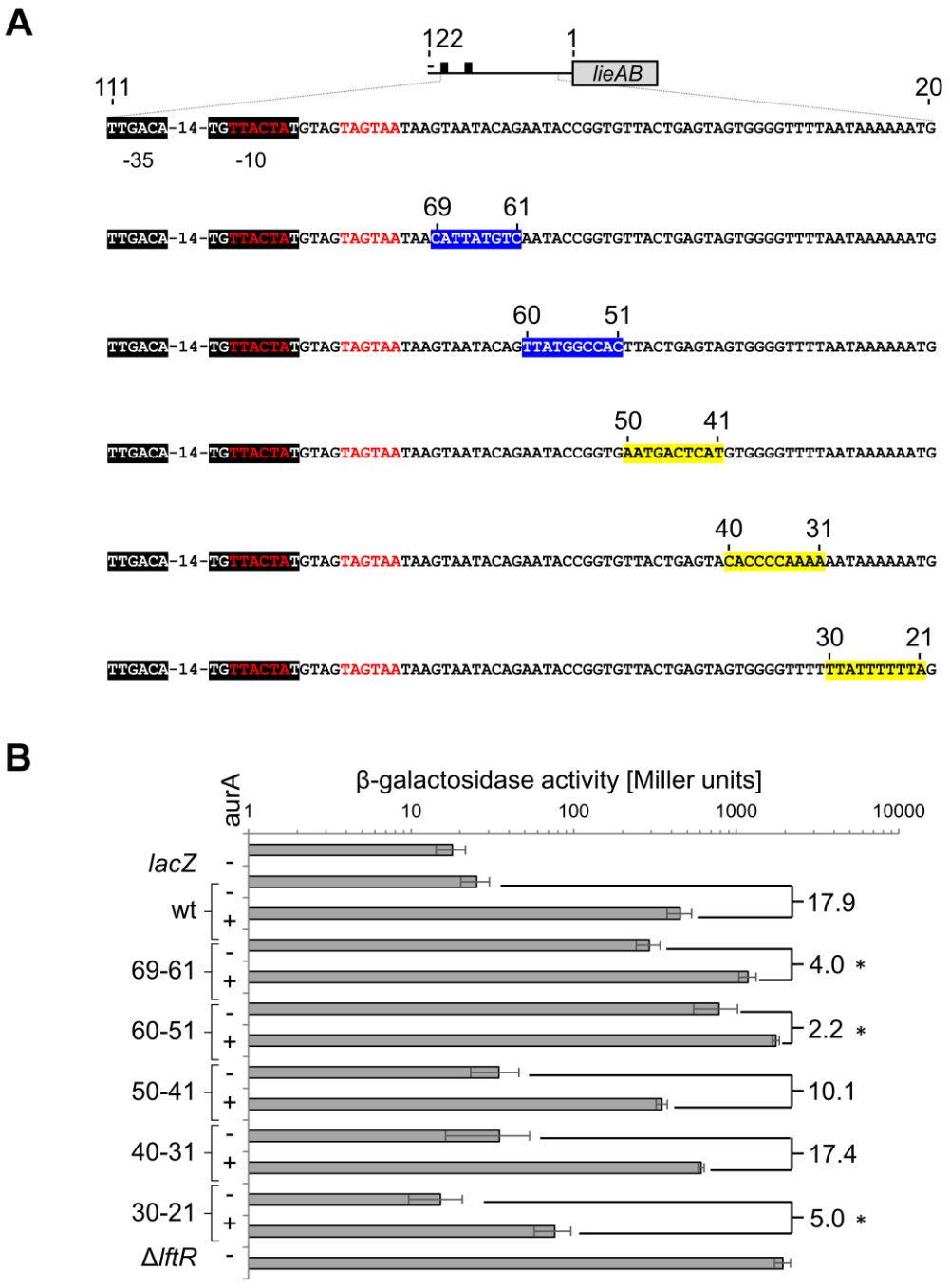

Figure 3-21: Identification of the LftR operator site. (A) Scheme illustrating the systematic nucleotide transversions on the *lieAB* promoter. The putative LftR binding motif is shown in red and the -35 and -10 boxes of the promoter fragment marked in black. Transversions leading to a significantly elevated P_{lieAB} activity in the absence of aurantimycin are marked in blue, while transversion having no effect on the promoter activity are shown in yellow. **(B)** Quantification of promoter activity of the constructs shown in (A) using a β-galactosidase assay. Strains LMSH16 (promoter-less *lacZ*) and LMSH98 (Δ*liftR* P_{lieAB}-*lacZ*) were used as controls. Each strain was grown until mid-log phase ±100 ng/µl aurantimycin at 37°C. The aurantimycin-mediated induction ratio for each strain is indicated. The experiment was conducted three times and average values and standard deviations are shown. Asterisks mark statistically significant differences (P<0.05, *t* test).

To confirm this theory, the nucleotides 69 to 56 on P_{lieAB} were transplanted into the *divIVA* promoter right downstream of its -10 box (Fig. 3-22A). An EMSA was performed investigating the binding of LftR to this synthetic construct. While LftR was unable to bind the native *divIVA* promoter, a shift towards a higher molecular complex could be seen, if LftR was incubated with P_{divIVA}-Op_{LftR} in a molar ratio of 6:1 (Fig. 3-22B). This validated the hypothesis, that the nucleotides 69 to 56 on P_{lieAB} function as the operator site for LftR.

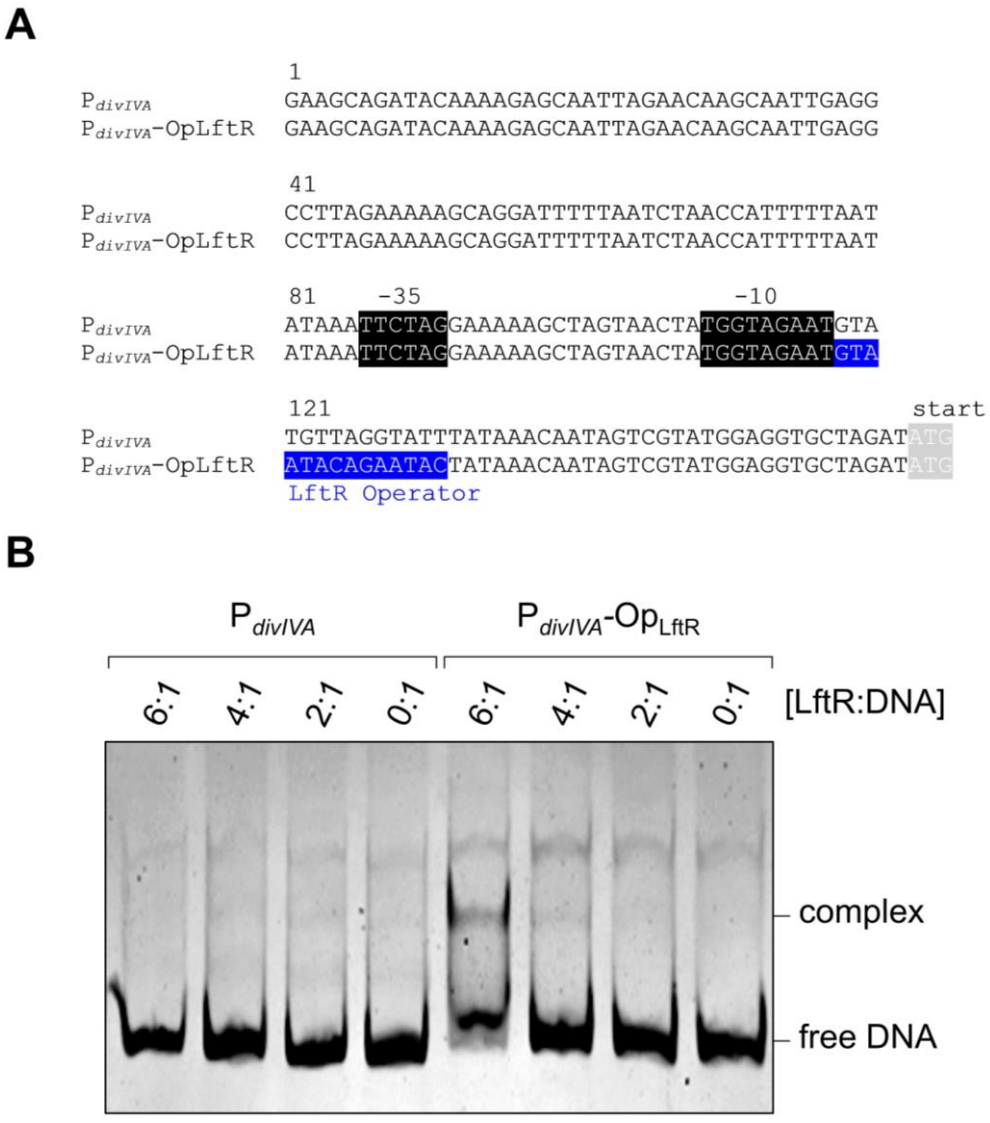

Figure 3-20: Validation of the LftR binding site on P_{lieAB}. (A) Schematic representation of the promoter fragments used for the EMSA experiment. **(B)** PA-gel for the analysis of LftR binding to the *divIVA* promoter with the transplanted LftR operator site (Op_{LftR}). Purified LftR was incubated with both promoter fragments in the molar ratios indicated and the indicated formation of a higher molecular complex visualized by ethidium bromide staining. The assay was performed three times, all repetitions showed similar results.

4 Discussion

4.1 Identification and screening of ABC-type MDR transporter genes

This project started with the identification of 20 putative ABC-type MDR transporter genes, which were identified *in silico* by using the TransportDB 2.0 database listed in Table 3-1. The database revealed ABC transporters which could potentially function as MDR transporters, since they are described as transporters having similarities to the daunorubicin transporters LmrCD (Lubelski *et al.*, 2006) or other multidrug transporters. The database did however get updated in 2023 (Elbourne *et al.*, 2023), and the improved algorithms identified four additional operons encoding ABC transporters with a potential function in drug export. ATPase and permease components of these transporters are listed in Table 4-1. None of these genes could yet be assigned with a general function.

Table 4-1: Further ABC transporter encoding genes involved in the detoxification of natural compounds.

ATPase	permease	class	operon
lmo0756	*lmo0757*	daunorubicin/multidrug	*lmo0755 lmo0756 lmo0757*
lmo0921	*lmo0920*	multidrug?	*lmo0920 lmo0921*
lmo1223	*lmo1224*	efflux (antimicrobial peptide)	*lmo1223 lmo1224*
lmo1505	*lmo1506*	efflux (antimicrobial peptide)	No operon detected

The transcript levels of the 20 originally identified ABC-type MDR transporters were analyzed as part of an earlier study (Hauf *et al.*, 2019). For each transporter gene, its promoter activity appeared weak in this dataset, which was good agreement with the activity observed when promoters were fused to *lacZ*, as β-galactosidase activity in the most active promoter (356±63 MU in $P_{lmo2214}$) was over 20-fold lower than the fully induced P_{lieA} promoter in the Δ*lftR*

background (8513±1507 MU). It therefore seemed likely that all promoters had the ability to be induced.

In order to screen the promoter-*lacZ* fusions for induction, a natural compound library was used, which included secondary metabolites from streptomycetes, myxobacteria and fungi. This library seemed well suited for this screen, since streptomycetes, myxobacteria and fungi co-occur with *L. monocytogenes* in the soil, making an adaptation against secondary metabolites secreted by these species quite likely. Additionally, streptomycetes are known to produce over 50% of all clinically relevant antibiotics (van der Heul *et al.*, 2018). However, only two promoters (P_{timA} and $P_{lmo0193}$) could be induced by any of the ~700 compounds tested.

4.2 The *timABR* operon mediates resistance to tartrolon B

4.2.1 Compound specificity of P_{timA} induction

The induction pattern of the *timA* promoter is very specific, since the induction can be visualized by minimal amounts of tartrolon B in the pg/ml scale, whereas tartrolon A mediated induction was only barely visible in agar-based diffusion assays. The induction circle obtained with tartrolon A was also very small, indicating that a much higher concentration of tartrolon A is needed to induce the promoter than the necessary amount of tartrolon B. No increase in β-galactosidase activity could be observed upon incubation of the P_{timA}-*lacZ* strain with tartrolon A concentrations right below the MIC. This is likely due to the fact, that the tartrolon A concentrations needed to induce the *timA* promoter are already inhibitory for *L. monocytogenes*.

In chapter 3.1.7, the underlying mechanism for P_{timA} induction was investigated in an EMSA experiment. Here, two complexes were formed representing different states of the promoter fragment bound to TimR. TimR is part of the TetR-like repressor family, which are known to form a homo-dimeric complex and interact with antibiotics (Ramos *et al.*, 2005, Bertram *et al.*,

2022). This binding of the antibiotic induces a conformational change in the repressor, which prevents interaction with its operator motif (Orth *et al.*, 2000). The two P_{timA}-TimR complexes formed could either indicate, that TimR has two binding sites on P_{timA} and the upper band represents the state in which two TimR dimers are bound to the promoter, or that TimR can also bind in its monomeric state to P_{timA}, forming the lower molecular complex. TetR-type repressors frequently only form a single complex with their corresponding nucleotide binding sites (Li *et al.*, 2012, Ray *et al.*, 2017, Grau *et al.*, 2020), which indicates, that TimR could indeed possess two binding sites on the *timA*-promoter.

In the previously described detoxification system for aurantimycin A, a similar system has been described. Here, the binding of the repressor protein LftR to the *lieAB* promoter could also be shown in an EMSA. However, this interaction could not be disturbed by aurantimycin A, even though the antibiotic is capable of inducing the promoter (Hauf *et al.*, 2021). However, the interaction of P_{timA} with TimR could be disturbed *in vitro* with tartrolon B, but not with tartrolon A, even though the structural formulas of their macrocycles are identical, with the only difference being the covalently bound boron atom in the hydrophilic center of tartrolon B.

This could be due to several reasons. One explanation could be the chemical properties of the macrocycle. Boronated tartrolons are macrodiolides with a C_2-symmetry (Mulzer & Berger, 2004), however tartrolon A undergoes rapid epimerization at its C2 atom, which leads to the loss of its C_2-symmetrical nature (Irschik *et al.*, 1995, Elshahawi *et al.*, 2013). The boron atom present in tartrolons B, C and E however fixes the configuration of the C2 atom, which forces the respective symmetric macrodiolide (Berger & Mulzer, 1999, Mulzer & Berger, 2004, Elshahawi *et al.*, 2013). Maintaining the C_2-symmetry might be the key for the improved binding of tartrolon B to dimeric TimR.

Another possibility is that the boron atom is needed because it directly interacts with TimR. There are examples of boron atoms binding directly to active centers of proteins (Bonvini *et al.*, 2007, Newman *et al.*, 2021), and in LexA, a transcriptional repressor has been shown to change its biological activity in presence of boronated compounds (Bellio *et al.*, 2020). However, the borate ester could also play a different role in the binding of tartrolon B to TimR, since the hydroxy-oxygens binding the boron in tartrolon B are quite far apart in tartrolon A. Binding of the boron atom in tartrolon B forces these oxygens into close proximity to each other. This leads to tartrolon A and B having quite different conformations regarding their macrocycle (Fig. 4-1). The different chemical properties of tartrolon A and tartrolon B were also investigated in a different work, where tartrolon B, but not tartrolon A was able to induce release of interleukin-1β in J774 macrophages and human peripheral blood mononuclear cells (Surup *et al.*, 2018).

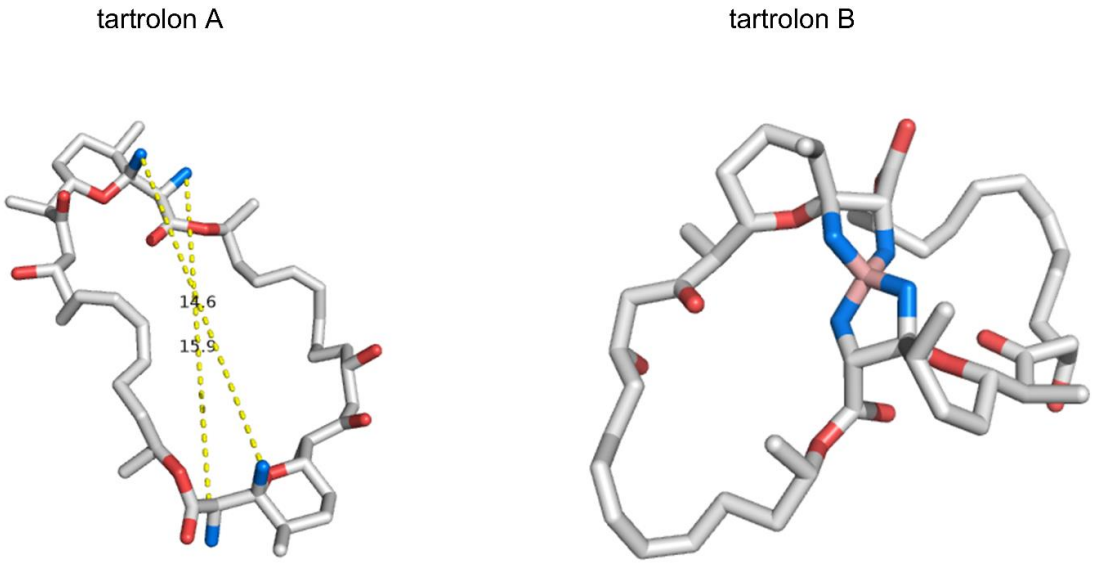

Figure 4-1: 3D-structures of tartrolon A (left) and tartrolon B (right). Chemical structures of both macrolides were drawn and their 3D-structure calculated using the software LEA3D (Douguet *et al.*, 2005) available on chemoinfo.ipmc.cnrs.fr/LEA3D/drawonline.html. The generated .pdb file was used to visualize both structures using the PyMOL software (DeLano, 2002). Carbon atoms are colored in gray and oxygen atoms in red. The oxygen atoms establishing the borate ester in tartrolon B are marked in blue in both macrolides and their intramolecular distances in tartrolon A measured in Å. The boron atom in tartrolon B is marked in pink.

4.2.2 Tartrolon resistance is dependent on TimAB

The tartrolon A and tartrolon B MICs for *L. monocytogenes* EGD-e were identical at 2 µg/ml. It is worth mentioning, that in later experiments, the tartrolon B MIC varied slightly in different experiments and ranged from 1-2 µg/ml for EGD-e. Overall, the MICs were in the same range as the ones reported for other gram-positive bacteria like *B. subtilis* and *S. aureus* at 0.31-0.62 µg/ml (Irschik *et al.*, 1995).

TimAB functioning as a tartrolon transporter could be confirmed by creation of a Δ*timAB* deletion strain, which became hyper-sensitive to the antibiotic as well as by transplantation of the *timAB* genes into *B. subtilis*, which conferred tartrolon resistance. The hypersensitivity of the Δ*timAB* mutant is remarkable when comparing the TimAB transporter to the previously found LieAB transporter exporting aurantimycin (Hauf *et al.*, 2019). In this work it was shown, that the aurantimycin MIC of the Δ*lieAB* mutant was only decreased 8-fold. Another *L. monocytogenes* transporter is the AnrAB transporter, which has recently been described as an export pump for multiple lantibiotics (Collins *et al.*, 2010). Among the substrates, bacitracin was the one being exported with the highest rate. Yet, a Δ*anrAB* strain only showed an 8-fold decreased MIC for bacitracin. These data led to the assumption that the TimAB transporter is able to export its substrates in a way higher efficiency than AnrAB or LieAB, since the tartrolon A and B MICs of a Δ*timAB* mutant decreased 20-fold and 200-fold compared to the wild type, respectively.

Reasons for the efficient detoxification of the tartrolons could be a high binding affinity of TimAB to both antibiotics or a higher activity of the transporter, which could be caused by an increased activity of the TimA-ATPase. When comparing TimA to previously studied ABC domains in *L. monocytogenes*, it becomes clear that TimA lacks the otherwise conserved glutamine in the Q-loop and the LSGGQ motif is altered in 3 out of the 5 amino acids

(LSGGQ↔MSLGN), which might cause a change in nucleotide binding affinity. The glutamate in the Q-loop present in all other ABC domains analyzed is exchanged to a serine in TimA, which might be a severe mutation, even though both amino acids possess polar side chains (Fig. 4-2). However, the exact effects of these structural differences in TimA are hard to predict.

The tartrolon B MIC being 200-fold lower in a Δ*timAB* strain compared to the wild type leads to a hypersensitive strain, in which toxic tartrolon B concentrations are far lower than the ones reported for other species (Irschik *et al.*, 1995). This is surprising, since no tartrolon transporters have been reported for any other bacteria, and therefore a *L. monocytogenes* Δ*timAB* mutant should have a similar tartrolon B resistance level as most other gram-positive bacteria. Since this is not the case, there is a possibility of other species possessing yet unidentified detoxification mechanisms for tartrolon. Alternatively, the tartrolons could be highly toxic to *L. monocytogenes* specifically, however, there is no evidence supporting this theory.

The theory of the existence of other tartrolon transporters unlike TimAB can be manifested when looking at TimAB homologs in the myxobacterium *Sorangium cellulosum*, which synthesizes tartrolon via its *trtA-trtJ* gene cluster (Elshahawi *et al.*, 2013). *S. cellulosum* is also mostly present in the soil and likely the reason for the evolved TimAB-mediated tartrolon resistance in *L. monocytogenes*. However, the TimAB transporter shows no significant homology to any transporter present in *S. cellulosum*. It was shown that tartrolon B is inactive against gram-negative bacteria like *S. cellulosum*, likely due to its inability to cross the outer membrane (Irschik *et al.*, 1995). Tartrolons might therefore not be toxic, even when inside *S. cellulosum*, however a transporter should still be mandatory in order to export the antibiotic into the environment. The production of secondary metabolites in a host is also often linked with its ability to pump out the antibiotic by transporter-mediated secretion (Martin *et al.*, 2005). Hence, it might indeed be possible, that an MDR transporter with no homology to

TimAB is also capable of secreting tartrolon and that homologs of this transporter are present in other gram-positive species, mediating tartrolon resistance.

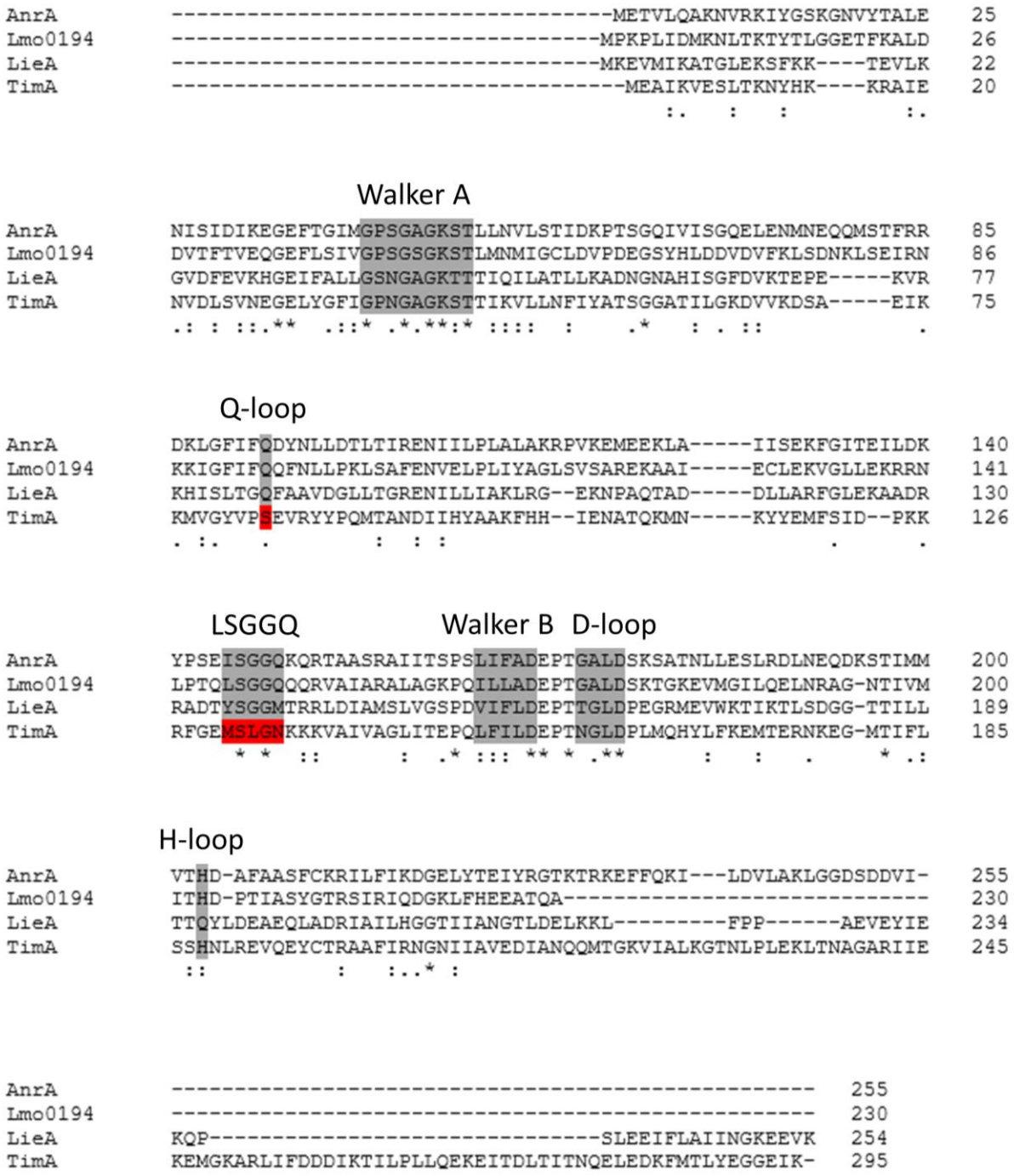

Figure 4-2: Sequence alignment of TimA with other ATPase proteins mentioned in this work. Conserved structural motifs are highlighted in each protein sequence, and the divergent sequences of TimA in the Q-loop and the LSGGQ motif marked in red. Dots below indicate similar (.) and very similar (:) amino acids in aligned sequences, while asterisks mark residues, which are identical in each ABC domain.

The hypothesis of different tartrolon B resistance mechanisms being present in other species, which are closely related to *L. monocytogenes* could also be undermined by testing several *Listeria sensu strico* and *sensu lato* species on their tartrolon B resistance. In this experiment, the *Mesolisteria*, which are lacking the *timABR* genes all showed a way higher tartrolon B MIC than the Δ*timAB* mutant strain, with *L. floridensis* exhibiting a resistance level comparable to *L. monocytogenes*, and *L. fleischmanii* and *L. aquatica* being almost unaffected to tartrolon B. As expected, *Listeria sensu stricto* species represented by *L. ivanovii*, *L. seeligeri* and *L. innocua* all showed tartrolon B resistance levels comparable to wild type *L. monocytogenes*. A Δ*timAB*-like tartrolon B resistance level could only be observed for the *Murraya* species *L. grayi*, which is also lacking the transporter genes.

Several TimAB homologs were however found in various *Carnobacteria* species, with sequence identities of up to 60% for TimA and up to 45% for TimB with similar length. *Carnobacteria* belong to the *Lactobacillales* which degrade carbohydrates to lactic acid. Just like *L. monocytogenes*, *Carnobacteria* can be found in saline waters and their shared occurrence on multiple food products such as fish and cheese are the main sources for direct interaction with *L. monocytogenes* (Leisner *et al.*, 2007, Afzal *et al.*, 2013). One of the most commonly found *Carnobacterium* species on contaminated food - *C. maltaromaticum* - possesses highly homologous proteins for TimAB (Genes *BN424-RS09320* - *BN424-RS09330*, 60% identity, 76% homology for BN424-RS09330 to TimA; 45% identity, 70% homology for BN424-RS09325 to TimB). The organization of this operon is identical to the *timABR* operon, with TimR having a 38% sequence identity (62% homology) to the corresponding TetR protein (BN424-RS09320). Protein sequences as well as the operons are shown in Fig 4-3A-B. No information regarding the function of these genes has yet been published, but it seems possible, that this *C. maltaromaticum* operon also mediates tartrolon resistance.

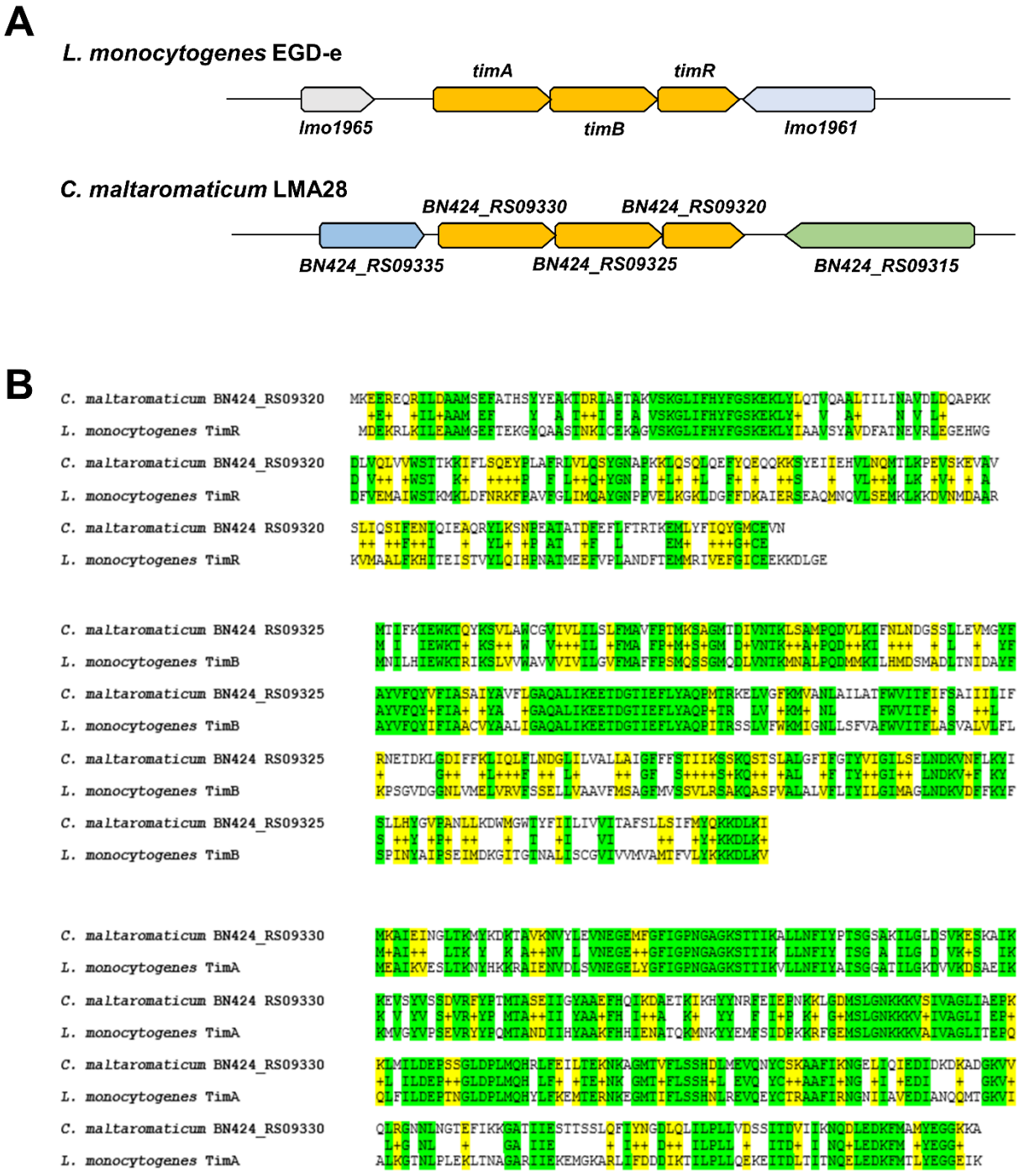

Figure 4-3: Comparison of the *C. maltaromaticum* LMA28 *BN424_RS09320-BN424_RS09330* genes with the *timABR* genes from *L. monocytogenes* EGD-e. (A) Schematic representation of the respective genomic loci **(B)** Sequence alignment of the respective homologous proteins. Identical residues are highlighted in green, while similar residues are indicated by the "+" and marked in yellow.

The tartrolon B MIC of a Δ*timR* strain was 4-fold higher compared to the wild type, while the tartrolon A resistance remained unchanged in this strain. The MIC for tartrolon A not changing upon deletion of the TimAB repressor protein might seem unexpected, since TimAB is also an exporter for tartrolon A, and while tartrolon A can not induce P_{timA}, an increased TimAB-level like the one present in Δ*timR* should also confer tartolon A resistance. Considering the fact, that the tartrolon A MIC only decreased 20-fold upon deletion of *timAB* (compared to the 200-fold tartrolon B MIC decrease), one could argue that TimAB is less efficient in the detoxification of tartrolon A compared to the one for tartrolon B and the minor P_{timA} activity increase upon deletion of *timR* is not sufficient to have an effect on tartrolon A resistance.

4.3 Tartrolon B functions as a potassium ionophore

The mode of action of tartrolon B was investigated by determination of the MIC of the wild type in potassium- and sodium-rich media. In these experiments, it could be shown, that potassium, but not sodium, counteracts the mode of action of tartrolon B. This suggested, that tartrolon B functions as an ionophore, which breaks down the membrane potential of potassium ions specifically. There are multiple reports on potassium ionophores, such as boromycin or valinomycin (Daniele & Holian, 1976, Moreira *et al.*, 2016). These types of ionophores are described as having a hydrophilic pocket, which can reversibly bind to specific ions (Sharma *et al.*, 2021).

For valinomycin, the binding site is in the center of the molecule, to which the oxygens of 12 carbonyl groups are pointing. However, only 6 of these oxygens are required for binding of K^+, since potassium is known to form an octahedral complex with macrolide oxygens, while the others point in other directions (Sato *et al.*, 2021). This octahedral complex is also present in tartrolon B, however it is in quite a remarkable relation to the tetrahedrally coordinated boron, since the boron already occupies 4 oxygen atoms in the center. Therefore, a tartrolon B crystal

structure revealed, that the octahedral potassium complex in tartrolon B is acquired by sharing the two C2-oxygens with the boron complex, making boron and potassium form an inner ion pair, which forces the alkali metal further towards the inside of the macrolide (Schummer *et al.*, 1996, Mulzer & Berger, 2004). This leads to a distinct difference regarding the confirmation of the macrocycle compared to tartrolon A. In addition to the previously mentioned gain of C_2-symmetry in tartrolon B caused by binding of the boron atom, this could also explain the differences between tartrolon A and tartrolon B regarding their observed biochemical characteristics, like the efficiency of potassium transport over the membrane, but also the binding affinity to TimR and therefore the rate of P_{timA} induction. The conformational differences between these two tartrolon derivates is however diminished in presence of potassium compared to their potassium unbound states (Fig. 4-4, see Fig. 4-1 for comparison).

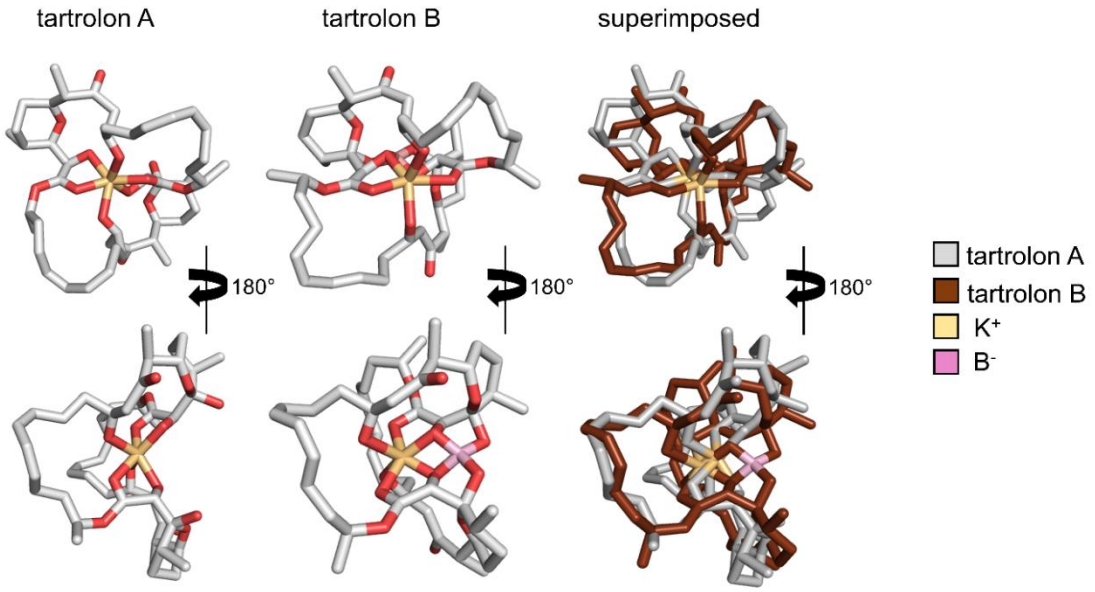

Figure 4-4: Putative conformations of tartrolon A and tartrolon B bound to potassium. Chemical structures of tartrolon A and tartrolon B complexed with potassium were drawn according to literature (Schummer *et al.*, 1996) and their 3D-structure calculated using the software LEA3D (Douguet *et al.*, 2005), which is available on chemoinfo.ipmc.cnrs.fr/LEA3D/drawonline.html. The generated .pdb file was used to visualize both structures using the PyMOL software (DeLano, 2002). Carbon atoms are colored in gray and oxygen atoms in red in the separate tartrolon A and tartrolon B structures.

The ionophore-activity of tartrolon B also shines new light on the TimAB-mediated detoxification of the antibiotic. In a scenario where no TimAB is present, tartrolon B can freely diffuse through the membrane of gram-positive bacteria, and by the law of entropy would be present in an identical concentration on the inside of the cell as on the outside. Once tartrolon B is inside the cell, it probably immediately binds to potassium, which it carries to the cell outside. If TimAB is present, tartrolon B loses a lot of its toxicity. However, if TimAB would export tartrolon B from the cytoplasm, a large proportion of the macrodiolide would be bound to potassium, and transporting this complex to the outside of the cell would only enhance its potassium deficiency. Since the data obtained clearly suggest, that this is not the case, there are two possibilities for TimAB mediated tartrolon B transport. In the first scenario, TimAB binds specifically to potassium-unbound tartrolon B in the cytoplasm. This theory can not be excluded, since the conformation of the macrocycle of tartrolon B slightly changes upon binding to potassium and hence it could be possible, that only the unbound state is recognized by TimAB (Fig 4-5). Another possibility is that TimAB functions in a similar manner as the other previously reported *L. lactis* MDR transporters LmrA and LmrP and is able to export tartrolon B already from the cytoplasmic membrane, where the macrodiolide has no opportunity to bind to internal potassium (Bolhuis *et al.*, 1996a, Bolhuis *et al.*, 1996b).

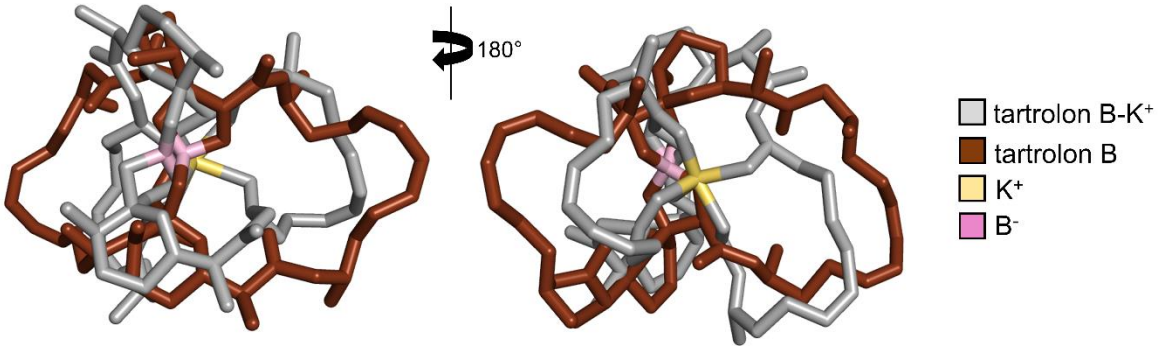

Figure 4-5: Putative conformational changes in tartrolon B upon binding to potassium. Chemical structures of tartrolon B in its potassium-bound and -unbound state were drawn according to literature (Schummer *et al.*, 1996) and their 3D-structure calculated using the software LEA3D (Douguet *et al.*, 2005), which is available on chemoinfo.ipmc.cnrs.fr/LEA3D/drawonline.html. The generated .pdb file was used to analyze both structures using the PyMOL software (DeLano, 2002).

4.4 The contribution of ClpP2 proteases to tartrolon B resistance

4.4.1 Tartrolon B suppressor screen

In order to isolate tartrolon B resistant clones, multiple tartrolon B suppressor screens were performed. As a first approach, the P_{timA}-*lacZ* strain was used with the intention to find suppressors, whose resistance is not caused by an increased activity of the *timA* promoter. This experiment was however unsuccessful, since the fully induced *timA* promoter in a Δ*timR* background only showed a 3-fold increased activity, which is not distinguishable from the wild type level on agar plates containing X-Gal.

Observing differences in β-galactosidase activity was however not necessary since colonies carrying mutations in *clpP2* were significantly smaller on an agar plate than normal sized clones, while also having the highest tartrolon B resistance level out of any clones isolated from these type of experiments (32-fold). This resistance level was likely the reason for the high frequency of smaller colonies in these suppressor screens, as any other suppressors found in *timR*, P_{timA} or *ybjH* were rare and only showed a 2 to 4-fold increased tartrolon B MIC.

The two SNPs found in *clpP2* - E9K and T90I - caused the inactivation of the protease as confirmed by a MurA-specific Western blot. MurA is being degraded by the ClpCP2 proteasome and a Δ*clpC* mutant has been shown to have a ~6-fold increased MurA level, as its degradation in this strain is likely completely absent (Wamp *et al.*, 2020). While the relative MurA levels in the strains carrying *clpP2* E9K and *clpP2* T90I were only 3-fold higher compared to the wild type, they were on a similar level as in the Δ*clpC* and the Δ*clpP2* strains, in which MurA proteolysis is stopped completely. Hence, the differences of the relative MurA level described in the literature is likely just of experimental nature and it could be concluded that both SNPs identified in *clpP2* lead to almost complete inactivation of the protease.

However, a small residual activity should still be present, since the strains carrying these mutated *clpP2* alleles only showed a slight growth deficit compared to the wild type, while growth of the Δ*clpP2* mutant was more strongly impaired in every experiment. Furthermore, the strains carrying *clpP2* E9K or *clpP2* T90I showed considerable growth at 42°C - a temperature, where Δ*clpP2* is unable to grow and the tartrolon B MIC of the suppressor strains was also slightly lower than the of the Δ*clpP2* deletion mutant, supporting the hypothesis of a slight ClpP2 activity still being present in these strains.

4.4.2 How does a Δ*clpP2* deletion mutant acquire resistance to tartrolon B?

One theory as to why inactivation of ClpP2 provides resistance to tartrolon B was that the antibiotic increases the enzymatic activity of the protease. In a previous work, the acyldepsipeptide ADEP has been assigned with the function of binding to a hydrophobic pocket on the entry pore of *B. subtilis* ClpP and thus activating the protease in an uncontrolled, ATPase independent manner (Brötz-Oesterhelt *et al.*, 2005, Kirstein *et al.*, 2009). It has also been shown, that multiple species belonging to the *Bacillota*, such as *B. subtilis*, *E. faecalis* or *S. pyrogenes* frequently mutate in all regions in *clpP* upon exposure to high ADEP concentrations, often by inactivation of the protease (Malik *et al.*, 2020).

When comparing the functions of tartrolon B and ADEP via a ClpP2 activity assay, it became clear that these two antibiotics work in different manners, as ADEP could activate ClpP2, and to a lesser extend even ClpP2 E9K. Tartrolon B however did not affect the activity of ClpP2 or ClpP2 E9K. Since tartrolon B did not activate ClpP2, the reason for a Δ*clpP2* mutant being hyper-resistant to the macrolide could not be caused by a direct interaction of tartrolon B with ClpP2, making it more likely, that accumulation of a ClpP2 substrate is mediating tartrolon B resistance in Δ*clpP2*. Identification of this substrate was hard, since there are 226 proteins accumulating in a *L. monocytogenes* Δ*clpP2* mutant (Balogh *et al.*, 2022), all of which could

impact tartrolon B resistance in several manners. The substrate of interest could not be found in a tartrolon B suppressor screen, likely because its corresponding gene would need to acquire gain of function mutations to increase its effect on tartrolon detoxification or mutations escaping ClpP2-mediated proteolysis.

Many approaches were used in the identification of said ClpP2 substrates. At first, it was postulated that the reason for the resistance gain in Δ*clpP2* is due to the accumulation of potassium importers, which could counteract the tartrolon B mediated depletion of potassium ions inside the cell. The only data undermining such a mechanism would be the fact, that the tartrolon B resistance-gain of a Δ*clpP2* mutant upon supplementation of the medium with high potassium concentrations is fairly low compared to the wild type (2-fold in Δ*clpP2* compared to 64-fold in the wild type). Importantly, the high potassium responsiveness present in the Δ*timAB* mutant could also be found for Δ*clpP2* Δ*timAB*, suggesting that a Δ*clpP2* mutant does not accumulate potassium importers to a level, which impacts tartrolon B resistance. The Δ*clpP2* Δ*timAB* strain matching the high potassium responsiveness of the Δ*timAB* mutant also provided solid proof that deletion of Δ*clpP2* only has a tartrolon B phenotype if *timAB* is present and supports the theory of TimAB accumulation in a Δ*clpP2* background.

Another trend seen in this data is, that the potassium responsiveness of a strain correlates with its tartrolon B sensitivity, with the hypersensitive Δ*timAB* strain having a 250-fold increased tartrolon B MIC upon supplementation of the medium with potassium, whereas the resistant Δ*clpP2* mutant showed almost no resistance gain. The same observation could also be made when strains overexpressing *timAB* were analyzed regarding their tartrolon B resistance in presence and absence of potassium, with the tartrolon B MIC of the hyper-resistant strain carrying an additional, IPTG-inducible copy of *timAB* in a Δ*timR* background only increasing two-fold upon potassium supplementation. This suggests, that the reason for this small

resistance gain in the Δ*clpP2* mutant and the Δ*timR* P_{help}-*timAB* mutant upon potassium supplementation could be the same – the increased activity of TimAB, which leads to a more stable potassium gradient by detoxifying tartrolon B, making these strains less dependent on high external potassium concentrations.

4.4.3 The level of SpxA1 impacts tartrolon B resistance

At this point, the hypothesis of the accumulation of a ClpP2 substrate being the reason for the resistance gain in Δ*clpP2* seemed very likely. However, TimAB itself is not this sought-after substrate of ClpP2 as shown via Western blotting of strep-tagged TimA, and in a recently published work analyzing the ClpP2 proteasome, the TimAB levels are not mentioned to be elevated either (Balogh *et al.*, 2022). To further understand the underlying mechanism mediating tartrolon B resistance, the three Clp ATPase genes (*clpC*, *clpE* and *clpX*) were deleted, yielding the result that both *clpC* and *clpX* need to be knocked out for a strain to acquire tartrolon B resistance. While the possibility of multiple relevant substrates accumulating - some of which are being degraded by ClpCP2 and some by ClpXP2 - could not be excluded, the finding of the suppressor carrying a frameshift mutation in *yjbH* suggested that the protein of interest is SpxA1, since YjbH mediates proteolytic degradation of this protein by the *B. subtilis* ClpXP proteasome, and *B. subtilis* Spx can also be degraded *in vitro* by ClpCP (Nakano *et al.*, 2002, Rojas-Tapias & Helmann, 2019). For degradation of Spx, a Spx-YjbH heterodimer is established, enhancing the rate of proteolysis of Spx by the ClpXP proteasome specifically (Awad *et al.*, 2019). However, Spx can also be degraded by ClpXP *in vitro* in absence of YjbH at a lower rate (Garg *et al.*, 2009). In *B. subtilis*, ClpCP-mediated degradation is enhanced by a different adapter protein, namely MecA (Garg *et al.*, 2009).

The resistance level of a Δ*yjbH* mutant was increased two-fold and hence the same as the one of the strain overexpressing *spxA1* in a wild type background. The common trait of these two

strains is their increased level of SpxA1, however, the reasons for accumulation of SpxA1 are different. While deletion of *yjbH* is causing a decreased degradation rate of SpxA1 by ClpP2, the proteolysis in the strain overexpressing *spxA1* is unaffected. Since both strains show the same tartrolon B resistance level, it is therefore unlikely that the Δ*yjbH* strain has a different cause for its resistance gain other than the resulting accumulation of SpxA1. This also means, that the resistance-gain of the strain overexpressing *spxA1* can not be caused by ClpP2 being too "busy" with the increased proteolysis caused by SpxA1 overproduction to degrade the actual protein of interest at the same rate as in the wild type background, since the opposite scenario, namely a decreased SpxA1 proteolysis in Δ*yjbH* also mediates resistance.

One problem with the hypothesis of SpxA1 being the ClpP2 substrate mediating tartrolon B resistance is, that no suppressor carrying mutations in the *spxA1* locus could ever be isolated in a tartrolon B suppressor screen. There are multiple mutations which could be possible: Firstly, mutations which lead to an increased *spxA1* expression level, like promoter up mutations, which should mediate resistance. These mutations were not possible, since the level of SpxA1 is likely very low in a wild type background, as the Spx level in a wild type *B. subtilis* strain is not detectable by Western blotting (Nakano *et al.*, 2003). This low level of Spx in the cell is not due to the low gene expression level, but due to the high degradation rate of the protein by the ClpCP and ClpXP proteasomes. The high degradation rate can likely also be applied to *L. monocytogenes* SpxA1. This makes an increased expression level negligible, which could also be shown in this work by overexpression of *spxA1*. Instead, mutations which can escape ClpP2 mediated proteolytic degradation would be needed to mediate a high level of SpxA1 and hence high-level resistance. However, since SpxA1 can be degraded by both ClpCP2 and ClpXP2, a single mutation in the protein might not be sufficient for the rescue from both proteasomes, since SpxA1 might be able to bind to another adaptor protein other than the known YbjH adapter via different residues. Also, previous works for *L. monocytogenes spxA1* suggested that

it is an essential gene under aerobic conditions, which likely means that only selective residues can be mutated within the *spxA1* gene itself for a strain to still be viable (Cesinger *et al.*, 2020, Fischer *et al.*, 2022).

The high level of SpxA1 being responsible for the hyper-resistant phenotype of a Δ*clpP2* mutant strain was confirmed by creating an i*spxA1* strain, which showed a slightly increased resistance to tartrolon B in the presence of IPTG, when SpxA1 is presumably overproduced compared to the wild type. However, the tartrolon B MIC of this strain in the absence of IPTG dropped to 0.25±0 µg/ml, which was 4-fold lower than the wild type MIC. This resistance level is not comparable to an MIC observed for any other strain tested in this work. Previously, the only strains sensitive to tartrolon B were strains lacking the *timAB* genes. While *spxA1* is another factor contributing to tartrolon B resistance, a *spxA1* depletion strain is still significantly more resistant to tartrolon B than strains lacking *timAB*. The precise role of *spxA1* in mediating tartrolon B resistance remains elusive. The most likely way *spxA1* mediates tartrolon B resistance is by transcriptional activation of certain genes, which are involved in tartrolon B detoxification.

4.5 A model for the tartrolon B detoxification mechanism in *L. monocytogenes*

In Fig. 4-6, a mechanism for the detoxification of tartrolon B in *L. monocytogenes* is postulated. The data obtained regarding the *timABR* operon (sensing of tartrolon B by TimR and the detoxification by TimAB) is not challenged by any data suggesting a different mechanism than the one presented here, the role of SpxA1 in mediating tartrolon B resistance is more complex. SpxA1 is a transcription factor binding to the RNA polymerase (RNAP) and is involved in the regulation of >140 genes required mostly for heme biosynthesis and aerobic growth, while the

catalase encoding gene *kat* is by far the most downregulated gene in a Δ*spxA1* mutant (Cesinger *et al.*, 2020). Since a high level of SpxA1 mediates tartrolon B resistance, the transcription factor likely functions as an activator of a gene beneficial for tartrolon B detoxification. Reasons for this SpxA1 mediated gene activation are however not clear, since *B. subtilis* Spx mainly activates genes involved in the stress response to high temperatures, disulfide or oxidative stress (Zuber, 2009, Schäfer & Turgay, 2019). However, Spx also accumulates upon exposure to antibiotics inducing cell wall stress such as ampicillin, which has been shown to promote the formation of reactive oxygen species in *E. coli* (Dwyer *et al.*, 2014, Rojas-Tapias & Helmann, 2018). While tartrolon B functions as a potassium ionophore and does not target cell wall biosynthesis like ampicillin, it seems possible that tartrolon B also induces oxidative stress, making a high level of *L. monocytogenes* SpxA1 beneficial for tartrolon B resistance of the pathogen.

While this theory would explain the hyper-resistance of a Δ*clpP2* mutant, it disregards the fact, that the resistance level of this mutant is dependent on the presence of *timAB*. A hypothesis considering this fact would revolve around SpxA1 activating a versatile adaptor protein, which binds to TimAB and increases its activity, but also plays a role in the SpxA1-mediated response to the stress factors described above. One factor supporting the theory of an unknown factor binding to TimAB is the fact, that the cytoplasmic TimA possesses an ~50 aa elongated C-terminus, which is absent in both AnrA and LieA (Fig. 4-2), which might serve as a docking site for this unknown protein.

To identify this factor, a Tn-Seq experiment could be performed. In this experiment, the wild type carrying a Tn-Seq library would need to be grown in tartrolon B concentrations right below its MIC and subsequently sequenced. Genes, which would be beneficial for tartrolon B resistance would carry a decreased amount of transposon insertions. After comparison of these

candidate genes to the ones known to be activated by SpxA1, knock-out mutations of candidate genes would have to be generated and tested regarding their tartrolon B MIC. The tartrolon B MIC of a strain, where the gene of interest in knocked out could be around the MIC observed for the i*spxA1* strain in the absence of IPTG, where the gene of interest presumably is transcribed at a low rate. Also, this deletion mutant should be unresponsive to subsequent deletions of *clpP2* or *spxA1*.

Genes, which would certainly be identified in a Tn-Seq experiment would be the *timAB* genes. While at this point, it can not be excluded that SpxA1 activates expression of the *timABR* operon, the fact that a strain expressing *timAB* from a heterologous promoter like the one present in the strain i*timAB* Δ*clpP2* phenocopies the tartrolon B resistance level of a Δ*clpP2* mutant in the presence of IPTG is a strong argument against this theory.

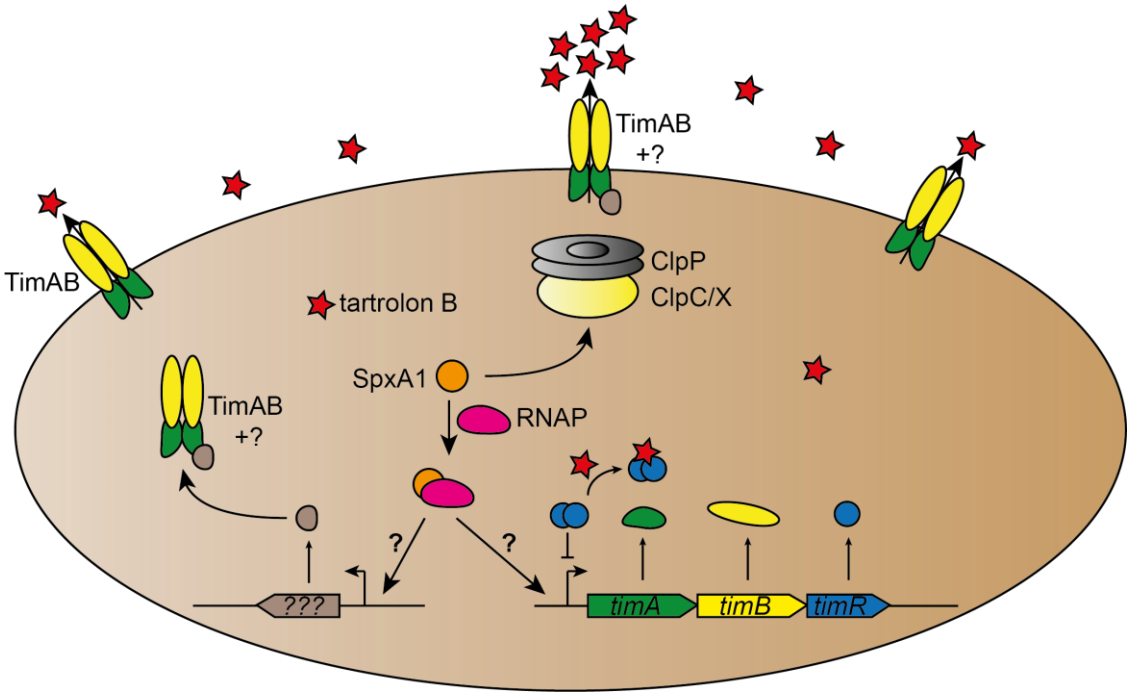

Figure 4-6: Model for *timABR* dependent detoxification of tartrolon B in *L. monocytogenes*. The TimAB transporter exports tartrolon B. Expression of the *timABR* genes is repressed by TimR in absence of tartrolon B, but induced upon contact of *L. monocytogenes* with tartrolon B, since tartrolon B prevents TimR from binding to its own operator sequence. The efficiency of TimAB-dependent tartrolon B efflux is positively correlated to the level of SpxA1, a transcriptional regulator binding to the RNAP. The reason for this correlation is not clear, as SpxA1 could activate expression of the *timABR* operon, or activate the expression of an unknown gene, which impacts the activity of TimAB.

Abbreviations

°C	degree Celsius
% (v/v)	percent volume
% (w/v)	percent weight
A	adenine
Å	Ångström
A_λ	absorption at wavelength λ
aa	amino acid
ad.	fill to
APS	ammonium persulfate
ATPase	adenosin triphosphatase
BHI	brain heart infusion
bla	beta lactamase
bp	base pair
BSA	bovine serum albumin
C	cytosine
c-di-AMP	cyclic di-adenosine monophosphate
d	days
dd	double distilled
DMSO	dimethyl sulfoxide
DNA	desoxyribonucleic acid
dNTP	desoxynukleoside triphosphate
EDTA	ethylenediaminetetraacetic acid
erm	erythromycin
fw	forward
G	guanine
g	gram
h	hour
HEPES	4-(2-hydroxyethyl)-1-piperazineethanesulfonic acid
HRP	horseradish peroxidase
i	IPTG inducible
IgG	immunoglobulin G

IPTG	isopropyl-β-D-thiogalactopyranoside
kbp	kilo base pair
l	liter
LB	Luria Bertani
LLO	listeriolysin
kan	kanamycin
kDa	kilodalton
M	molar
mg	milligram
ml	milliliters
mM	millimolar
min	minutes
nm	nanometres
OD	optical density
ONPG	o-nitrophenyl-β-galactoside
PAGE	polyacrylamide gel electrophoresis
PBS	phosphate buffered saline
PCR	polymerase chain reaction
P_{help}	IPTG inducible promoter
PMSF	phenylmethylsulfonyl fluoride
PVDF	polyvinylidene fluoride
rev	reverse
RNA	ribonucleic acid
RNAP	RNA polymerase
rpm	rotations per minute
s	seconds
SDS	sodium dodecyl sulfate
SGWB	sucrose glycerol wash buffer
strep	streptavidin
T	thymine
t	time
TAE	Tris-acetate-EDTA
TEMED	tetramethylethylenediamine
Tris	tris(hydroxymethyl)aminomethane

UV	ultraviolet
V	volt
wt	wild type
X-Gal	5-bromo-4-chloro-3-indolyl-β-D-galactopyranoside
x g	relative centrifugal force
µF	microfarad
µg	microgram
µl	microliter
µm	micrometre
λ	wavelength
Ω	ohm

Acknowledgements

I would like to thank everyone who supported me during my time as a doctoral student:

- My supervisor PD Dr. Sven Halbedel for his calm nature, constant engagement in my project and his invaluable advices not only regarding my project, but also in several other aspects of life.

- all members of the *Listeria* working group, who helped me acquire new skills in the lab.

- Dr. Sabrina Wamp, Sandra Freier, Susan Scheffler and especially Patricia Rothe for the interesting conversations in the lab, which made every day even more fun.

- Jacqueline Schürmann for her invaluable friendship, jolly nature and constant positive attitude. Without her writing this thesis would have been a lot harder.

- All other collegues from the RKI, who supported me mentally or technically in the lab, mostly Dr. Martin Fischer, Tobias Größl and Dr. Michael Pietsch.

- My collaboration partners in the German Centre of Infection Research, namely Dr. Jennifer Herrmann and Prof. Dr. Rolf Müller for providing me with tartrolon B.

- My girlfriend Gina Schlott, who distracted me from constantly thinking about work on the weekends and made me have a good time instead.

- All of my friends, especially the ones around Coburg, which I was able to see way less than I wished for in the last 3 years.

- At last, my family, especially my parents and my sister, who have supported me throughout my whole life and certainly are the main reason I was able to write this work.

5 Literature

Abdelhamed, H., Lawrence, M.L., and Karsi, A. (2015) A novel suicide plasmid for efficient gene mutation in Listeria monocytogenes. *Plasmid* **81**: 1-8.

Abou-Zeid, A.Z., Khalil, A.e.-G., and Rabei, M. (1980) Spiramycin, a macrolide antibiotic. *Zentralbl Bakteriol Naturwiss* **135**: 443-453.

Afzal, M.I., Ariceaga, C.C.G., Lhomme, E., Ali, N.K., Payot, S., Burgain, J., Gaiani, C., Borges, F., Revol-Junelles, A.-M., and Delaunay, S. (2013) Characterization of Carnobacterium maltaromaticum LMA 28 for its positive technological role in soft cheese making. *Food microbiology* **36**: 223-230.

Ahmed, M., Lyass, L., Markham, P.N., Taylor, S.S., Vazquez-Laslop, N., and Neyfakh, A.A. (1995) Two highly similar multidrug transporters of Bacillus subtilis whose expression is differentially regulated. *Journal of bacteriology* **177**: 3904-3910.

Aittoniemi, J., de Wet, H., Ashcroft, F.M., and Sansom, M.S. (2010) Asymmetric switching in a homodimeric ABC transporter: a simulation study. *PLoS Comput Biol* **6**: e1000762.

Alexopoulos, J.A., Guarne, A., and Ortega, J. (2012) ClpP: a structurally dynamic protease regulated by AAA+ proteins. *J Struct Biol* **179**: 202-210.

Aljghami, M.E., Barghash, M.M., Majaesic, E., Bhandari, V., and Houry, W.A. (2022) Cellular functions of the ClpP protease impacting bacterial virulence. *Front Mol Biosci* **9**: 1054408.

Altenberg, G.A., Vanoye, C.G., Horton, J.K., and Reuss, L. (1994) Unidirectional fluxes of rhodamine 123 in multidrug-resistant cells: evidence against direct drug extrusion from the plasma membrane. *Proc Natl Acad Sci U S A* **91**: 4654-4657.

Anast, J.M., and Schmitz-Esser, S. (2021) Certain Listeria monocytogenes plasmids contribute to increased UVC ultraviolet light stress. *FEMS Microbiol Lett* **368**.

Angelidis, A.S., and Smith, G.M. (2003) Three transporters mediate uptake of glycine betaine and carnitine by Listeria monocytogenes in response to hyperosmotic stress. *Applied and Environmental Microbiology* **69**: 1013-1022.

Arnaud, M., Chastanet, A., and Debarbouille, M. (2004) New vector for efficient allelic replacement in naturally nontransformable, low-GC-content, gram-positive bacteria. *Appl Environ Microbiol* **70**: 6887-6891.

Arslan, S., and Özdemir, F. (2008) Prevalence and antimicrobial resistance of Listeria spp. in homemade white cheese. *Food control* **19**: 360-363.

Awad, W., Al-Eryani, Y., Ekstrom, S., Logan, D.T., and von Wachenfeldt, C. (2019) Structural Basis for YjbH Adaptor-Mediated Recognition of Transcription Factor Spx. *Structure* **27**: 923-936 e926.

Balogh, D., Eckel, K., Fetzer, C., and Sieber, S.A. (2022) Listeria monocytogenes utilizes the ClpP1/2 proteolytic machinery for fine-tuned substrate degradation at elevated temperatures. *RSC Chemical Biology* **3**: 955-971.

Baquero, F., F. Lanza, V., Duval, M., and Coque, T.M. (2020) Ecogenetics of antibiotic resistance in Listeria monocytogenes. *Molecular microbiology* **113**: 570-579.

Beasley, D.E., Koltz, A.M., Lambert, J.E., Fierer, N., and Dunn, R.R. (2015) The Evolution of Stomach Acidity and Its Relevance to the Human Microbiome. *PLoS One* **10**: e0134116.

Beauchamp, S., and Lacroix, M. (2012) Resistance of the genome of Escherichia coli and Listeria monocytogenes to irradiation evaluated by the induction of cyclobutane pyrimidine dimers and 6-4 photoproducts using gamma and UV-C radiations. *Radiation Physics and Chemistry* **81**: 1193-1197.

Becattini, S., Littmann, E.R., Carter, R.A., Kim, S.G., Morjaria, S.M., Ling, L., Gyaltshen, Y., Fontana, E., Taur, Y., Leiner, I.M., and Pamer, E.G. (2017) Commensal microbes provide first line defense against Listeria monocytogenes infection. *J Exp Med* **214**: 1973-1989.

Begley, M., Hill, C., and Ross, R.P. (2006) Tolerance of Listeria monocytogenes to cell envelope-acting antimicrobial agents is dependent on SigB. *Applied and Environmental Microbiology* **72**: 2231-2234.

Begley, M., Sleator, R.D., Gahan, C.G., and Hill, C. (2005) Contribution of three bile-associated loci, bsh, pva, and btlB, to gastrointestinal persistence and bile tolerance of Listeria monocytogenes. *Infect Immun* **73**: 894-904.

Bellio, P., Mancini, A., Di Pietro, L., Cracchiolo, S., Franceschini, N., Reale, S., de Angelis, F., Perilli, M., Amicosante, G., Spyrakis, F., Tondi, D., Cendron, L., and Celenza, G. (2020) Inhibition of the transcriptional repressor LexA: Withstanding drug resistance by inhibiting the bacterial mechanisms of adaptation to antimicrobials. *Life Sci* **241**: 117116.

Berger, M., and Mulzer, J. (1999) Total synthesis of tartrolon B. *Journal of the American Chemical Society* **121**: 8393-8394.

Bertram, R., Neumann, B., and Schuster, C.F. (2022) Status quo of tet regulation in bacteria. *Microb Biotechnol* **15**: 1101-1119.

Bervoets, I., and Charlier, D. (2019) Diversity, versatility and complexity of bacterial gene regulation mechanisms: opportunities and drawbacks for applications in synthetic biology. *FEMS Microbiol Rev* **43**: 304-339.

Beuchat, L.R. (1996) Listeria monocytogenes: incidence on vegetables. *Food control* **7**: 223-228.

Beumer, R.R., Te Giffel, M.C., Cox, L.J., Rombouts, F.M., and Abee, T. (1994) Effect of exogenous proline, betaine, and carnitine on growth of Listeria monocytogenes in a minimal medium. *Appl Environ Microbiol* **60**: 1359-1363.

Bhandari, V., Wong, K.S., Zhou, J.L., Mabanglo, M.F., Batey, R.A., and Houry, W.A. (2018) The Role of ClpP Protease in Bacterial Pathogenesis and Human Diseases. *ACS Chem Biol* **13**: 1413-1425.

Bien, J., Palagani, V., and Bozko, P. (2013) The intestinal microbiota dysbiosis and Clostridium difficile infection: is there a relationship with inflammatory bowel disease? *Therapeutic advances in gastroenterology* **6**: 53-68.

Bienfait, B., and Ertl, P. (2013) JSME: a free molecule editor in JavaScript. *Journal of cheminformatics* **5**: 1-6.

Bolhuis, H., Van Veen, H.W., Brands, J.R., Putman, M., Poolman, B., Driessen, A.J., and Konings, W.N. (1996a) Energetics and mechanism of drug transport mediated by the lactococcal multidrug transporter LmrP. *Journal of Biological Chemistry* **271**: 24123-24128.

Bolhuis, H., van Veen, H.W., Molenaar, D., Poolman, B., Driessen, A., and Konings, W.N. (1996b) Multidrug resistance in Lactococcus lactis: evidence for ATP-dependent drug extrusion from the inner leaflet of the cytoplasmic membrane. *The EMBO Journal* **15**: 4239-4245.

Bolhuis, H., van Veen, H.W., Poolman, B., Driessen, A.J., and Konings, W.N. (1997) Mechanisms of multidrug transporters. *FEMS Microbiol Rev* **21**: 55-84.

Bonvini, P., Zorzi, E., Basso, G., and Rosolen, A. (2007) Bortezomib-mediated 26S proteasome inhibition causes cell-cycle arrest and induces apoptosis in CD-30+ anaplastic large cell lymphoma. *Leukemia* **21**: 838-842.

Bourgin, M., Kriaa, A., Mkaouar, H., Mariaule, V., Jablaoui, A., Maguin, E., and Rhimi, M. (2021) Bile Salt Hydrolases: At the Crossroads of Microbiota and Human Health. *Microorganisms* **9**.

Braun, L., Ghebrehiwet, B., and Cossart, P. (2000) gC1q-R/p32, a C1q-binding protein, is a receptor for the InlB invasion protein of Listeria monocytogenes. *The EMBO journal* **19**: 1458-1466.

Briggs, G.S., Smits, W.K., and Soultanas, P. (2012) Chromosomal replication initiation machinery of low-G+C-content Firmicutes. *J Bacteriol* **194**: 5162-5170.

Brigham, R.B., and Pittenger, R.C. (1956) Streptomyces orientalis, n. sp., the source of vancomycin. *Antibiot Chemother (Northfield)* **6**: 642-647.

Brötz-Oesterhelt, H., Beyer, D., Kroll, H.P., Endermann, R., Ladel, C., Schroeder, W., Hinzen, B., Raddatz, S., Paulsen, H., Henninger, K., Bandow, J.E., Sahl, H.G., and Labischinski, H. (2005) Dysregulation of bacterial proteolytic machinery by a new class of antibiotics. *Nat Med* **11**: 1082-1087.

Buchaklian, A.H., and Klug, C.S. (2006) Characterization of the LSGGQ and H motifs from the Escherichia coli lipid A transporter MsbA. *Biochemistry* **45**: 12539-12546.

Bucur, F.I., Grigore-Gurgu, L., Crauwels, P., Riedel, C.U., and Nicolau, A.I. (2018) Resistance of Listeria monocytogenes to Stress Conditions Encountered in Food and Food Processing Environments. *Front Microbiol* **9**: 2700.

Cavanagh, D., Fitzgerald, G.F., and McAuliffe, O. (2015) From field to fermentation: the origins of Lactococcus lactis and its domestication to the dairy environment. *Food Microbiol* **47**: 45-61.

Cepeda, J., Millar, M., Sheridan, E., Warwick, S., Raftery, M., Bean, D., and Wareham, D. (2006) Listeriosis due to infection with a catalase-negative strain of Listeria monocytogenes. *Journal of clinical Microbiology* **44**: 1917-1918.

Cesinger, M.R., Thomason, M.K., Edrozo, M.B., Halsey, C.R., and Reniere, M.L. (2020) Listeria monocytogenes SpxA1 is a global regulator required to activate genes encoding catalase and heme biosynthesis enzymes for aerobic growth. *Molecular microbiology* **114**: 230-243.

Charpentier, E., and Courvalin, P. (1999) Antibiotic resistance in Listeria spp. *Antimicrobial agents and chemotherapy* **43**: 2103-2108.

Charpentier, E., Gerbaud, G., and Courvalin, P. (1999) Conjugative mobilization of the rolling-circle plasmid pIP823 from Listeria monocytogenes BM4293 among gram-positive and gram-negative bacteria. *Journal of Bacteriology* **181**: 3368-3374.

Chávez-Arroyo, A., and Portnoy, D.A. (2020) Why is Listeria monocytogenes such a potent inducer of CD8+ T-cells? *Cellular microbiology* **22**: e13175.

Collins, B., Curtis, N., Cotter, P.D., Hill, C., and Ross, R.P. (2010) The ABC transporter AnrAB contributes to the innate resistance of Listeria monocytogenes to nisin, bacitracin, and various beta-lactam antibiotics. *Antimicrob Agents Chemother* **54**: 4416-4423.

Collins, M.D., Wallbanks, S., Lane, D.J., Shah, J., Nietupski, R., Smida, J., Dorsch, M., and Stackebrandt, E. (1991) Phylogenetic analysis of the genus Listeria based on reverse transcriptase sequencing of 16S rRNA. *Int J Syst Bacteriol* **41**: 240-246.

Commichau, F.M., Gibhardt, J., Halbedel, S., Gundlach, J., and Stulke, J. (2018) A Delicate Connection: c-di-AMP Affects Cell Integrity by Controlling Osmolyte Transport. *Trends Microbiol* **26**: 175-185.

Cornforth, D.M., and Foster, K.R. (2013) Competition sensing: the social side of bacterial stress responses. *Nat Rev Microbiol* **11**: 285-293.

Cossart, P., Vicente, M.F., Mengaud, J., Baquero, F., Perez-Diaz, J., and Berche, P. (1989) Listeriolysin O is essential for virulence of Listeria monocytogenes: direct evidence obtained by gene complementation. *Infection and immunity* **57**: 3629-3636.

Cotter, P.D., Gahan, C.G., and Hill, C. (2000) Analysis of the role of the Listeria monocytogenes F0F1 -AtPase operon in the acid tolerance response. *Int J Food Microbiol* **60**: 137-146.

Cotter, P.D., Gahan, C.G., and Hill, C. (2001) A glutamate decarboxylase system protects Listeria monocytogenes in gastric fluid. *Mol Microbiol* **40**: 465-475.

Cotter, P.D., Ryan, S., Gahan, C.G., and Hill, C. (2005) Presence of GadD1 glutamate decarboxylase in selected Listeria monocytogenes strains is associated with an ability to grow at low pH. *Applied and environmental microbiology* **71**: 2832-2839.

Cremers, C.M., Knoefler, D., Vitvitsky, V., Banerjee, R., and Jakob, U. (2014) Bile salts act as effective protein-unfolding agents and instigators of disulfide stress in vivo. *Proceedings of the National Academy of Sciences* **111**: E1610-E1619.

Csonka, L.N. (1989) Physiological and genetic responses of bacteria to osmotic stress. *Microbiol Rev* **53**: 121-147.

Cummins, A.J., Fielding, A.K., and McLauchlin, J. (1994) Listeria ivanovii infection in a patient with AIDS. *J Infect* **28**: 89-91.

Dahmen, M., Vielberg, M.T., Groll, M., and Sieber, S.A. (2015) Structure and mechanism of the caseinolytic protease ClpP1/2 heterocomplex from Listeria monocytogenes. *Angew Chem Int Ed Engl* **54**: 3598-3602.

Daniele, R.P., and Holian, S.K. (1976) A potassium ionophore (valinomycin) inhibits lymphocyte proliferation by its effects on the cell membrane. *Proc Natl Acad Sci U S A* **73**: 3599-3602.

Darken, M.A., Berenson, H., Shirk, R.J., and Sjolander, N.O. (1960) Production of tetracycline by Streptomyces aureofaciens in synthetic media. *Appl Microbiol* **8**: 46-51.

Davis, M.L., Ricke, S.C., and Donaldson, J.R. (2019) Establishment of Listeria monocytogenes in the Gastrointestinal Tract. *Microorganisms* **7**.

Dawson, R.J., and Locher, K.P. (2006) Structure of a bacterial multidrug ABC transporter. *Nature* **443**: 180-185.

de Carvalho, L.P., Groeger-Otero, S., Kreidenweiss, A., Kremsner, P.G., Mordmüller, B., and Held, J. (2022) Boromycin has rapid-onset antibiotic activity against asexual and sexual blood stages of Plasmodium falciparum. *Frontiers in Cellular and Infection Microbiology* **11**: 802294.

DeLano, W.L. (2002) Pymol: An open-source molecular graphics tool. *CCP4 Newsl. Protein Crystallogr* **40**: 82-92.

Derré, I., Rapoport, G., Devine, K., Rose, M., and Msadek, T. (1999) ClpE, a novel type of HSP100 ATPase, is part of the CtsR heat shock regulon of Bacillus subtilis. *Molecular microbiology* **32**: 581-593.

Derre, I., Rapoport, G., and Msadek, T. (1999) CtsR, a novel regulator of stress and heat shock response, controls clp and molecular chaperone gene expression in gram-positive bacteria. *Mol Microbiol* **31**: 117-131.

Dickey, S.W., Burgin, D.J., Huang, S., Maguire, D., and Otto, M. (2023) Two transporters cooperate to secrete amphipathic peptides from the cytoplasmic and membranous milieus. *Proceedings of the National Academy of Sciences* **120**: e2211689120.

Disson, O., Moura, A., and Lecuit, M. (2021) Making Sense of the Biodiversity and Virulence of Listeria monocytogenes. *Trends Microbiol* **29**: 811-822.

Douguet, D., Munier-Lehmann, H., Labesse, G., and Pochet, S. (2005) LEA3D: a computer-aided ligand design for structure-based drug design. *Journal of medicinal chemistry* **48**: 2457-2468.

Dramsi, S., Biswas, I., Maguin, E., Braun, L., Mastroeni, P., and Cossart, P. (1995) Entry of Listeria monocytogenes into hepatocytes requires expression of inIB, a surface protein of the internalin multigene family. *Molecular microbiology* **16**: 251-261.

Dwyer, D.J., Belenky, P.A., Yang, J.H., MacDonald, I.C., Martell, J.D., Takahashi, N., Chan, C.T., Lobritz, M.A., Braff, D., and Schwarz, E.G. (2014) Antibiotics induce redox-related physiological alterations as part of their lethality. *Proceedings of the National Academy of Sciences* **111**: E2100-E2109.

Ehrlich, J., Gottlieb, D., Burkholder, P.R., Anderson, L.E., and Pridham, T.G. (1948) Streptomyces venezuelae, n. sp., the source of chloromycetin. *J Bacteriol* **56**: 467-477.

Eiki, H., Gushima, H., Saito, T., Ishida, H., Oka, Y., and Osono, T. (1988) Product inhibition and its removal on josamycin fermentation by Streptomyces narbonensis var. josamyceticus. *Journal of Fermentation Technology* **66**: 559-565.

Ekiert, D.C., Coudray, N., and Bhabha, G. (2022) Structure and mechanism of the bacterial lipid ABC transporter, MlaFEDB. *Curr Opin Struct Biol* **76**: 102429.

Elbourne, L.D., Tetu, S.G., Hassan, K.A., and Paulsen, I.T. (2017) TransportDB 2.0: a database for exploring membrane transporters in sequenced genomes from all domains of life. *Nucleic Acids Res* **45**: D320-D324.

Elbourne, L.D., Wilson-Mortier, B., Ren, Q., Hassan, K.A., Tetu, S.G., and Paulsen, I.T. (2023) TransAAP: an automated annotation pipeline for membrane transporter prediction in bacterial genomes. *Microbial Genomics* **9**: 000927.

Elshahawi, S.I., Trindade-Silva, A.E., Hanora, A., Han, A.W., Flores, M.S., Vizzoni, V., Schrago, C.G., Soares, C.A., Concepcion, G.P., Distel, D.L., Schmidt, E.W., and Haygood, M.G. (2013) Boronated tartrolon antibiotic produced by symbiotic cellulose-degrading bacteria in shipworm gills. *Proc Natl Acad Sci U S A* **110**: E295-304.

Fang, X., Tiyanont, K., Zhang, Y., Wanner, J., Boger, D., and Walker, S. (2006) The mechanism of action of ramoplanin and enduracidin. *Molecular BioSystems* **2**: 69-76.

Farady, C.J., and Craik, C.S. (2010) Mechanisms of macromolecular protease inhibitors. *Chembiochem* **11**: 2341-2346.

Farber, J.M., and Peterkin, P.I. (1991) Listeria monocytogenes, a food-borne pathogen. *Microbiol Rev* **55**: 476-511.

Fischer, M.A., Engelgeh, T., Rothe, P., Fuchs, S., Thurmer, A., and Halbedel, S. (2022) Listeria monocytogenes genes supporting growth under standard laboratory cultivation conditions and during macrophage infection. *Genome Res* **32**: 1711-1726.

Flynn, J.M., Levchenko, I., Seidel, M., Wickner, S.H., Sauer, R.T., and Baker, T.A. (2001) Overlapping recognition determinants within the ssrA degradation tag allow modulation of proteolysis. *Proceedings of the National Academy of Sciences* **98**: 10584-10589.

Frees, D., Gerth, U., and Ingmer, H. (2014) Clp chaperones and proteases are central in stress survival, virulence and antibiotic resistance of Staphylococcus aureus. *Int J Med Microbiol* **304**: 142-149.

Frees, D., Savijoki, K., Varmanen, P., and Ingmer, H. (2007) Clp ATPases and ClpP proteolytic complexes regulate vital biological processes in low GC, Gram-positive bacteria. *Mol Microbiol* **63**: 1285-1295.

Freitag, N.E., Port, G.C., and Miner, M.D. (2009) Listeria monocytogenes - from saprophyte to intracellular pathogen. *Nat Rev Microbiol* **7**: 623-628.

Gaillard, J., Jaubert, F., and Berche, P. (1996) The inlAB locus mediates the entry of Listeria monocytogenes into hepatocytes in vivo. *The Journal of experimental medicine* **183**: 359-369.

Gaillard, J.L., Berche, P., Mounier, J., Richard, S., and Sansonetti, P. (1987) In vitro model of penetration and intracellular growth of Listeria monocytogenes in the human enterocyte-like cell line Caco-2. *Infect Immun* **55**: 2822-2829.

Gaillot, O., Bregenholt, S., Jaubert, F., Di Santo, J.P., and Berche, P. (2001) Stress-induced ClpP serine protease of Listeria monocytogenes is essential for induction of listeriolysin O-dependent protective immunity. *Infect Immun* **69**: 4938-4943.

Gaillot, O., Pellegrini, E., Bregenholt, S., Nair, S., and Berche, P. (2000) The ClpP serine protease is essential for the intracellular parasitism and virulence of Listeria monocytogenes. *Molecular microbiology* **35**: 1286-1294.

Gardan, R., Cossart, P., Labadie, J., and European Listeria Genome, C. (2003) Identification of Listeria monocytogenes genes involved in salt and alkaline-pH tolerance. *Appl Environ Microbiol* **69**: 3137-3143.

Garg, S.K., Kommineni, S., Henslee, L., Zhang, Y., and Zuber, P. (2009) The YjbH protein of Bacillus subtilis enhances ClpXP-catalyzed proteolysis of Spx. *J Bacteriol* **191**: 1268-1277.

Gartley, S., Anderson-Coughlin, B., Sharma, M., and Kniel, K.E. (2022) Listeria monocytogenes in Irrigation Water: An Assessment of Outbreaks, Sources, Prevalence, and Persistence. *Microorganisms* **10**.

Gatsogiannis, C., Balogh, D., Merino, F., Sieber, S.A., and Raunser, S. (2019) Cryo-EM structure of the ClpXP protein degradation machinery. *Nat Struct Mol Biol* **26**: 946-954.

Gayan, E., Serrano, M.J., Pagan, R., Alvarez, I., and Condon, S. (2015) Environmental and biological factors influencing the UV-C resistance of Listeria monocytogenes. *Food Microbiol* **46**: 246-253.

Gellin, B.G., and Broome, C.V. (1989) Listeriosis. *JAMA* **261**: 1313-1320.

Ghebrehiwet, B., Lim, B.-L., Peerschke, E., Willis, A.C., and Reid, K. (1994) Isolation, cDNA cloning, and overexpression of a 33-kD cell surface glycoprotein that binds to the globular" heads" of C1q. *The Journal of experimental medicine* **179**: 1809-1821.

Ghosh, P., and Higgins, D.E. (2018) Listeria monocytogenes Infection of the Brain. *J Vis Exp*.

Gibbons, N., and Murray, R. (1978) Proposals concerning the higher taxa of bacteria. *International Journal of Systematic and Evolutionary Microbiology* **28**: 1-6.

Gibhardt, J., Hoffmann, G., Turdiev, A., Wang, M., Lee, V.T., and Commichau, F.M. (2019) c-di-AMP assists osmoadaptation by regulating the Listeria monocytogenes potassium transporters KimA and KtrCD. *J Biol Chem* **294**: 16020-16033.

Girma, L., Geteneh, A., Amenu, D., and Kassa, T. (2021) Isolation and characterization of Listeria monocytogenes among women attending Jimma University medical center, Southwest Ethiopia. *BMC Infectious Diseases* **21**: 1-6.

Godreuil, S., Galimand, M., Gerbaud, G., Jacquet, C., and Courvalin, P. (2003) Efflux pump Lde is associated with fluoroquinolone resistance in Listeria monocytogenes. *Antimicrobial Agents and Chemotherapy* **47**: 704-708.

Gottesman, M.M., and Pastan, I. (1993) Biochemistry of multidrug resistance mediated by the multidrug transporter. *Annu Rev Biochem* **62**: 385-427.

Gouin, E., Mengaud, J., and Cossart, P. (1994) The virulence gene cluster of Listeria monocytogenes is also present in Listeria ivanovii, an animal pathogen, and Listeria seeligeri, a nonpathogenic species. *Infection and immunity* **62**: 3550-3553.

Gräfe, U., Schlegel, R., Ritzau, M., Ihn, W., Dornberger, K., Stengel, C., Fleck, W.F., Gutsche, W., Hartl, A., and Paulus, E.F. (1995) Aurantimycins, new depsipeptide antibiotics from Streptomyces aurantiacus IMET 43917. Production, isolation, structure elucidation, and biological activity. *J Antibiot (Tokyo)* **48**: 119-125.

Grandvalet, C., Rapoport, G., and Mazodier, P. (1998) hrcA, encoding the repressor of the groEL genes in Streptomyces albus G, is associated with a second dnaJ gene. *Journal of bacteriology* **180**: 5129-5134.

Grau, F.C., Jaeger, J., Groher, F., Suess, B., and Muller, Y.A. (2020) The complex formed between a synthetic RNA aptamer and the transcription repressor TetR is a structural and functional twin of the operator DNA–TetR regulator complex. *Nucleic Acids Research* **48**: 3366-3378.

Guillet, C., Join-Lambert, O., Le Monnier, A., Leclercq, A., Mechai, F., Mamzer-Bruneel, M.F., Bielecka, M.K., Scortti, M., Disson, O., Berche, P., Vazquez-Boland, J., Lortholary, O., and Lecuit, M. (2010) Human listeriosis caused by Listeria ivanovii. *Emerg Infect Dis* **16**: 136-138.

Gutierrez, A., Laureti, L., Crussard, S., Abida, H., Rodriguez-Rojas, A., Blazquez, J., Baharoglu, Z., Mazel, D., Darfeuille, F., Vogel, J., and Matic, I. (2013) beta-Lactam antibiotics promote bacterial mutagenesis via an RpoS-mediated reduction in replication fidelity. *Nat Commun* **4**: 1610.

Haavik, H.I. (1974) Studies on the formation of bacitracin by Bacillus licheniformis: role of catabolite repression and organic acids. *J Gen Microbiol* **84**: 321-326.

Hadjilouka, A., Paramithiotis, S., and Drosinos, E.H. (2018) Genetic Analysis of the Listeria Pathogenicity Island 1 of Listeria monocytogenes 1/2a and 4b Isolates. *Curr Microbiol* **75**: 857-865.

Halbedel, S., Sperle, I., Lachmann, R., Kleta, S., Fischer, M.A., Wamp, S., Holzer, A., Lüth, S., Murr, L., and Freitag, C. (2023) Large Multicountry Outbreak of Invasive Listeriosis by a Listeria monocytogenes ST394 Clone Linked to Smoked Rainbow Trout, 2020 to 2021. *Microbiology Spectrum*: e03520-03522.

Hamon, M., Bierne, H., and Cossart, P. (2006) Listeria monocytogenes: a multifaceted model. *Nat Rev Microbiol* **4**: 423-434.

Hanawa, T., Kai, M., Kamiya, S., and Yamamoto, T. (2000) Cloning, sequencing, and transcriptional analysis of the dnaK heat shock operon of Listeria monocytogenes. *Cell Stress Chaperones* **5**: 21-29.

Hauf, S., Engelgeh, T., and Halbedel, S. (2021) Elements in the LftR Repressor Operator Interface Contributing to Regulation of Aurantimycin Resistance in Listeria monocytogenes. *J Bacteriol* **203**.

Hauf, S., Herrmann, J., Miethke, M., Gibhardt, J., Commichau, F.M., Muller, R., Fuchs, S., and Halbedel, S. (2019) Aurantimycin resistance genes contribute to survival of Listeria monocytogenes during life in the environment. *Mol Microbiol* **111**: 1009-1024.

Hellmich, U.A., Monkemeyer, L., Velamakanni, S., van Veen, H.W., and Glaubitz, C. (2015) Effects of nucleotide binding to LmrA: A combined MAS-NMR and solution NMR study. *Biochim Biophys Acta* **1848**: 3158-3165.

Hendlin, D., Stapley, E.O., Jackson, M., Wallick, H., Miller, A.K., Wolf, F.J., Miller, T.W., Chaiet, L., Kahan, F.M., Foltz, E.L., Woodruff, H.B., Mata, J.M., Hernandez, S., and Mochales, S. (1969) Phosphonomycin, a new antibiotic produced by strains of streptomyces. *Science* **166**: 122-123.

Higashide, E., Hatano, K., Shibata, M., and Nakazawa, K. (1968) Enduracidin, a new antibiotic. I. Streptomyces fungicidicus No. B5477, an enduracidin producing organism. *J Antibiot (Tokyo)* **21**: 126-137.

Higgins, C.F. (1992) ABC transporters: from microorganisms to man. *Annual review of cell biology* **8**: 67-113.

Hirooka, K., Kunikane, S., Matsuoka, H., Yoshida, K., Kumamoto, K., Tojo, S., and Fujita, Y. (2007) Dual regulation of the Bacillus subtilis regulon comprising the lmrAB and yxaGH operons and yxaF gene by two transcriptional repressors, LmrA and YxaF, in response to flavonoids. *J Bacteriol* **189**: 5170-5182.

Holland, I.B., and Blight, M.A. (1999) ABC-ATPases, adaptable energy generators fuelling transmembrane movement of a variety of molecules in organisms from bacteria to humans. *J Mol Biol* **293**: 381-399.

Horwitz, J.P., Chua, J., Curby, R.J., Tomson, A.J., Darooge, M.A., Fisher, B.E., Mauricio, J., and Klundt, I. (1964) Substrates for Cytochemical Demonstration of Enzyme Activity. I. Some Substituted 3-Indolyl-Beta-D-Glycopyranosides. *J Med Chem* **7**: 574-575.

Huang, L. (2004) Thermal resistance of Listeria monocytogenes, Salmonella Heidelberg, and Escherichia coli O157:H7 at elevated temperatures. *J Food Prot* **67**: 1666-1670.

Irschik, H., Schummer, D., Gerth, K., Hofle, G., and Reichenbach, H. (1995) The tartrolons, new boron-containing antibiotics from a myxobacterium, Sorangium cellulosum. *J Antibiot (Tokyo)* **48**: 26-30.

Jiang, X., Geng, Y., Ren, S., Yu, T., Li, Y., Liu, G., Wang, H., Meng, H., and Shi, L. (2019) The VirAB-VirSR-AnrAB multicomponent system is involved in resistance of Listeria monocytogenes EGD-e to cephalosporins, bacitracin, nisin, benzalkonium chloride, and ethidium bromide. *Applied and Environmental Microbiology* **85**: e01470-01419.

Johnson, L.J., Azari, S., Webb, A., Zhang, X., Gavrilin, M.A., Marshall, J.M., Rood, K., and Seveau, S. (2021) Human Placental Trophoblasts Infected by Listeria monocytogenes Undergo a Pro-Inflammatory Switch Associated With Poor Pregnancy Outcomes. *Front Immunol* **12**: 709466.

Jones, E.M., and MacGowan, A.P. (1995) Antimicrobial chemotherapy of human infection due to Listeria monocytogenes. *Eur J Clin Microbiol Infect Dis* **14**: 165-175.

Jones, P.M., and George, A.M. (2002) Mechanism of ABC transporters: a molecular dynamics simulation of a well characterized nucleotide-binding subunit. *Proc Natl Acad Sci U S A* **99**: 12639-12644.

Jonquières, R., Pizarro-Cerdá, J., and Cossart, P. (2001) Synergy between the N-and C-terminal domains of InlB for efficient invasion of non-phagocytic cells by Listeria monocytogenes. *Molecular microbiology* **42**: 955-965.

Karatzas, K.-A.G., Suur, L., and O'Byrne, C.P. (2012) Characterization of the intracellular glutamate decarboxylase system: analysis of its function, transcription, and role in the acid resistance of various strains of Listeria monocytogenes. *Applied and Environmental Microbiology* **78**: 3571-3579.

Karatzas, K.A., Wouters, J.A., Gahan, C.G., Hill, C., Abee, T., and Bennik, M.H. (2003) The CtsR regulator of Listeria monocytogenes contains a variant glycine repeat region that affects piezotolerance, stress resistance, motility and virulence. *Molecular Microbiology* **49**: 1227-1238.

Katayama, Y., Gottesman, S., Pumphrey, J., Rudikoff, S., Clark, W.P., and Maurizi, M.R. (1988) The two-component, ATP-dependent Clp protease of Escherichia coli. Purification, cloning, and mutational analysis of the ATP-binding component. *J Biol Chem* **263**: 15226-15236.

Kaval, K.G., Hahn, B., Tusamda, N., Albrecht, D., and Halbedel, S. (2015) The PadR-like transcriptional regulator LftR ensures efficient invasion of Listeria monocytogenes into human host cells. *Frontiers in microbiology* **6**: 772.

Kellner, R., Jung, G., Horner, T., Zahner, H., Schnell, N., Entian, K.D., and Gotz, F. (1988) Gallidermin: a new lanthionine-containing polypeptide antibiotic. *Eur J Biochem* **177**: 53-59.

Kibbe, W.A. (2007) OligoCalc: an online oligonucleotide properties calculator. *Nucleic Acids Res* **35**: W43-46.

Kiernan, J.A. (2007) Indigogenic substrates for detection and localization of enzymes. *Biotech Histochem* **82**: 73-103.

Kim, H.J., Mittal, M., and Sonenshein, A.L. (2006a) CcpC-dependent regulation of citB and lmo0847 in Listeria monocytogenes. *J Bacteriol* **188**: 179-190.

Kim, S., Fei, X., Sauer, R.T., and Baker, T.A. (2022) AAA+ protease-adaptor structures reveal altered conformations and ring specialization. *Nat Struct Mol Biol* **29**: 1068-1079.

Kim, S.H., Gorski, L., Reynolds, J., Orozco, E., Fielding, S., Park, Y.H., and Borucki, M.K. (2006b) Role of uvrA in the growth and survival of Listeria monocytogenes under UV radiation and acid and bile stress. *J Food Prot* **69**: 3031-3036.

Kirstein, J., Hoffmann, A., Lilie, H., Schmidt, R., Rubsamen-Waigmann, H., Brotz-Oesterhelt, H., Mogk, A., and Turgay, K. (2009) The antibiotic ADEP reprogrammes ClpP, switching it from a regulated to an uncontrolled protease. *EMBO Mol Med* **1**: 37-49.

Knudsen, G.M., Olsen, J.E., Aabo, S., Barrow, P., Rychlik, I., and Thomsen, L.E. (2013) ClpP deletion causes attenuation of Salmonella Typhimurium virulence through mis-regulation of RpoS and indirect control of CsrA and the SPI genes. *Microbiology (Reading)* **159**: 1497-1509.

Ko, R., and Smith, L.T. (1999) Identification of an ATP-driven, osmoregulated glycine betaine transport system in Listeria monocytogenes. *Appl Environ Microbiol* **65**: 4040-4048.

Kock, H., Gerth, U., and Hecker, M. (2004) MurAA, catalysing the first committed step in peptidoglycan biosynthesis, is a target of Clp-dependent proteolysis in Bacillus subtilis. *Molecular Microbiology* **51**: 1087-1102.

Komaki, H. (2023) Recent Progress of Reclassification of the Genus Streptomyces. *Microorganisms* **11**.

Konosonoka, I.H., Jemeljanovs, A., Osmane, B., Ikauniece, D., and Gulbe, G. (2012) Incidence of Listeria spp. in Dairy Cows Feed and Raw Milk in Latvia. *ISRN Vet Sci* **2012**: 435187.

Konz, D., Klens, A., Schorgendorfer, K., and Marahiel, M.A. (1997) The bacitracin biosynthesis operon of Bacillus licheniformis ATCC 10716: molecular characterization of three multi-modular peptide synthetases. *Chem Biol* **4**: 927-937.

Krüger, E., Zuhlke, D., Witt, E., Ludwig, H., and Hecker, M. (2001) Clp-mediated proteolysis in Gram-positive bacteria is autoregulated by the stability of a repressor. *EMBO J* **20**: 852-863.

Kuipers, O.P., Beerthuyzen, M.M., Siezen, R.J., and De Vos, W.M. (1993) Characterization of the nisin gene cluster nisABTCIPR of Lactococcus lactis. Requirement of expression of the nisA and nisI genes for development of immunity. *Eur J Biochem* **216**: 281-291.

Kuttappan, D., Muyyarikkandy, M.S., Mathew, E., and Amalaradjou, M.A. (2021) Listeria monocytogenes Survival on Peaches and Nectarines under Conditions Simulating Commercial Stone-Fruit Packinghouse Operations. *Int J Environ Res Public Health* **18**.

Kvistholm Jensen, A., Simonsen, J., and Ethelberg, S. (2017) Use of Proton Pump Inhibitors and the Risk of Listeriosis: A Nationwide Registry-based Case-Control Study. *Clin Infect Dis* **64**: 845-851.

Larsson, J.T., Rogstam, A., and von Wachenfeldt, C. (2007) YjbH is a novel negative effector of the disulphide stress regulator, Spx, in Bacillus subtilis. *Mol Microbiol* **66**: 669-684.

Lecuit, M. (2005) Understanding how Listeria monocytogenes targets and crosses host barriers. *Clinical Microbiology and Infection* **11**: 430-436.

Lecuit, M., Ohayon, H., Braun, L., Mengaud, J., and Cossart, P. (1997) Internalin of Listeria monocytogenes with an intact leucine-rich repeat region is sufficient to promote internalization. *Infection and immunity* **65**: 5309-5319.

Lee, S. (2020) Bacteriocins of Listeria monocytogenes and their potential as a virulence factor. *Toxins* **12**: 103.

Leisner, J.J., Laursen, B.G., Prevost, H., Drider, D., and Dalgaard, P. (2007) Carnobacterium: positive and negative effects in the environment and in foods. *FEMS Microbiol Rev* **31**: 592-613.

Lewis, P.J., and Marston, A.L. (1999) GFP vectors for controlled expression and dual labelling of protein fusions in Bacillus subtilis. *Gene* **227**: 101-110.

Lewis, V.G., Ween, M.P., and McDevitt, C.A. (2012) The role of ATP-binding cassette transporters in bacterial pathogenicity. *Protoplasma* **249**: 919-942.

Li, D.H., Chung, Y.S., Gloyd, M., Joseph, E., Ghirlando, R., Wright, G.D., Cheng, Y.Q., Maurizi, M.R., Guarne, A., and Ortega, J. (2010) Acyldepsipeptide antibiotics induce the formation of a structured axial channel in ClpP: A model for the ClpX/ClpA-bound state of ClpP. *Chem Biol* **17**: 959-969.

Li, T., Zhao, K., Huang, Y., Li, D., Jiang, C.-Y., Zhou, N., Fan, Z., and Liu, S.-J. (2012) The TetR-type transcriptional repressor RolR from Corynebacterium glutamicum regulates resorcinol catabolism by binding to a unique operator, rolO. *Applied and environmental microbiology* **78**: 6009-6016.

Lightfield, J., Fram, N.R., and Ely, B. (2011) Across bacterial phyla, distantly-related genomes with similar genomic GC content have similar patterns of amino acid usage. *PLoS One* **6**: e17677.

Locher, K.P. (2004) Structure and mechanism of ABC transporters. *Current opinion in structural biology* **14**: 426-431.

Locher, K.P. (2009) Structure and mechanism of ATP-binding cassette transporters. *Philos Trans R Soc Lond B Biol Sci* **364**: 239-245.

Loughlin, M.F., Arandhara, V., Okolie, C., Aldsworth, T.G., and Jenks, P.J. (2009) Helicobacter pylori mutants defective in the clpP ATP-dependant protease and the chaperone clpA display reduced macrophage and murine survival. *Microb Pathog* **46**: 53-57.

Lubelski, J., De Jong, A., Van Merkerk, R., Agustiandari, H., Kuipers, O.P., Kok, J., and Driessen, A.J. (2006) LmrCD is a major multidrug resistance transporter in Lactococcus lactis. *Molecular microbiology* **61**: 771-781.

Lubelski, J., Konings, W.N., and Driessen, A.J. (2007) Distribution and physiology of ABC-type transporters contributing to multidrug resistance in bacteria. *Microbiol Mol Biol Rev* **71**: 463-476.

Lubelski, J., Mazurkiewicz, P., van Merkerk, R., Konings, W.N., and Driessen, A.J. (2004) ydaG and ydbA of Lactococcus lactis encode a heterodimeric ATP-binding cassette-type multidrug transporter. *J Biol Chem* **279**: 34449-34455.

Luque-Sastre, L., Arroyo, C., Fox, E.M., McMahon, B.J., Bai, L., Li, F., and Fanning, S. (2018) Antimicrobial Resistance in Listeria Species. *Microbiol Spectr* **6**.

Mabanglo, M.F., Leung, E., Vahidi, S., Seraphim, T.V., Eger, B.T., Bryson, S., Bhandari, V., Zhou, J.L., Mao, Y.-Q., and Rizzolo, K. (2019) ClpP protease activation results from the reorganization of the electrostatic interaction networks at the entrance pores. *Communications Biology* **2**: 410.

Mackey, B., and Bratchell, N. (1989) The heat resistance of Listeria monocytogenes. *Letters in Applied Microbiology* **9**: 89-94.

Madad, A., Marshall, K.E., Blessington, T., Hardy, C., Salter, M., Basler, C., Conrad, A., Stroika, S., Luo, Y., and Dwarka, A. (2023) Investigation of a multistate outbreak of Listeria monocytogenes infections linked to frozen vegetables produced at individually quick-frozen vegetable manufacturing facilities. *Journal of Food Protection* **86**: 100117.

Madoori, P.K., Agustiandari, H., Driessen, A.J., and Thunnissen, A.M. (2009) Structure of the transcriptional regulator LmrR and its mechanism of multidrug recognition. *EMBO J* **28**: 156-166.

Malik, I.T., Pereira, R., Vielberg, M.T., Mayer, C., Straetener, J., Thomy, D., Famulla, K., Castro, H., Sass, P., Groll, M., and Brotz-Oesterhelt, H. (2020) Functional Characterisation of ClpP Mutations Conferring Resistance to Acyldepsipeptide Antibiotics in Firmicutes. *Chembiochem* **21**: 1997-2012.

Mandin, P., Fsihi, H., Dussurget, O., Vergassola, M., Milohanic, E., Toledo-Arana, A., Lasa, I., Johansson, J., and Cossart, P. (2005) VirR, a response regulator critical for Listeria monocytogenes virulence. *Mol Microbiol* **57**: 1367-1380.

Marston, A.L., Thomaides, H.B., Edwards, D.H., Sharpe, M.E., and Errington, J. (1998) Polar localization of the MinD protein of Bacillus subtilis and its role in selection of the mid-cell division site. *Genes Dev* **12**: 3419-3430.

Martin, J.F., Casqueiro, J., and Liras, P. (2005) Secretion systems for secondary metabolites: how producer cells send out messages of intercellular communication. *Curr Opin Microbiol* **8**: 282-293.

Mascher, T., Zimmer, S.L., Smith, T.A., and Helmann, J.D. (2004) Antibiotic-inducible promoter regulated by the cell envelope stress-sensing two-component system LiaRS of Bacillus subtilis. *Antimicrob Agents Chemother* **48**: 2888-2896.

Matle, I., Mbatha, K.R., and Madoroba, E. (2020) A review of Listeria monocytogenes from meat and meat products: Epidemiology, virulence factors, antimicrobial resistance and diagnosis. *Onderstepoort J Vet Res* **87**: e1-e20.

Maupin-Furlow, J. (2011) Proteasomes and protein conjugation across domains of life. *Nat Rev Microbiol* **10**: 100-111.

Mengaud, J., Chenevert, J., Geoffroy, C., Gaillard, J., and Cossart, P. (1987) Identification of the structural gene encoding the SH-activated hemolysin of Listeria monocytogenes: listeriolysin O is homologous to streptolysin O and pneumolysin. *Infection and immunity* **55**: 3225-3227.

Miller, J.H., (1972) Experiments in Molecular Genetics. In: Cold Spring Harbor. Cold Spring Harbor Laboratory: Cold Spring Harbor, pp. 352-355.

Monk, I.R., Gahan, C.G., and Hill, C. (2008) Tools for functional postgenomic analysis of listeria monocytogenes. *Appl Environ Microbiol* **74**: 3921-3934.

Moreira, W., Aziz, D.B., and Dick, T. (2016) Boromycin kills mycobacterial persisters without detectable resistance. *Frontiers in microbiology* **7**: 199.

Moreno-Cinos, C., Goossens, K., Salado, I.G., Van Der Veken, P., De Winter, H., and Augustyns, K. (2019) ClpP Protease, a Promising Antimicrobial Target. *Int J Mol Sci* **20**.

Msadek, T., Dartois, V., Kunst, F., Herbaud, M.L., Denizot, F., and Rapoport, G. (1998) ClpP of Bacillus subtilis is required for competence development, motility, degradative enzyme synthesis, growth at high temperature and sporulation. *Molecular microbiology* **27**: 899-914.

Muchaamba, F., Stephan, R., and Tasara, T. (2021) Listeria monocytogenes Cold Shock Proteins: Small Proteins with A Huge Impact. *Microorganisms* **9**.

Müller, A., Rychli, K., Zaiser, A., Wieser, C., Wagner, M., and Schmitz-Esser, S. (2014) The Listeria monocytogenes transposon Tn 6188 provides increased tolerance to various quaternary ammonium compounds and ethidium bromide. *FEMS microbiology letters* **361**: 166-173.

Mulzer, J., and Berger, M. (2004) Total synthesis of the boron-containing ion carrier antibiotic macrodiolide tartrolon B. *J Org Chem* **69**: 891-898.

Murata, M., Ohno, S., Kumano, M., Yamane, K., and Ohki, R. (2003) Multidrug resistant phenotype of Bacillus subtilis spontaneous mutants isolated in the presence of puromycin and lincomycin. *Can J Microbiol* **49**: 71-77.

Murray, E.G.D., Webb, R.A., and Swann, M.B.R. (1926) A disease of rabbits characterised by a large mononuclear leucocytosis, caused by a hitherto undescribed bacillus Bacterium monocytogenes (n. sp.). *The Journal of Pathology and Bacteriology* **29**: 407-439.

Nair, S., Derre, I., Msadek, T., Gaillot, O., and Berche, P. (2000) CtsR controls class III heat shock gene expression in the human pathogen Listeria monocytogenes. *Mol Microbiol* **35**: 800-811.

Nair, S., Frehel, C., Nguyen, L., Escuyer, V., and Berche, P. (1999) ClpE, a novel member of the HSP100 family, is involved in cell division and virulence of Listeria monocytogenes. *Molecular microbiology* **31**: 185-196.

Nakano, M.M., Hajarizadeh, F., Zhu, Y., and Zuber, P. (2001) Loss-of-function mutations in yjbD result in ClpX- and ClpP-independent competence development of Bacillus subtilis. *Mol Microbiol* **42**: 383-394.

Nakano, S., Küster-Schöck, E., Grossman, A.D., and Zuber, P. (2003) Spx-dependent global transcriptional control is induced by thiol-specific oxidative stress in Bacillus subtilis. *Proceedings of the National Academy of Sciences* **100**: 13603-13608.

Nakano, S., Zheng, G., Nakano, M.M., and Zuber, P. (2002) Multiple pathways of Spx (YjbD) proteolysis in Bacillus subtilis. *J Bacteriol* **184**: 3664-3670.

Newman, H., Krajnc, A., Bellini, D., Eyermann, C.J., Boyle, G.A., Paterson, N.G., McAuley, K.E., Lesniak, R., Gangar, M., von Delft, F., Brem, J., Chibale, K., Schofield, C.J., and Dowson, C.G. (2021) High-Throughput Crystallography Reveals Boron-Containing Inhibitors of a Penicillin-Binding Protein with Di- and Tricovalent Binding Modes. *J Med Chem* **64**: 11379-11394.

Nguyen, T.K., Tran, N.P., and Cavin, J.F. (2011) Genetic and biochemical analysis of PadR-padC promoter interactions during the phenolic acid stress response in Bacillus subtilis 168. *J Bacteriol* **193**: 4180-4191.

Nishino, K., Yamasaki, S., Nakashima, R., Zwama, M., and Hayashi-Nishino, M. (2021) Function and inhibitory mechanisms of multidrug efflux pumps. *Frontiers in Microbiology* **12**: 737288.

Nyarko, E.B., and Donnelly, C.W. (2015) Listeria monocytogenes: Strain Heterogeneity, Methods, and Challenges of Subtyping. *J Food Sci* **80**: M2868-2878.

Nyfeldt, A. (1929) Etiologie de la mononucleose infectieuse. *CR Soc. Biol* **101**: 590-591.

Okami, Y., Tazaki, T., Katumata, S., Honda, K., Suzuki, M., and Umezawa, H. (1959) Studies on Streptomyces kanamyceticus, producer of kanamycin. *J Antibiot (Tokyo)* **12**: 252-256.

Olaimat, A.N., Al-Holy, M.A., Shahbaz, H.M., Al-Nabulsi, A.A., Abu Ghoush, M.H., Osaili, T.M., Ayyash, M.M., and Holley, R.A. (2018) Emergence of Antibiotic Resistance in Listeria monocytogenes Isolated from Food Products: A Comprehensive Review. *Compr Rev Food Sci Food Saf* **17**: 1277-1292.

Olivares, A.O., Baker, T.A., and Sauer, R.T. (2016) Mechanistic insights into bacterial AAA+ proteases and protein-remodelling machines. *Nature Reviews Microbiology* **14**: 33-44.

Oren, A., and Garrity, G.M. (2021) Valid publication of the names of forty-two phyla of prokaryotes. *Int J Syst Evol Microbiol* **71**.

Orsi, R.H., and Wiedmann, M. (2016) Characteristics and distribution of Listeria spp., including Listeria species newly described since 2009. *Applied microbiology and biotechnology* **100**: 5273-5287.

Orth, P., Schnappinger, D., Hillen, W., Saenger, W., and Hinrichs, W. (2000) Structural basis of gene regulation by the tetracycline inducible Tet repressor-operator system. *Nat Struct Biol* **7**: 215-219.

Panina, I., Taldaev, A., Efremov, R., and Chugunov, A. (2021) Molecular Dynamics Insight into the Lipid II Recognition by Type A Lantibiotics: Nisin, Epidermin, and Gallidermin. *Micromachines (Basel)* **12**.

Patrick, J.E., and Kearns, D.B. (2008) MinJ (YvjD) is a topological determinant of cell division in Bacillus subtilis. *Mol Microbiol* **70**: 1166-1179.

Phelps, C.C., Vadia, S., Arnett, E., Tan, Y., Zhang, X., Pathak-Sharma, S., Gavrilin, M.A., and Seveau, S. (2018) Relative Roles of Listeriolysin O, InlA, and InlB in Listeria monocytogenes Uptake by Host Cells. *Infect Immun* **86**.

Pistor, S., Chakraborty, T., Niebuhr, K., Domann, E., and Wehland, J. (1994) The ActA protein of Listeria monocytogenes acts as a nucleator inducing reorganization of the actin cytoskeleton. *The EMBO journal* **13**: 758-763.

Pizarro-Cerda, J., Charbit, A., Enninga, J., Lafont, F., and Cossart, P. (2016) Manipulation of host membranes by the bacterial pathogens Listeria, Francisella, Shigella and Yersinia. *Semin Cell Dev Biol* **60**: 155-167.

Poelarends, G.J., Mazurkiewicz, P., and Konings, W.N. (2002) Multidrug transporters and antibiotic resistance in Lactococcus lactis. *Biochim Biophys Acta* **1555**: 1-7.

Quereda, J.J., Andersson, C., Cossart, P., Johansson, J., and Pizarro-Cerda, J. (2018) Role in virulence of phospholipases, listeriolysin O and listeriolysin S from epidemic Listeria monocytogenes using the chicken embryo infection model. *Vet Res* **49**: 13.

Quereda, J.J., Meza-Torres, J., Cossart, P., and Pizarro-Cerdá, J. (2017) Listeriolysin S: A bacteriocin from epidemic Listeria monocytogenes strains that targets the gut microbiota. *Gut Microbes* **8**: 384-391.

Quereda, J.J., Moron-Garcia, A., Palacios-Gorba, C., Dessaux, C., Garcia-Del Portillo, F., Pucciarelli, M.G., and Ortega, A.D. (2021) Pathogenicity and virulence of Listeria monocytogenes: A trip from environmental to medical microbiology. *Virulence* **12**: 2509-2545.

Radisky, E.S., Lee, J.M., Lu, C.-J.K., and Koshland Jr, D.E. (2006) Insights into the serine protease mechanism from atomic resolution structures of trypsin reaction intermediates. *Proceedings of the National Academy of Sciences* **103**: 6835-6840.

Radoshevich, L., and Cossart, P. (2018) Listeria monocytogenes: towards a complete picture of its physiology and pathogenesis. *Nat Rev Microbiol* **16**: 32-46.

Ramos, J.L., Martinez-Bueno, M., Molina-Henares, A.J., Teran, W., Watanabe, K., Zhang, X., Gallegos, M.T., Brennan, R., and Tobes, R. (2005) The TetR family of transcriptional repressors. *Microbiol Mol Biol Rev* **69**: 326-356.

Ray, S., Maitra, A., Biswas, A., Panjikar, S., Mondal, J., and Anand, R. (2017) Functional insights into the mode of DNA and ligand binding of the TetR family regulator TylP from Streptomyces fradiae. *Journal of Biological Chemistry* **292**: 15301-15311.

Razzaq, A., Shamsi, S., Ali, A., Ali, Q., Sajjad, M., Malik, A., and Ashraf, M. (2019) Microbial Proteases Applications. *Front Bioeng Biotechnol* **7**: 110.

Rey, M.W., Ramaiya, P., Nelson, B.A., Brody-Karpin, S.D., Zaretsky, E.J., Tang, M., Lopez de Leon, A., Xiang, H., Gusti, V., Clausen, I.G., Olsen, P.B., Rasmussen, M.D., Andersen, J.T., Jorgensen, P.L., Larsen, T.S., Sorokin, A., Bolotin, A., Lapidus, A., Galleron, N., Ehrlich, S.D., and Berka, R.M. (2004) Complete genome sequence of the industrial bacterium Bacillus licheniformis and comparisons with closely related Bacillus species. *Genome Biol* **5**: R77.

Rietkötter, E., Hoyer, D., and Mascher, T. (2008) Bacitracin sensing in Bacillus subtilis. *Mol Microbiol* **68**: 768-785.

Rismondo, J., Bender, J.K., and Halbedel, S. (2017) Suppressor Mutations Linking gpsB with the First Committed Step of Peptidoglycan Biosynthesis in Listeria monocytogenes. *J Bacteriol* **199**.

Rismondo, J., Gibhardt, J., Rosenberg, J., Kaever, V., Halbedel, S., and Commichau, F.M. (2016) Phenotypes Associated with the Essential Diadenylate Cyclase CdaA and Its Potential Regulator CdaR in the Human Pathogen Listeria monocytogenes. *J Bacteriol* **198**: 416-426.

Rojas-Tapias, D.F., and Helmann, J.D. (2018) Induction of the Spx regulon by cell wall stress reveals novel regulatory mechanisms in Bacillus subtilis. *Mol Microbiol* **107**: 659-674.

Rojas-Tapias, D.F., and Helmann, J.D. (2019) Roles and regulation of Spx family transcription factors in Bacillus subtilis and related species. *Adv Microb Physiol* **75**: 279-323.

Rouquette, C., Ripio, M.T., Pellegrini, E., Bolla, J.M., Tascon, R.I., Vazquez-Boland, J.A., and Berche, P. (1996) Identification of a ClpC ATPase required for stress tolerance and in vivo survival of Listeria monocytogenes. *Mol Microbiol* **21**: 977-987.

Rozov, A., Khusainov, I., El Omari, K., Duman, R., Mykhaylyk, V., Yusupov, M., Westhof, E., Wagner, A., and Yusupova, G. (2019) Importance of potassium ions for ribosome structure and function revealed by long-wavelength X-ray diffraction. *Nat Commun* **10**: 2519.

Runde, S., Moliere, N., Heinz, A., Maisonneuve, E., Janczikowski, A., Elsholz, A.K., Gerth, U., Hecker, M., and Turgay, K. (2014) The role of thiol oxidative stress response in heat-induced protein aggregate formation during thermotolerance in Bacillus subtilis. *Mol Microbiol* **91**: 1036-1052.

Ryan, S., Begley, M., Gahan, C.G., and Hill, C. (2009) Molecular characterization of the arginine deiminase system in Listeria monocytogenes: regulation and role in acid tolerance. *Environmental Microbiology* **11**: 432-445.

Saklani-Jusforgues, H., Fontan, E., and Goossens, P.L. (2000) Effect of acid-adaptation on Listeria monocytogenes survival and translocation in a murine intragastric infection model. *FEMS Microbiol Lett* **193**: 155-159.

Sallami, L., Marcotte, M., Naim, F., Ouattara, B., Leblanc, C., and Saucier, L. (2006) Heat inactivation of Listeria monocytogenes and Salmonella enterica serovar Typhi in a typical bologna matrix during an industrial cooking-cooling cycle. *Journal of food protection* **69**: 3025-3030.

Sanger, F., Nicklen, S., and Coulson, A.R. (1977) DNA sequencing with chain-terminating inhibitors. *Proc Natl Acad Sci U S A* **74**: 5463-5467.

Saraste, M., Sibbald, P.R., and Wittinghofer, A. (1990) The P-loop—a common motif in ATP- and GTP-binding proteins. *Trends in biochemical sciences* **15**: 430-434.

Sato, E., Hirata, K., Lisy, J.M., Ishiuchi, S.I., and Fujii, M. (2021) Rethinking Ion Transport by Ionophores: Experimental and Computational Investigation of Single Water Hydration in Valinomycin-K(+) Complexes. *J Phys Chem Lett* **12**: 1754-1758.

Sauer, R.T., and Baker, T.A. (2011) AAA+ proteases: ATP-fueled machines of protein destruction. *Annu Rev Biochem* **80**: 587-612.

Schäfer, H., and Turgay, K. (2019) Spx, a versatile regulator of the Bacillus subtilis stress response. *Curr Genet* **65**: 871-876.

Schlech III, W.F., Lavigne, P.M., Bortolussi, R.A., Allen, A.C., Haldane, E.V., Wort, A.J., Hightower, A.W., Johnson, S.E., King, S.H., and Nicholls, E.S. (1983) Epidemic listeriosis—evidence for transmission by food. *New england journal of medicine* **308**: 203-206.

Schmees, G., Stein, A., Hunke, S., Landmesser, H., and Schneider, E. (1999) Functional consequences of mutations in the conserved 'signature sequence' of the ATP-binding-cassette protein MalK. *Eur J Biochem* **266**: 420-430.

Schmid, B., Klumpp, J., Raimann, E., Loessner, M.J., Stephan, R., and Tasara, T. (2009) Role of cold shock proteins in growth of Listeria monocytogenes under cold and osmotic stress conditions. *Appl Environ Microbiol* **75**: 1621-1627.

Schmitt, L., Benabdelhak, H., Blight, M.A., Holland, I.B., and Stubbs, M.T. (2003) Crystal structure of the nucleotide-binding domain of the ABC-transporter haemolysin B: identification of a variable region within ABC helical domains. *Journal of molecular biology* **330**: 333-342.

Schummer, D., Schomburg, D., Irschik, H., Reichenbach, H., and Höfle, G. (1996) Antibiotics from gliding bacteria, LXXV. Absolute configuration and biosynthesis of tartrolon B, a boron-containing macrodiolide from Sorangium cellulosum. *Liebigs Annalen* **1996**: 965-969.

Schwedt, I., Wang, M., Gibhardt, J., and Commichau, F.M. (2023) Cyclic di-AMP, a multifaceted regulator of central metabolism and osmolyte homeostasis in Listeria monocytogenes. *Microlife* **4**: uqad005.

Selby, T., Berzins, A., Gerrard, D., Corvalan, C., Grant, A., and Linton, R. (2006) Microbial heat resistance of Listeria monocytogenes and the impact on ready-to-eat meat quality after post-package pasteurization. *Meat Science* **74**: 425-434.

Seno, E.T., Pieper, R.L., and Huber, F.M. (1977) Terminal stages in the biosynthesis of tylosin. *Antimicrob Agents Chemother* **11**: 455-461.

Sharma, P., Reddy, P.K., and Kumar, B. (2021) Trace Element Zinc, a Nature's Gift to Fight Unprecedented Global Pandemic COVID-19. *Biol Trace Elem Res* **199**: 3213-3221.

Shen, Y., Naujokas, M., Park, M., and Ireton, K. (2000) InlB-dependent internalization of Listeria is mediated by the Met receptor tyrosine kinase. *Cell* **103**: 501-510.

Simonetti, T., Peter, K., Chen, Y., Jin, Q., Zhang, G., LaBorde, L.F., and Macarisin, D. (2021) Prevalence and Distribution of Listeria monocytogenes in Three Commercial Tree Fruit Packinghouses. *Front Microbiol* **12**: 652708.

Sivalingam, J.J., Martin, P., Fraimow, H.S., Yarze, J.C., and Friedman, L.S. (1992) Listeria monocytogenes peritonitis: case report and literature review. *Am J Gastroenterol* **87**: 1839-1845.

Sleator, R.D., Gahan, C.G., Abee, T., and Hill, C. (1999) Identification and disruption of BetL, a secondary glycine betaine transport system linked to the salt tolerance of Listeria monocytogenes LO28. *Appl Environ Microbiol* **65**: 2078-2083.

Sleator, R.D., Wemekamp-Kamphuis, H.H., Gahan, C.G., Abee, T., and Hill, C. (2005) A PrfA-regulated bile exclusion system (BilE) is a novel virulence factor in Listeria monocytogenes. *Molecular microbiology* **55**: 1183-1195.

Smith, B., Kemp, M., Ethelberg, S., Schiellerup, P., Bruun, B.G., Gerner-Smidt, P., and Christensen, J.J. (2009) Listeria monocytogenes: maternal-foetal infections in Denmark 1994-2005. *Scand J Infect Dis* **41**: 21-25.

Smith, G.A., Marquis, H., Jones, S., Johnston, N.C., Portnoy, D.A., and Goldfine, H. (1995) The two distinct phospholipases C of Listeria monocytogenes have overlapping roles in escape from a vacuole and cell-to-cell spread. *Infection and immunity* **63**: 4231-4237.

Solanki, P., Putatunda, C., Kumar, A., Bhatia, R., and Walia, A. (2021) Microbial proteases: ubiquitous enzymes with innumerable uses. *3 Biotech* **11**: 428.

Subramaniam-Niehaus, B., Schneider, T., Metzger, J.W., and Wohlleben, W. (1997) Isolation and analysis of moenomycin and its biosynthetic intermediates from Streptomyces ghanaensis (ATCC 14672) wildtype and selected mutants. *Z Naturforsch C J Biosci* **52**: 217-226.

Surup, F., Chauhan, D., Niggemann, J., Bartok, E., Herrmann, J., Keck, M., Zander, W., Stadler, M., Hornung, V., and Muller, R. (2018) Activation of the NLRP3 Inflammasome by Hyaboron, a New Asymmetric Boron-Containing Macrodiolide from the Myxobacterium Hyalangium minutum. *ACS Chem Biol* **13**: 2981-2988.

Svensson, M.-L.G., Sten (1982) The pathway of D-cycloserine biosynthesis in Streptomyces garyphalus. *Archives of Microbiology* **131**: 129-131.

Swaminathan, B., and Gerner-Smidt, P. (2007) The epidemiology of human listeriosis. *Microbes Infect* **9**: 1236-1243.

Sweet, M.E., Larsen, C., Zhang, X., Schlame, M., Pedersen, B.P., and Stokes, D.L. (2021) Structural basis for potassium transport in prokaryotes by KdpFABC. *Proc Natl Acad Sci U S A* **118**.

Swier, L.J., Slotboom, D.-J., and Poolman, B. (2016) ABC importers. *ABC Transporters-40 Years on*: 3-36.

Takatsuki, A., Arima, K., and Tamura, G. (1971) Tunicamycin, a new antibiotic. I. Isolation and characterization of tunicamycin. *J Antibiot (Tokyo)* **24**: 215-223.

Urban, A., Eckermann, S., Fast, B., Metzger, S., Gehling, M., Ziegelbauer, K., Rubsamen-Waigmann, H., and Freiberg, C. (2007) Novel whole-cell antibiotic biosensors for compound discovery. *Appl Environ Microbiol* **73**: 6436-6443.

van der Heul, H.U., Bilyk, B.L., McDowall, K.J., Seipke, R.F., and van Wezel, G.P. (2018) Regulation of antibiotic production in Actinobacteria: new perspectives from the post-genomic era. *Nat Prod Rep* **35**: 575-604.

Vasseur, C., Baverel, L., Hebraud, M., and Labadie, J. (1999) Effect of osmotic, alkaline, acid or thermal stresses on the growth and inhibition of Listeria monocytogenes. *J Appl Microbiol* **86**: 469-476.

Vazquez-Boland, J.A., Dominguez-Bernal, G., Gonzalez-Zorn, B., Kreft, J., and Goebel, W. (2001) Pathogenicity islands and virulence evolution in Listeria. *Microbes Infect* **3**: 571-584.

Walker, J.E., Saraste, M., Runswick, M.J., and Gay, N.J. (1982) Distantly related sequences in the alpha- and beta-subunits of ATP synthase, myosin, kinases and other ATP-requiring enzymes and a common nucleotide binding fold. *EMBO J* **1**: 945-951.

Walker, S. (1987) Growth of Listeria monocytogenes and Aeromonas hydrophila at chill temperatures.

Walsh, D., Duffy, G., Sheridan, J., Blair, I., and McDowell, D. (2001) Antibiotic resistance among Listeria, including Listeria monocytogenes, in retail foods. *Journal of Applied Microbiology* **90**: 517-522.

Wamp, S., Rutter, Z.J., Rismondo, J., Jennings, C.E., Moller, L., Lewis, R.J., and Halbedel, S. (2020) PrkA controls peptidoglycan biosynthesis through the essential phosphorylation of ReoM. *Elife* **9**.

Wampler, J.L., Kim, K.-P., Jaradat, Z., and Bhunia, A.K. (2004) Heat shock protein 60 acts as a receptor for the Listeria adhesion protein in Caco-2 cells. *Infection and Immunity* **72**: 931-936.

Wang, J., Hartling, J.A., and Flanagan, J.M. (1997) The structure of ClpP at 2.3 Å resolution suggests a model for ATP-dependent proteolysis. *Cell* **91**: 447-456.

Wang, M., Wamp, S., Gibhardt, J., Holland, G., Schwedt, I., Schmidtke, K.U., Scheibner, K., Halbedel, S., and Commichau, F.M. (2022) Adaptation of Listeria monocytogenes to perturbation of c-di-AMP metabolism underpins its role in osmoadaptation and identifies a fosfomycin uptake system. *Environ Microbiol* **24**: 4466-4488.

Webb, A.J., Homer, K.A., and Hosie, A.H. (2008) Two closely related ABC transporters in Streptococcus mutans are involved in disaccharide and/or oligosaccharide uptake. *J Bacteriol* **190**: 168-178.

Weber, J.M., Wierman, C.K., and Hutchinson, C.R. (1985) Genetic analysis of erythromycin production in Streptomyces erythreus. *J Bacteriol* **164**: 425-433.

Weis, J., and Seeliger, H.P. (1975) Incidence of Listeria monocytogenes in nature. *Appl Microbiol* **30**: 29-32.

Wemekamp-Kamphuis, H.H., Wouters, J.A., Sleator, R.D., Gahan, C.G., Hill, C., and Abee, T. (2002) Multiple deletions of the osmolyte transporters BetL, Gbu, and OpuC of Listeria monocytogenes affect virulence and growth at high osmolarity. *Applied and environmental microbiology* **68**: 4710-4716.

Westfahl, K.M., Merten, J.A., Buchaklian, A.H., and Klug, C.S. (2008) Functionally important ATP binding and hydrolysis sites in Escherichia coli MsbA. *Biochemistry* **47**: 13878-13886.

Wex, K.W., Saur, J.S., Handel, F., Ortlieb, N., Mokeev, V., Kulik, A., Niedermeyer, T.H.J., Mast, Y., Grond, S., Berscheid, A., and Brötz-Oesterhelt, H. (2021) Bioreporters for direct mode of action-informed screening of antibiotic producer strains. *Cell Chem Biol* **28**: 1242-1252 e1244.

Whiteley, A.T., Ruhland, B.R., Edrozo, M.B., and Reniere, M.L. (2017) A Redox-Responsive Transcription Factor Is Critical for Pathogenesis and Aerobic Growth of Listeria monocytogenes. *Infect Immun* **85**.

Wilkens, S. (2015) Structure and mechanism of ABC transporters. *F1000Prime Rep* **7**: 14.

Yoshida, K.-i., Ohki, Y.-h., Murata, M., Kinehara, M., Matsuoka, H., Satomura, T., Ohki, R., Kumano, M., Yamane, K., and Fujita, Y. (2004) Bacillus subtilis LmrA is a repressor of the lmrAB and yxaGH operons: identification of its binding site and functional analysis of lmrB and yxaGH. *Journal of bacteriology* **186**: 5640-5648.

Yücel, N., Cıtak, S., and Önder, M. (2005) Prevalence and antibiotic resistance of Listeria species in meat products in Ankara, Turkey. *Food microbiology* **22**: 241-245.

Zarrella, T.M., and Bai, G. (2020) The Many Roles of the Bacterial Second Messenger Cyclic di-AMP in Adapting to Stress Cues. *J Bacteriol* **203**.

Zhao, B.B., Li, X.H., Zeng, Y.L., and Lu, Y.J. (2016) ClpP-deletion impairs the virulence of Legionella pneumophila and the optimal translocation of effector proteins. *BMC Microbiol* **16**: 174.

Zolnerciks, J.K., Akkaya, B.G., Snippe, M., Chiba, P., Seelig, A., and Linton, K.J. (2014) The Q loops of the human multidrug resistance transporter ABCB1 are necessary to couple drug binding to the ATP catalytic cycle. *FASEB J* **28**: 4335-4346.

Zuber, P. (2009) Management of oxidative stress in Bacillus. *Annu Rev Microbiol* **63**: 575-597.

Ehrenerklärung

Ich versichere hiermit, dass ich die vorliegende Arbeit ohne unzulässige Hilfe Dritter und ohne Benutzung anderer als der angegebenen Hilfsmittel angefertigt habe; verwendete fremde und eigene Quellen sind als solche kenntlich gemacht.

Ich habe insbesondere nicht wissentlich:

- Ergebnisse erfunden oder widersprüchliche Ergebnisse verschwiegen,
- statistische Verfahren absichtlich missbraucht, um Daten in ungerechtfertigter Weise zu interpretieren,
- fremde Ergebnisse oder Veröffentlichungen plagiiert,
- fremde Forschungsergebnisse verzerrt wiedergegeben.

Mir ist bekannt, dass Verstöße gegen das Urheberrecht Unterlassungs- und Schadensersatzansprüche des Urhebers sowie eine strafrechtliche Ahndung durch die Strafverfolgungsbehörden begründen kann.

Ich erkläre mich damit einverstanden, dass die Arbeit ggf. mit Mitteln der elektronischen Datenverarbeitung auf Plagiate überprüft werden kann,

Die Arbeit wurde bisher weder im Inland noch im Ausland in gleicher oder ähnlicher Form als Dissertation eingereicht und ist als Ganzes auch noch nicht veröffentlicht.

Wernigerode, den 12.11.2023

Tim Engelgeh